DEXAMETHASONE ENHANCED MICRODIALYSIS FOR EXTENDED INTRACRANIAL CHEMICAL MONITORING

by

Erika Lynne Varner

B.S. Chemistry, California University of Pennsylvania, 2012

Submitted to the Graduate Faculty of the

Kenneth P. Dietrich School of Arts and Sciences in partial fulfillment

of the requirements for the degree of

Doctor of Philosophy

University of Pittsburgh

2017

UNIVERSITY OF PITTSBURGH

DIETRICH SCHOOL OF ARTS AND SCIENCES

This dissertation was presented

by

Erika Lynne Varner

It was defended on

June 27, 2017

and approved by

Renã A. S. Robinson, Assistant Professor, Department of Chemistry

Stephen G. Weber, Professor, Department of Chemistry

Xinyan Tracy Cui, Professor, Bioengineering Department

Dissertation Advisor: Adrian C. Michael, Professor, Department of Chemistry

DEXAMETHASONE ENHANCED MICRODIALYSIS FOR EXTENDED INTRACRANIAL CHEMICAL MONITORING

Erika Lynne Varner, PhD

University of Pittsburgh, 2017

Microdialysis is a popular method for real-time monitoring of neurotransmitters in the brain, applicable for a variety of research areas. Nonetheless, insertion of the probe into the brain tissue results in a penetration injury that triggers ischemia, activates astrocytes and microglia, and damages neurons in the surrounding area. This insertion injury significantly affects the ability of the microdialysis probe to collect samples from the surrounding tissue, a consequence that is further exacerbated with time. Incorporating dexamethasone, a glucocorticoid anti-inflammatory steroid, into the microdialysis perfusion fluid is a simple yet effective strategy for mitigating the probe insertion injury. The benefits of dexamethasone retrodialysis for long-term sampling from the rat brain are presented herein.

First, stimulated dopamine release was monitored with fast scan cyclic voltammetry next to and at the outlet of microdialysis probes at 4 hours, 24 hours, and 5 days after probe insertion into the rat striatum. Perfusing the microdialysis probe with dexamethasone and allowing the tissue 5 days to recover reinstated normal evoked dopamine activity adjacent to the probe. This provided quantitative agreement between responses measured directly in the striatal tissue and those measured at the probe outlet.

Second, transient changes in K^+ and glucose were monitored in the rat cortex following the induction of spreading depolarization at 2 hours, 5 days, and 10 days after probe insertion. At all three time points the retrodialysis of dexamethasone improved the detection of K^+ and glucose transients following spreading depolarization. When microdialysis probes were

implanted for 5 days without dexamethasone the glucose responses became essentially undetectable, however 5 days of dexamethasone retrodialysis preserved consistent glucose responses at both 5 and 10 days after probe insertion. For the 10 day study dexamethasone was removed from the perfusion fluid on day 5, showing the benefits of dexamethasone outlast the retrodialysis itself.

The significance of enhancing microdialysis through anti-inflammatory mitigation strategies extends beyond the analytes and conditions investigated thus far. The ability to accurately and reproducibly quantify neurochemicals days after microdialysis probe implantation is invaluable and will aid in improving our understanding of the complex chemical events occurring in the brain.

TABLE OF CONTENTS

LIST OF TABLES

LIST OF FIGURES

PREFACE

I would like to begin by acknowledging everyone who has supported me throughout the years. First I would like to thank my research advisor, Dr. Adrian Michael for the opportunities and advice he has provided me. His support both in and out of the lab has meant so much to me. Along with mentoring me in research he has also encouraged my interest in teaching and mentored me as I taught my first class.

Many thanks to all of the members of the Michael lab that I had the pleasure of working with: Andrea Jaquins-Gerstl, Katy Nesbitt, Mitch Taylor, Zhan Shu, Seth Walters, Elaine Robbins, and Rebecca Wu. A special thanks to Katy who trained me in both microdialysis and voltammetry. I am also grateful for the opportunity to work closely with Andrea throughout my projects, especially our collaboration with the Boutelle lab. I would like to thank Martyn Boutelle and his lab, specifically Agnes Leong, for their help in the spreading depolarization project and for welcoming Andrea and I into their lab. I am also appreciate of my other collaborations with Dr. Stephen Weber and his group members Khanh Ngo and Hui Gu.

I would like to thank Dr. Renã Robinson, Dr. Stephen Weber, and Dr. X. Tracy Cui for serving as my committee members. I would also like to thank Dr. Shigeru Amemiya for mentoring my original proposal. I am grateful the additional support I have received from the University of Pittsburgh's department of chemistry including the staff, machine and electronic shops, and Stan Paul and the other teaching faculty. I would also like to acknowledge my former

Finally, I need to thank my friends and family for always being there for me. Thank you to my fellow graduate students and Scott, it has been amazing to have you with me through this whole process. Words cannot describe the how grateful I am for the love and support I receive from my parents, siblings, and family, I could not have done this without them.

1.0   INTRODUCTION

1.1   MICRODIALYSIS

Microdialysis is a powerful technique with numerous benefits and advantages for intracranial chemical monitoring in both animal models and human patients.[1-7] Implanting a microdialysis probe into the brain tissue allows investigators to monitor in vivo chemical changes occurring in real time. The samples collected with the probe are compatible with a variety of highly sensitive and selective analytical methods such as high-performance liquid chromatography, capillary electrophoresis, electrochemical sensors and mass spectrometry.[8-13] This versatile technique is commonly used in studies of brain functions, neurological disorders, behavior and monitoring during neurointensive care.[1, 4, 14-17]

A microdialysis probe is constructed by connecting inlet and outlet tubing to a semipermeable membrane. The probe is perfused with a solution, typically artificial cerebrospinal fluid (aCSF), and diffusion across the membrane allows the collection of any molecule below the molecular weight cutoff of the membrane. Adding drugs or other compounds to the perfusate provides a localized delivery to the tissue around the probe, a process known as retrodialysis.

The samples collected by the probe, known as the dialysate, will contain a lower analyte concentration (C_{out}) when compared to the external environment (C_{ext}). The probe recovery of a specific analyte is defined as a ratio of C_{out}/C_{ext}. Probe recovery is influenced by several factors including the flow rate, temperature, diffusion and the active sampling area of probe's

1

membrane.[3] Due to the environmental differences affecting diffusion, such as tortuosity and uptake, it has been established that in vitro calibrations based on the probe recovery are not suitable for in vivo analysis.[18] While several in vivo calibrations have been developed,[19-21] they are limited by the tissue response to the probe insertion. This response creates a zone of abnormal tissue and disrupted neurochemical activity surrounding the microdialysis probe.[22-24]

1.2   TISSUE RESPONSE TO PROBE IMPLANTATION

Although microdialysis is a well-established technique, one drawback is that insertion of the probe into living brain tissue results in a penetration injury and tissue response.[22-35] Inserting the probe disrupts the blood-brain barrier and activates microglia within minutes.[32] The penetration injury develops over time with additional signs of tissue disruption including ischemia, astrocyte activation, and neuronal damage in the vicinity of the probe track.[25-31, 33-35]

Since microdialysis samples from the tissue surrounding the probe, the penetration injury results in the samples being obtained from tissue in an abnormal state. This complicates data interpretation and limits the capabilities of microdialysis. The tissue response to the foreign object develops over time which in turn creates an instability in microdialysis measurements.[36-40] To account for this many microdialysis studies are performed with a careful time interval between probe insertion and sample collection and often do not sample from the probe for more than a few hours or days.[3, 41]

The penetration injury is not unique to microdialysis, as the tissue response also affects other devices used for intracranial monitoring.[42-44] It is important to note there is no indication that the penetration injury adversely affects the subject's overall brain function or behavior.

Microdialysis is well tolerated by both animal models and human patients. The significance of the penetration injury is its impact on the ability of the microdialysis probe to provide an accurate report of the chemical events occurring in the brain.

1.2.1 Dexamethasone retrodialysis

The work detailed herein describes the benefits of utilizing dexamethasone (DEX) retrodialysis to mitigate the penetration injury. Dexamethasone, an anti-inflammatory and immunosuppressant glucocorticoid, has been used with both microdialysis and neuroprosthetic devices to suppress the tissue response to the foreign object and enhance long-term sampling.[31-35, 45-47] Incorporating DEX into the microdialysis perfusion fluid is a simple yet effective strategy that reduces ischemia, suppresses glial cell activation, and protects neurons and neuronal terminals in the vicinity of microdialysis probes.[31-35] Using retrodialysis provides a localized delivery method that allows for careful control over the dose and duration of DEX provided.

1.3   DOPAMINE MICRODIALYIS AND DETECTION WITH FAST SCAN CYCLIC VOLTAMMETRY

Dopamine is one of the analytes commonly sampled with microdialysis. Dopamine is an important neurotransmitter with numerous roles in normal brain function and it is also involved in a variety of disorders including substance abuse, schizophrenia, and Parkinson's disease.[48-51] When triggered by an action potential dopamine is released from vesicles within a neuron into the extracellular space where it can be measured with microdialysis. Once it is released

dopamine comes into contact with both receptors and transporters that regulate the extracellular concentration of dopamine.[52, 53] When dopamine binds to presynaptic D2 autoreceptors it serves as an inhibitory mechanism to decrease further dopamine release. The extracellular concentration of dopamine is also regulated by uptake through the dopamine transporter protein (DAT).

Along with microdialysis, fast scan cyclic voltammetry (FSCV) is another method commonly used for studying dopamine in vivo.[53-55] This technique involves applying a potential to a carbon fiber microelectrode and measuring the changes in current from the oxidation and reduction between dopamine and dopamine o-quinone. Applying a waveform that scans at 400 V/s from the rest potential of 0 V to 1 V, then to -0.5 V, and back to the resting potential (vs. Ag/AgCl) can selectively measure changes in dopamine with high temporal resolution. This high scan rate produces a background nonfaradaic charging current, therefore requiring background subtraction to identify the faradaic current from the oxidation and reduction of dopamine.[56]

1.4   VOLTAMMETRY NEXT TO AND AT THE OUTLET OF THE MICRODIALYSIS PROBE

To understand the impact of the probe insertion injury, voltammetry has been used to measure dopamine next to the microdialysis probe. This method involves measuring stimulated dopamine release with FSCV before and after implanting a microdialysis probe into the striatum of an anesthetized rat. The carbon fiber microelectrode is ideal for this comparison as its small diameter, 7 µm, results in minimal tissue disruption in comparison to the 300 µm diameter of the microdialysis probe. Within hours of implanting a microdialysis probe, the evoked dopamine

response in the tissue next to the probe is significantly decreased.[24, 33-35, 40, 57] The impact of the penetration injury is dependent on the distance between the microelectrode and probe, forming a decreasing gradient of evoked dopamine the closer the microelectrode is positioned to the probe.[24] The gradient of release is still present when the sampling time is extended beyond acute, 4 h, studies.[34, 35, 40] The dopamine terminals around the probe survive the implantation, but are suppressed, showing the decrease in signal is not from the terminals being completely destroyed, but remaining in a perturbed state.[33, 57]

The gradient of responses observed around the microdialysis probe leads to the question, how well do the samples collected with the probe represent normal, undisturbed tissue? Microdialysis studies do not typically use an additional technique to sample from the tissue next to the probe, therefore it is important to correlate the responses next to the probe to those obtained at the probe outlet.[23, 34, 35, 40, 58] Carbon fiber microelectrodes were placed next to and at the outlet of microdialysis probes for the measurement of electrically evoked release of striatal dopamine. In most cases, evoked release was undetectable at the probe outlet without the addition of a dopamine uptake inhibitor, nomifensine. Under these conditions nomifensine increased the in vivo recovery of dopamine. Theoretical models have suggested the increase in vivo probe recovery observed with DAT inhibition results from the zone of disrupted tissue surrounding the probe wherein dopamine uptake exceeds release.[22, 23, 58-60] The next two chapters discuss benefits of utilizing DEX retrodialysis to mitigate the probe penetration injury and enhance long-term microdialysis sampling of dopamine measured with FSCV.

1.5   SPREADING DEPOLARIZATION AND CLINCAL MICRODIALYSIS

Microdialysis, initially developed for use in the animal brain, has since been adapted for neurochemical monitoring in clinical settings.[5] One application of clinical microdialysis is monitoring brain injured patients in the intensive care unit (ICU) to identify chemical markers of secondary brain injuries. Traumatic brain injury (TBI) is a significant public health problem, often referred to as a silent epidemic due to the numerous complications associated with a TBI.[61, 62] In the United States 1.7 million TBI cases result in 53,000 deaths and 275,000 hospitalizations a year.[63] The primary injury can expand into the surrounding at risk tissue, termed the penumbra, resulting in secondary brain injuries.[64-67] Forms of secondary injury include rises in intracranial pressure, ischemia, hypoxia, seizures, and spreading depolarization (SD).

In the hours and days following the primary injury episodes of SD occur spontaneously in approximately 60% of TBI patients.[68-71] The occurrence and frequency of SD is a major source of the heterogeneity of this complex disease and is proving to be a major factor in predicting patient outcome. Incidences of SD are significantly correlated with poor patient outcomes, including death, vegetative state, and severe disability.[64-66]

Spreading depolarization is characterized by a wave of near-complete depolarization of neurons and glia resulting in a temporary disruption of the ion homeostasis and silencing of electrical activity.[65] Excess K^+ released into the extracellular space during SD can diffuses to and depolarizes neighboring cells, thus creating a wave that propagates across the cortex at a rate of 2-5 mm/minute. Following the SD there is a large energy demand essential for the repolarization of cell membranes. The brain tissue depends on the vasculature to deliver glucose and oxygen to meet these energy demands, however swelling and restricted blood flow, commonly observed

after a TBI, can hinder this process. Clusters of SD impose particularly severe energy demands on the injured brain and can result in long-lasting declines in basal glucose.[16, 67-73]

The importance of SD monitoring during neurointensive care has been widely recognized and numerous animal studies have been dedicated to improving SD monitoring.[64-66, 74] Methods for SD monitoring include electrocortiography (ECoG), blood flow analysis, and microdialysis. The Boutelle lab has developed a rapid sampling microdialysis (rsMD) system that monitors SD-associated changes in glucose and lactate at the patient's bedside.[75] Combining the rsMD system with an online K^+ ion-selective electrode (ISE) and ECoG provides a multimodal analysis system that can detect episodes of SD in the days following the patient's primary injury.[76-78] The fourth chapter describes the DEX enhanced sampling of SD-induced changes in K^+ and glucose 10 days after inserting a microdialysis probe into the rat cortex.

2.0   MICRODIALYSIS IN THE RAT STRIATUM: EFFECTS OF 24 HOUR DEXAMETHASONE RETRODIALYSIS ON EVOKED DOPAMINE RELEASE AND PENETRATION INJURY

The contents of this chapter have been adapted with permission from: Nesbitt, K.M., Varner, E.L., Jaquin-Gerstl, A., Michael, A.C., ACS Chem. Neurosci. 2015, 6, 163-173. Copyright 2014 American Chemical Society.

Dr. Andrea Jaquins-Gerstl contributed the immunohistochemistry and fluorescence microscopy work presented in this chapter.

2.1   INTRODUCTION

Intracranial microdialysis is ideally suited for real-time chemical monitoring in the brain,[16, 41, 79-90] the benefits of which are well-known and have been reviewed often.[1-4, 91-95] The microdialysis membrane keeps the dialysate samples free of large molecules and other debris, thus the dialysate is compatible with numerous analytical techniques. Many studies have been dedicated to refining both the microdialysis probes themselves and the analytical methods used to analyze the dialysate samples.[8, 12, 96-104] Here, we wish to contribute to this ongoing refinement effort by focusing attention on what happens when the probes are implanted into brain tissue.

In practice, two major and intertwined challenges remain to be solved. First, when microdialysis probes are inserted into brain tissue, a wound response is triggered.[22, 25-31, 33, 105-109] Consequently, the dialysate samples are derived from the injured, abnormal tissue near the probe track. The wound response involves a cascade of events, some of which begin right away and some of which develop over the course of several days. Microglia respond within minutes to focal brain injury, whereas astrocytes respond later forming a barrier around the microdialysis probe after 5 days.[31, 42, 110] Probe implantation also causes ischemia, disruption of the blood-brain barrier, and neuronal loss.[30-31, 33, 105]

Second, minimal quantitative information is available as to how the concentration of substances in the outflow of microdialysis probes are related to the concentration of substances in the injured tissue next to the probes, or how concentrations in the injured tissue next to the probes are related to concentrations in the non-injured surroundings. These concentration relationships have been the subject of theoretical considerations but relatively few direct measurements.[59, 111, 112] Neurochemical instability over the postimplantation intervals has been a long-standing issue in the field of microdialysis.[24, 36-38, 57, 113-115] Even so, the dialysate content of neurotransmitters exhibits sensitivity to tetrodotoxin,[41] responds predictably to various drugs,[100, 116-118] and correlates with behaviors.[1, 4, 15, 80, 83] These observations show that microdialysis provides valid and useful indices of neurochemical activity.

A prior study from our laboratory demonstrated the beneficial effects of the retrodialysis of dexamethasone (DEX), a potent anti-inflammatory steroid, on the tissue penetration injury and dopamine (DA) concentrations in the tissue surrounding the probe 4 h after probe insertion.[33] DEX diminished the loss in amplitude of evoked DA responses measured directly next to the probe with fast-scan cyclic voltammetry (FSCV). Histochemical data provided clear evidence

9

that the anti-inflammatory actions of DEX prevented ischemia, astrocyte and microglia activation, and the loss of neurons near the probe track.[31, 33]

Herein, we implanted microdialysis probes in the rat striatum for 4 and 24 h, both with and without DEX in the perfusion fluid, and then measured evoked DA release at the outlet of the probes with FSCV. Responses at the probe outlet were below the detection limits of FSCV unless animals were treated with the DA uptake inhibitor, nomifensine, which increases the microdialysis recovery of evoked dopamine transients.[23, 116, 119] When probes were perfused without DEX, post-nomifensine responses at the probe outlet exhibited a significant decline in amplitude between 4 and 24 h postimplantation. However, DEX abolished this instability, both in animals treated first with nomifensine and then with raclopride. Thus, we report here for the first time that DEX stabilizes, but does not alter, evoked dopamine responses at the outlet of microdialysis probes. DEX had no significant effect on two key tissue markers for dopamine terminals, tyrosine hydroxylase (TH) and the dopamine transporter (DAT). We therefore attribute DEX's effects on evoked dopamine responses at the outlet of microdialysis probes to its anti-inflammatory actions, as opposed to any direct actions on dopamine terminals. Finally, we report for the first time that the penetration of DEX into the tissue near the probe is extremely limited. Fluorescein-labeled DEX was found no further than 80 μm from its delivery probe. We therefore conclude that DEX's anti-inflammatory actions are tightly confined to the immediate, local vicinity of the probe.

2.2 RESULTS AND DISCUSSION

2.2.1 Voltammetry Next to the Probe

Electrical stimulation of DA axons in the medial forebrain bundle (MFB) evokes DA release in the ipsilateral striatum, which is easily measurable by FSCV.[120-123] Previous studies have shown when microelectrodes are implanted into the tissue next to the microdialysis probe there is a decreasing gradient of evoked DA release the closer the microelectrode is placed to the microdialysis probe.[24, 40] When microelectrodes are implanted next to the microdialysis probe (70-100 μm from the probe) evoked DA responses are abolished by 4 h after probe implantation.[33] Previously, the retrodialysis of DEX diminished, but did not eliminate, the loss in amplitude of the evoked responses next to the microdialysis probe.[33] Additional data obtained next to the microdialysis probe is provided in the original version of this research article.

2.2.2 Voltammetry at the Probe Outlet

FSCV was performed at the outlet of microdialysis probes to quantify evoked responses in the dialysate stream (Figure 2-1). The stimulus parameters were 45 Hz, 300 μA, 25 s. The evoked responses are reported in Figure 2-2, in which the time axes have been adjusted to account for the time needed for the dialysate to flow from the probe to the end of the outlet line: the transit time was confirmed by calibration and agreed with calculated values. The vertical axes in Figure 2-2 were obtained by postcalibration of the detection electrode in a flow cell apparatus without correction for probe recovery, so the vertical axes report dialysate, not in vivo,

11

DA concentrations. The DA responses in Figure 2-2 exhibit some baseline drift: this is due to the

electrode pretreatment strategy used to optimize the sensitivity of the electrodes (see Methods).
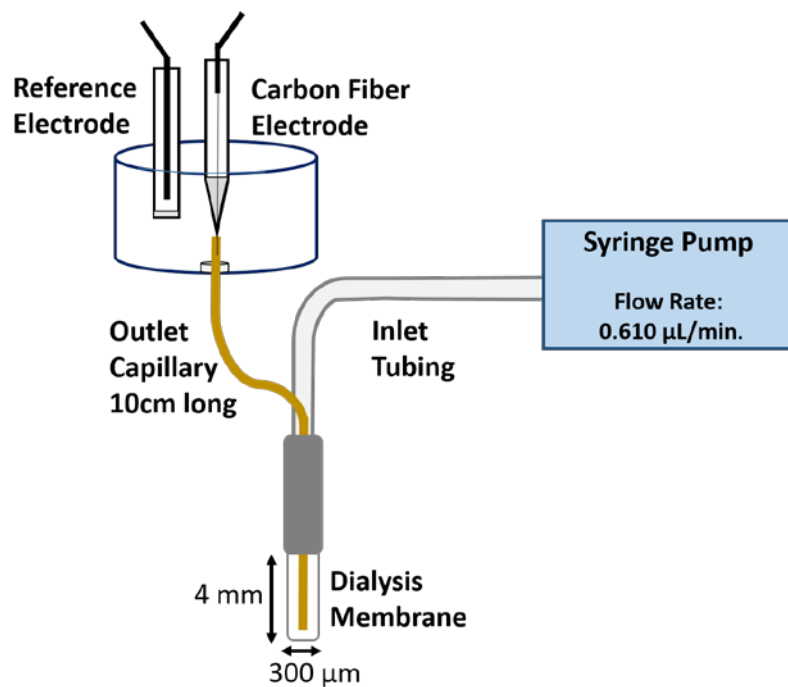
Figure 2-1.
Diagram for voltammetry at the microdialysis probe outlet.
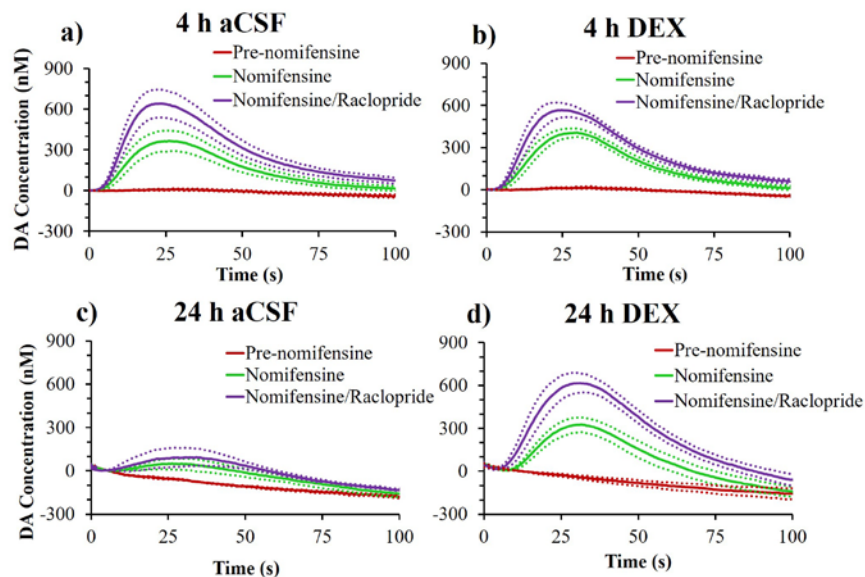
Figure 2-2.
Effect of aCSF and DEX on the average (±SEM) evoked DA release measured at the probe outlet pre-nomifensine (red), after nomifensine (green), and after both nomifensine and raclopride (purple). Evoked release was measured (a, b) 4 h and (c, d) 24 h after probe implantation (n = 6 per group). A negative dopamine concentration means that the current dropped below the baseline current response as a result of the baseline drift from the electrochemical pretreatment of the carbon fiber (see Methods).

Evoked DA release was nondetectable at the outlet of probes perfused with aCSF or DEX for 4 or 24 h (Figure 2-2, red lines). This is consistent with our prior experience that evoked DA responses at the probe outlet are below the detection limits of FSCV unless the DA uptake mechanism is inhibited.[23, 40, 58] This observation is also consistent with the results of our measurements next to the microdialysis probe.[33] In the case of perfusion with aCSF, evoked responses are below FSCV detection limits next to the probe, which explains why no response was detected at the probe outlet. DEX significantly increased the response amplitude next to the probe but evidently, not sufficiently enough to produce a detectable response at the probe outlet.

Evoked DA release was detected at the probe outlet following administration of the dopamine uptake inhibitor, nomifensine (20 mg/kg i.p., Figure 2-2, green lines), consistent with the ability of nomifensine to increase evoked responses next to the probe. In the case of probes

13

perfused with aCSF, the post-nomifensine response was not stable: the response amplitude declined significantly between 4 and 24 h after implantation (Figure 2-3, statistics reported in figure legend). No such instability was observed next to the probe, which suggests that responses closer to the probe are affected more, as we have previously suggested.[24] DEX eliminated this instability: in the presence of DEX, there was no significant difference in the responses at the probe outlet at 4 and 24 h postimplantation (Figure 2-3). Hence, we report here for the first time on DEX's ability to stabilize evoked responses at the probe outlet over the 4–24 h postimplantation interval.
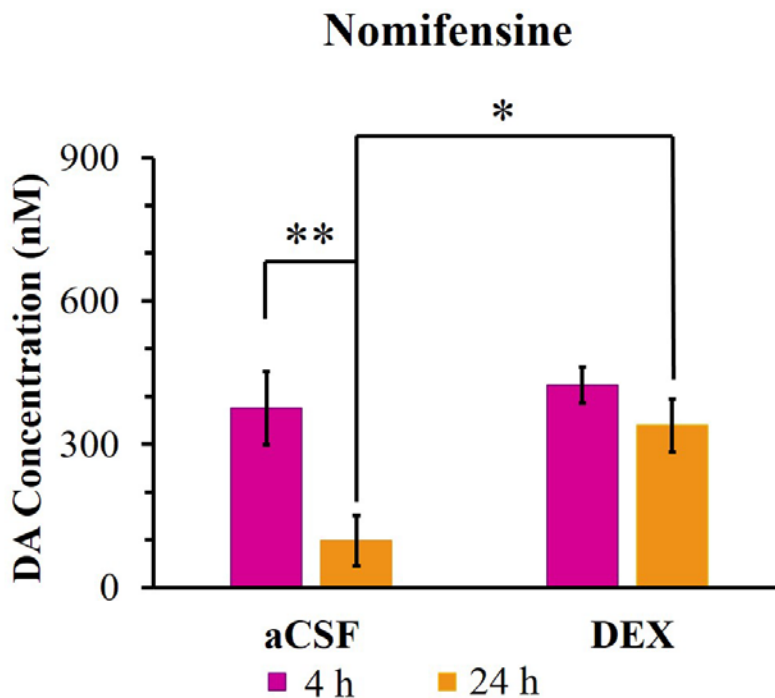
Figure 2-3.
Average maximum evoked DA concentration (±SEM) observed at the outlet of microdialysis probes after nomifensine comparing 4 h (pink, n = 6) and 24 h (orange, n = 6) after probe implantation. In a two-way ANOVA time (4, 24 h), $F_{(1,20)} = 9.86$, $p < 0.01$, and treatment (aCSF, DEX), $F_{(1,20)} = 6.37$, $p < 0.05$, were significant effects on the DA concentration post-nomifensine. There was no significant interaction $F_{(1,20)} = 2.82$, $p > 0.05$. In a post hoc pairwise comparisons with Bonferroni corrections, there is a significant difference between aCSF at 4 and 24 h and between aCSF and DEX at 24 h. *$p < 0.01$ and **$p < 0.005$.

The statistical analysis also shows there were no significant differences between the response amplitudes measured at the outlet of probes perfused with DEX and those perfused for 4 h with aCSF (Figure 2-3). Thus, DEX stabilized, but does appear to have altered, the responses at the probe outlet.

Following the administration of nomifensine, rats received a single dose of the D2 DA receptor antagonist, raclopride (2 mg/kg i.p.), and a final evoked response was measured at the probe outlet (Figure 2-2, purple lines). As expected,[57, 121, 124, 125] the autoreceptor antagonist caused a further increase in the response amplitudes, as summarized in Figure 2-4. Statistical

15

analysis of Figure 2-4 was by a mixed-model three-way ANOVA of time (4 h, 24 h), perfusion medium (aCSF, DEX), and drug (nomifensine, raclopride, with repeated measure) as the main factors (details in the figure legend). The responses at the outlet of probes perfused with aCSF significantly diminished between 4 and 24 h postimplantation. There were no significant differences between the responses observed in the 4 h aCSF, 4 h DEX, and 24 h DEX cases: this shows that DEX stabilized but did not alter these responses. Raclopride significantly increased the evoked responses in the 4 h aCSF, 4 h DEX, and 24 h DEX cases but not in the 24 h aCSF case.
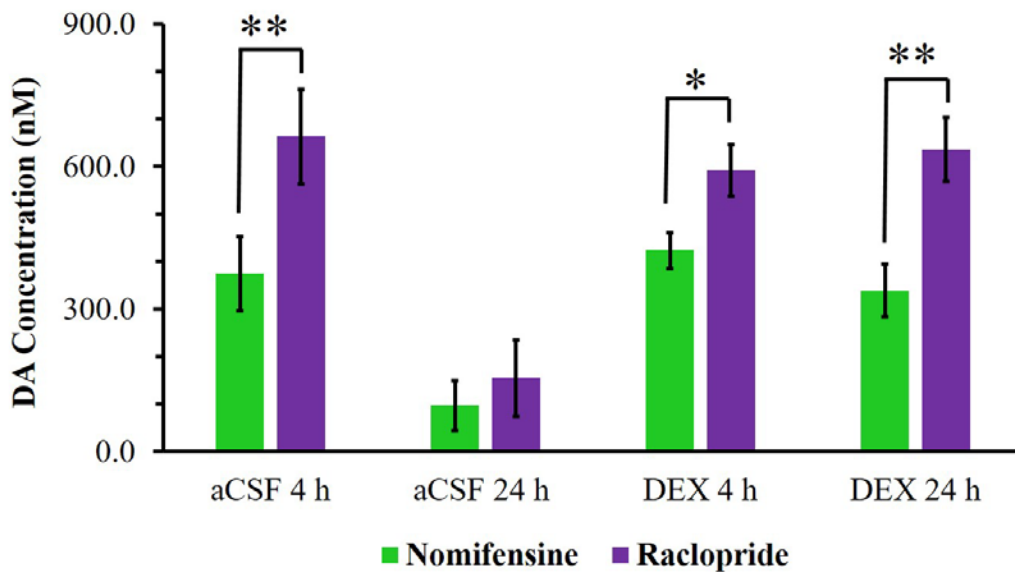
Figure 2-4.
Average maximum evoked DA concentration (±SEM) collected by the probe. A three-way ANOVA with repeated measures was completed comparing the effects of time (4, 24 h), treatment (aCSF, DEX), and drug (nomifensine, raclopride). As seen in the nomifensine data, time $F_{(1,20)} = 10.4$, $p < 0.005$; treatment $F_{(1,20)} = 7.52$, $p < 0.05$; and now the interaction between treatment and time $F_{(1,20)} = 8.47$, $p < 0.01$ are significant. The effect of drug (between nomifensine and raclopride) was significant $F_{(1,20)} = 74.7$, $p < 0.00000005$, and the interaction between time and treatment and drug was also significant $F_{(1,20)} = 14.5$, $p < 0.05$. A post hoc pairwise comparison with Bonferroni corrections shows a significant increase from nomifensine to raclopride in 3 of the 4 experiments. *$p < 0.005$ and **$p < 0.000005$.

16

Thus, as judged on the basis of evoked responses measured at the outlet of microdialysis probes, DEX eliminated the instability in DA neurochemistry between 4 and 24 h post implantation in animals treated first with nomifensine and then with raclopride. Perfusion with aCSF for 24 h caused a loss in the significance of the effects of both nomifensine and raclopride combination. The loss in amplitude reported here is consistent with several prior reports of instability of DA following probe implantation.[36-38, 40]

During the 24 h experiments a second carbon fiber microelectrode was inserted into the tissue to record in vivo evoked responses. The electrode was positioned 1.5 mm from the probe to ensure the electrode was outside of the zone of tissue disrupted during the probe insertion.[24, 40] While there was a significant difference in the outlet responses with and without DEX (Figures 2-3 and 2-4), there was no significant difference observed at the electrode 1.5 mm from the probe (Figure 2-5). This confirms the instability at the probe outlet is due to the disruption of the tissue in the immediate vicinity of the probe. In the 4 h experiment the in vivo electrode was removed prior to probe insertion, as described in the methods section.
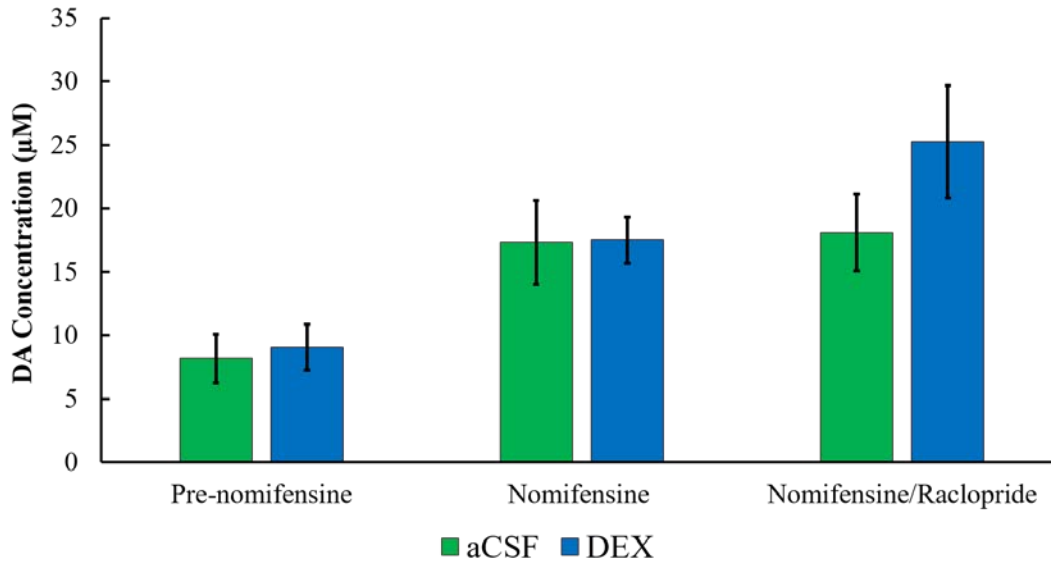
Figure 2-5.
Average (±SEM) in vivo evoked DA concentration recorded 24 h after probe insertion. The carbon fiber microelectrode was positioned 1.5 mm from the probe. A two-way ANOVA with repeated measures was completed with treatment (aCSF, DEX) and drug (pre-nomifensine, nomifensine, and nomifensine/raclopride) as the factors. Drug was a significant factor, $F_{(2,20)} = 24.579$, $p > 0.00005$, but treatment and the interaction were not significant.

2.2.3 Immunohistochemistry of the Probe Track

We performed histochemical analysis of striatal tissues using antibodies for two widely accepted markers of DA terminals, tyrosine hydroxylase (TH) and the DAT.[126-128] The tissue exhibited nonlabeled areas corresponding to myelinated axon bundles. Additionally, the probe tracks are clearly visible in the center of the images shown in Figure 2-6. Some diffuse labeling around probes perfused with aCSF is evident in the TH image (Figure 2-6, middle column): we have observed such binding before and consider it an edge effect.[33, 129] Overall, TH and DAT labeling was clearly evident near the tracks of probes perfused both with and without DEX (quantification is discussed, below).

18
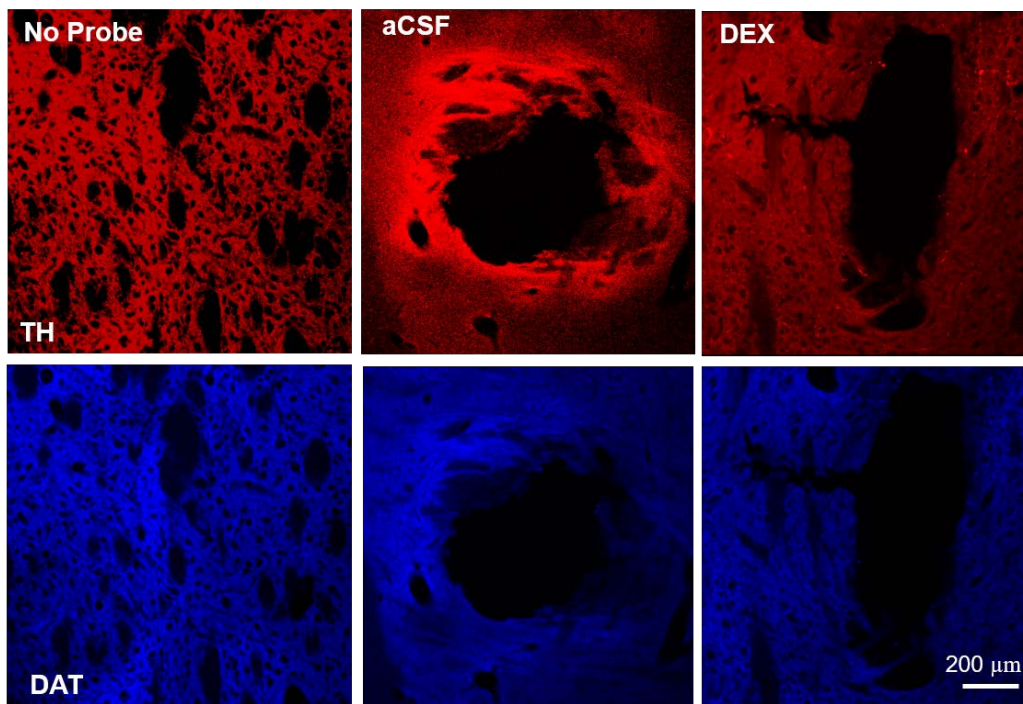
Figure 2-6.
Separate columns illustrate representative fluorescent images of striatal tissue with no probe, or after retrodialysis of aCSF, or DEX for 24 h. Separate rows provide tissue labeled with TH (top) or DAT (bottom). Scale bars are 200 μm.

The intense TH labeling near probe tracks perfused with aCSF for 24 h stands in clear contrast to the absence of TH labeling that we observed 4 h after implantation.[33] The exact mechanism whereby this interesting rebound of TH labeling occurs is not yet known: possibilities, to be explored further in future studies, might include the synthesis of new TH protein by surviving DA terminals and/or the sprouting of new DA terminals.[130, 131]

The TH and DAT images were converted to 2D intensity scatter plots, from which we determined Pearson's correlation coefficient (PCC) and Manders' overlay coefficient (MOC) (see the methods for explanations of these coefficients).[132] The correlation coefficients in images with and without probe tracks are indistinguishable for probes perfused with DEX (Figure 2-7). The correlation coefficients are only slightly reduced with aCSF compared to DEX, most likely

19

due to the nonspecific edge effect.[133] Overall, the probes with DEX had no significant effect on the correlation of TH and DAT labeling in the nearby tissue (see Figure 2-7 legend). Regions of interest in the TH and DAT labeled images were defined to eliminate the probe track. There were no significant differences in the quantitative TH and DAT labeling in nonimplanted control tissue and the regions of interest around the tracks of probes perfused for 24 h with either aCSF or DEX (Figure 2-7b).
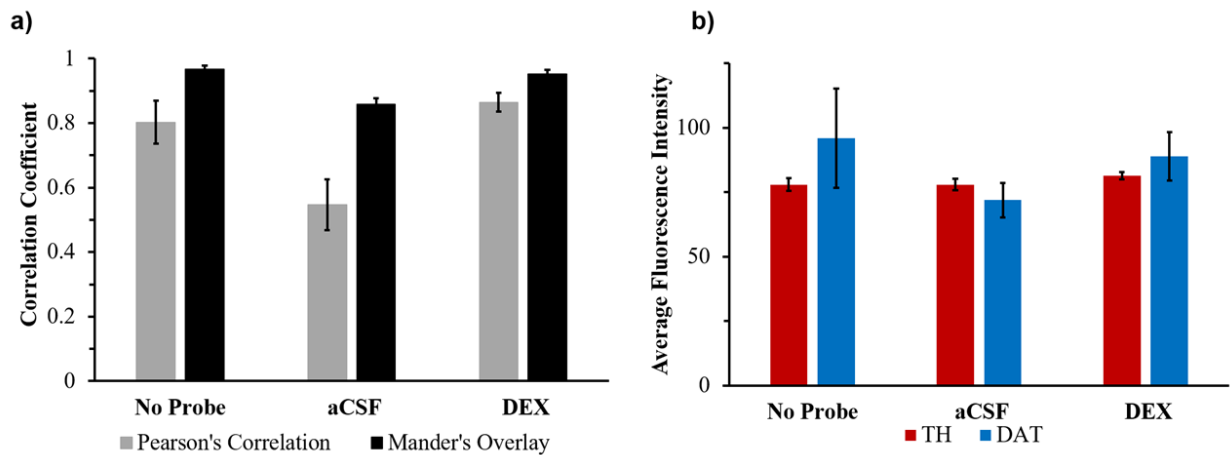
Figure 2-7.
(a) Correlation coefficients between TH and DAT pixels among the three groups (no probe, aCSF and DEX, n = 3 rats (total of 6 images per group)) for both Mander's overlay (black) and Pearson's correlation (green). A two-way ANOVA comparing the treatment (no probe, aCSF, and DEX) and analysis (Pearson's correlation and Mander's overlay) showed that there were significant differences in treatment $F_{(2,28)} = 14.2$, $p < 0.0001$, analysis $F_{(1,28)} = 29.7$, $p < 0.00001$, and the interaction treatment and analysis $F_{(2,28)} = 3.87$, $p < 0.05$. A post hoc Tukey test further showed aCSF correlation coefficients were significantly reduced compared to no probe ($p < 0.0005$) and DEX ($p < 0.0001$). A post hoc pairwise comparisons with Bonferroni corrections showed that Mander's overlay and Pearson's correlation differ from each other with no probes ($p < 0.05$) and aCSF ($p < 0.00005$). (b) Average fluorescent intensity for TH (red) and DAT (blue) for no probe, aCSF, and DEX (n = 3 rats (total of 6 images per group)). Fluorescent intensity ranges from 0 to 255 with 255 being the highest value. In a two-way ANOVA comparing treatment (no probe, aCSF, and DEX, $F_{(2,30)} = 0.97$, $p > 0.05$) and stain (TH and DAT, $F_{(2,30)} = 0.74$, $p > 0.05$), there were no significant differences in average fluorescent intensity.

Overall, probe implantation had no significant effect on TH and DAT, two key markers for DA terminals. This supports our conclusion that DEX's effects on evoked responses are attributable to its previously documented anti-inflammatory actions,[31, 33] as opposed to direct

actions on DA terminals. Our prior studies show that DEX profoundly decreases ischemia, glial activation, and neuron loss in the tissues near microdialysis probes.[31, 33] It appears that these actions are responsible for the effects of DEX on evoked DA responses next to and at the outlet of microdialysis probes over the 4−24 h post-implantation interval.

2.2.4 Evaluating the Tissue Penetration of Dexamethasone

We used fluorescein-labeled DEX (DEX-FL) to assess how far DEX penetrates into the tissue near microdialysis probes. After 4 h of retrodialysis, DEX-FL penetrated only to 78.6 ± 46.1 μm from the probe track (Figure 2-8). This result, however, might be affected by the detection limit of the fluorescence measurement and possibly by loss of soluble DEX-FL during tissue processing. We therefore conclude that DEX does not penetrate deeply into brain tissue and that its actions are confined to within close proximity to the delivery probe.
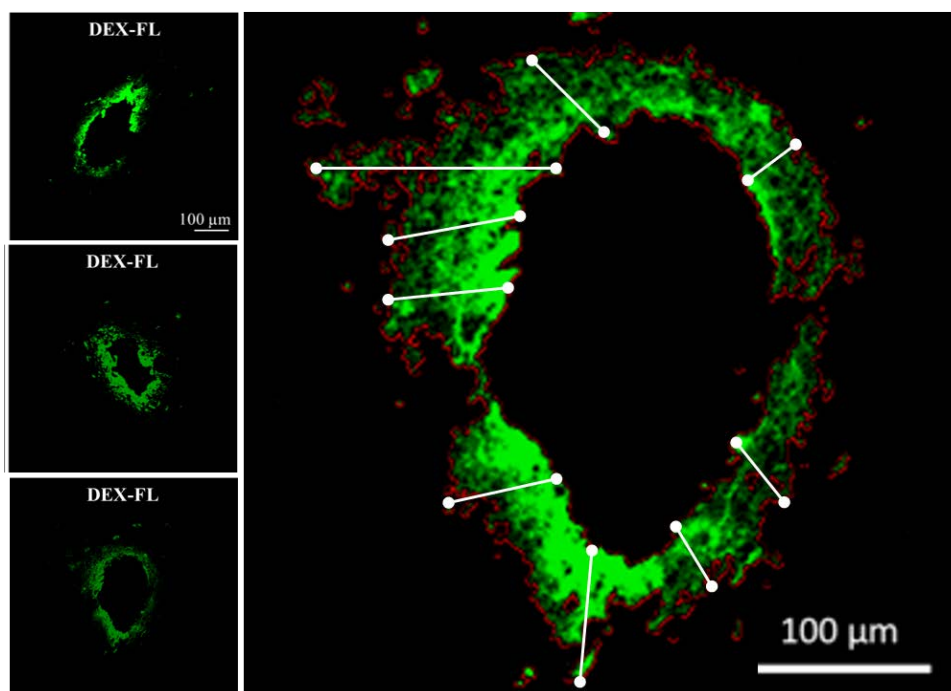
Figure 2-8.
Images of the microdialysis probe track, from three different rats, after 4 h perfusion of DEX-FL. DEX-FL is delivered locally only to the tissue directly surrounding the probe. The white lines mark the distance of DEX-FL from the microdialysis probe track.

2.3   CONCLUSIONS

Our findings reiterate that tissue damage occurs when a microdialysis probe is implanted into brain tissue.[25, 26, 28, 30, 31, 33, 105] The disruption of the tissue surrounding the microdialysis probe results in neurochemical and histological disruptions over the 4−24 h postimplant interval, a typical time frame for microdialysis studies.[3, 8, 41, 97] Here, based on the evoked DA responses measured at the outlet of the probe, we have documented for the first time that DEX eliminates such instability over the 4-24 h time interval following probe insertion. DEX stabilizes, but does not alter, evoked dopamine responses at the outlet of microdialysis probes following the sequential administration of nomifensine and raclopride. The actions of DEX reported here

22

appear to derive from its anti-inflammatory actions,[31, 33] rather than any direct neurochemical impact on the DA terminals. Additionally, the actions of DEX are confined to the tissue directly surrounding the microdialysis probe.

2.4   METHODS

The methods used during this study have been described previously.[23, 24, 30, 31, 33, 57, 105]

2.4.1   Reagents and Solutions

All solutions were prepared with ultrapure water (Nanopure, Barnstead, Dubuque, IA). All reagents were used as received from their suppliers. Artificial cerebrospinal fluid (aCSF: 142 mM NaCl, 1.2 mM $CaCl_2$, 2.7 mM KCl, 1.0 mM $MgCl_2$, 2.0 mM NaH_2PO_4, pH 7.4) was the perfusion fluid for microdialysis. DEX sodium phosphate (DEX, APP Pharmaceuticals LLC Schaumburg, IL) was diluted to 10 μM in aCSF. This dose was used as we have previously observed a dramatic reduction in tissue disruption at 10 μM DEX for 24 h.[31] DEX fluorescein (DEX-FL, Life Technologies Grand Island, NY) was diluted to 10 μM in aCSF. Nomifensine maleate and S(−)-raclopride (+)-tartrate salts (SigmaAldrich, St. Louis, MO) were dissolved in phosphate-buffered saline (PBS: 155 mM NaCl, 100 mM NaH_2PO_4, pH 7.4) and administered at 20 mg/kg (i.p.) and 2 mg/kg (i.p.), respectively. Isopropyl alcohol (Sigma-Aldrich, St. Louis, MO) and decolorizing carbon (Fisher, Pittsburgh, PA) were used to pretreat carbon fiber electrodes for DA voltammetry. DA (Sigma-Aldrich, St. Louis, MO) standards were prepared in N_2-purged aCSF.

2.4.2　Fast Scan Cyclic Voltammetry and Electrochemical Pretreatment

Carbon fiber electrodes were constructed by threading a single carbon fiber (7 µm diameter, T650, Cytec Carbon Fibers LLC., Piedmont, SC) through borosilicate capillaries (0.58 mm I.D., 1.0 mm O.D., Sutter Instruments, Novato, CA). The capillaries were pulled to fine tips around the carbon fiber with a vertical puller (Narishing Tokyo, Japan). Carbon fibers were glued in place with a low viscosity epoxy (Spurr Epoxy, Polysciences Inc., Warrington, PA) and cured overnight at 70 ºC. The exposed carbon fiber was cut to a length of 400 µm for in vivo studies or 800 µm for detection at the outlet of microdialysis probes. Capillaries were backfilled with mercury and a nichrome wire (Goodfellow, Oakdale, PA) was placed into the mercury to make an electrical connection.

Fast scan cyclic voltammetry (FSCV) was executed using a computer controlled EI-400 potentiostat (Ensman Instruments, Bloomington, IN) with CV Tarheels version 4.3 software (Michael Heien, University of Arizona, Tucson AZ). A triangular waveform was applied as a linear sweep (vs Ag/AgCl) from 0 V to 1 V, then to -0.5 V, and then back to the resting potential of 0 V at a scan rate of 400 V/s. Scans were performed at a frequency of 2.5 Hz unless otherwise noted. Background subtracted voltammograms were used to quantify DA on the initial potential sweep between 0.6 V and 0.8 V. The DA current was converted to concentrations by post-calibrations with freshly prepared standard solutions of DA (Sigma Aldrich, St. Louis, MO) dissolved in nitrogen purged aCSF.

In addition to the isopropyl alcohol pretreatment, 800 µm electrodes were electrochemically pretreated (0-2V vs. Ag/AgCl at 200 V/s for 3 s) exactly 10 min before each collection. The electrode was pulled out of the outlet before each pretreatment and re-lowered immediately after it was complete. To reduce resistance, the electrode was positioned so that

majority of the carbon fiber was inside the outlet. The pretreatment causes a drift in the signal, which is noticeable when detecting low concentrations close to the detection limit (~20-30 nM).[23] For this reason the pretreatment was completed exactly 10 min before each collection at the outlet, followed by a 60 Hz waveform scan for 60 s to help stabilize the drift. The pretreatment had no impact on the brain tissue because the in vivo electrode was outside of the path of the electrochemical cell.

2.4.3 Microdialysis Probes

Concentric microdialysis probes (300 μm diameter, 4 mm length) were constructed with hollow fiber membranes (13 kDa MWCO, Specta/Por RC, Spectrum Laboratories Inc., Ranco Dominguez, CA). The inlet tubing (PE, Becton Dickinson, Franklin Lakes, NJ) was connected to a 1 mL gastight syringe driven by a microliter syringe pump (Harvard Apparatus, Holliston, MA) at a rate of 0.610 μL/min. The outlet was a fused silica capillary (75 μM I.D., 150 μM O.D., 10 cm long; Polymicro Technologies, Phoenix, AZ). Probes were perfused with either aCSF or aCSF containing 10 μM DEX.

2.4.4 Surgical Procedures

All procedures involving animals were approved by the University of Pittsburgh's Animal Care and Use Committee. Male Sprague−Dawley rats (250−350 g; Hilltop, Scottsdale, PA) underwent sterile stereotaxic surgery under isoflurane anesthesia. The probes were lowered into the brain at 5 μm/s with an automated micropositioner (model 2660, David Kopf Instruments, Tujunga, CA). For all voltammetry experiments, the reference and stimulating

electrodes were placed in the same positions in the brain. Reference electrodes were connected to the brain via a salt bridge. Bipolar stimulating electrodes were lowered into the medial forebrain bundle (MFB) until maximum DA release was observed (4.3 mm posterior and 1.2 mm lateral from bregma). Electrically evoked DA release was recorded by FSCV during stimulation of the MFB (stimulus waveform: biphasic, square, constant current pulses 300 μA pulse height, 4 ms pulse width). The waveform was delivered for 25 s at 45 Hz.

2.4.5 Voltammetry at the Probe Outlet

Voltammetry at the probe outlet was performed in a custom-made Plexiglas detection chamber (Figure 2-1). A carbon fiber electrode (800 μm long) was inserted into the end of the capillary outlet line with a miniature micromanipulator (Fine Science Tools, Foster City, CA). As described previously,[23] the electrodes were electrochemically pretreated 10 min before each stimulus or calibration procedure.

Voltammetry at the outlet was performed in four groups of rats, 4 or 24 h (n = 6 per group) after probe implantation, with perfusion of aCSF or DEX. Animals in the 4 h group remained under isoflurane anesthesia throughout the experiment.

For the 4 h study, anesthetized rats were placed in a stereotaxic frame and adjusted to flat skull. Three holes were drilled in the skull and the dura was carefully removed to expose the brain. A carbon fiber electrode was inserted into the striatum (0.7 mm anterior to bregma, 2.5 mm lateral from bregma, and 5.0 mm below dura), and a stimulating electrode was lowered to the MFB. Three evoked DA responses were recorded in 20 min intervals to establish a stable, pre-probe response. The electrode was removed and a microdialysis probe was inserted using a micropositioner (5 μm/sec) in the same location except 7.0 mm below dura. After 2 h, evoked

DA release was monitored in the outlet. Following three initial 25s stimulations, nomifensine and raclopride were sequentially administered and evoked DA monitored 25 minutes later.

For the 24 h study, a microdialysis probe was lowered into the brain of an anesthetized rat (1.6 mm anterior to bregma, 2.5 mm lateral from bregma, and 7.0 mm below the dura) at 5 µm/s with an automated micropositioner and secured to the skull with bone screws and acrylic cement. Following surgery, the rats were placed in a Raturn microdialysis bowl (MD-1404, BASI, West Lafayette, IN) and the probes were perfused with aCSF or DEX for 24 h. After a 24 h recovery the rats were re-anesthetized and returned to the stereotactic frame. A 400 µm carbon fiber electrode was inserted into the striatum (0.45 mm anterior to bregma, 3.5 mm lateral from bregma, and 5.0 mm below dura), the stimulating electrode was positioned at the MFB, and detection at the outlet and in vivo were completed the in same order as the post-probe procedure in the 4 h study.

2.4.6   Tissue Immunohistochemistry

After the in vivo measurements, the rats were deeply anesthetized and the brain tissues were collected for immunohistochemical analysis.[30] Thin horizontal sections (35 µm) were cut in a cryostat at −21 to −22 °C and labeled together with antibody for tyrosine hydroxylase (TH; 1:1000, Millipore, Temecula, CA) and the DA transporter (DAT; 1:400, Synaptic Systems, Göttingen, Germany). The secondary antibody was goat anti-rabbit IgG-Cy3 or IgG-Cy5 (Invitrogen, Eugene, OR). In another group of rats, probes perfused with DEX-FL were implanted for 4 h. Fluorescence and optical differential interference contrast (DIC) images were acquired with an Olympus BX61 microscope (Olympus; Melville, NY) equipped with a 20× objective. Nonimplanted tissue (from the hemisphere opposite the microdialysis probe) was used

as control tissue. Quantitative image analysis was performed with NIS-Elements Advanced Research version 4.00 software (Nikon Instruments Inc., Melville, NY). Images were batched processed using the "smart threshold function" in the software to automatically set threshold limits and disregard background pixels.

2.4.7   Fluorescent Dexamethasone Procedure

Microdialysis probes were implanted for 4 hr during which dexamethasone fluorescein (10 µM) was perfused through the probe (n=3 rats). Horizontal sections (30 µm) were taken along the probe tract (130 slices per rat). Three random sections from each rat were imaged, thresholded and masked. Using NIS Element Advanced Research software random line measurements were perform in the area defined as a positive fluorescent signal. Nine different line measurements were made from each image for a total of 81 measurements (see Figure 2-8).

2.4.8   Defining TH and DAT Colocalization

Fluorescence microscopy was used to examine the colocalization of tissue labeled for tyrosine hydroxylase (TH) and dopamine transporters (DAT). For each probe track, images of both TH and DAT were collect using sequential mode, allowing for images to be merged and a composite image created. Since it is difficult to visualize the degree of colocalization from a pair of images, an important alternative is to display the intensities of the pairs of homologous pixels in a 2D scatterplot. The two antibodies were analyzed for the degree of colocalization by measuring the equivalent pixel position in each of the acquired images by generating a 2D-scatterplot (Fig. 2-7a). Each axis covers the range of intensities of the fluorophores, in our case

Cy3 and CY5 (respectively, TH and DAT). The scatterplot shows the frequency of occurrence between the pair of intensities which reveals any correlation between the fluorophores. The relationship between the intensities in the two images is calculated by linear regression. The slope of this linear approximation provides the rate of association of the two fluorophores.[134] Following the generation of the scatterplot it is possible to quantitatively evaluate colocalization between the fluorophores (TH and DAT). Values calculated for the scatterplot using NIS Element Advanced Research software include Pearson's Correlation Coefficient (PCC), and Manders' Overlap Coefficient (MOC). Pearson's Correlation and Manders' Overlap are mathematically similar differing in the use of either absolute intensities (Manders') or the deviation from the mean (Pearson's).[134, 135] Pearson's Correlation is well defined and is an accepted means for describing overlap between image pairs. It's computed values are between -1 to 1 with -1 being no overlap, 1 being perfect overlap and 0 representing random distributions between images. Only the similarities of shapes between images are account for not their intensities. PCC is defined as:[136, 137]

$$PCC = \frac{\sum_i (R_i - \bar{R}) * (G_i - \bar{G})}{\sqrt{\sum_i (R_i - \bar{R})^2 * \sum_i (G_i - \bar{G})^2}}$$

where R_i= intensity in red channel, $\bar{R}$= average intensity in red channel, G_i= intensity in green channel and $\bar{G}$= average intensity in green channel.

MOC is also used to describe overlap however this method does not perform any pixel averaging functions like that of PCC therefore values range from 0 to 1. This method is also not sensitive to intensity variations between images. MOC is defined as:[136]

$$MOC = \frac{\sum_1 (R_i * G_i)}{\sqrt{\sum_1 R_i^2 * \sum_i G_i^2}}$$

2.4.9   Statistics

IBM Statistical Package for the Social Sciences (SPSS) 22 software was used for all statistical analysis.

3.0 ENHANCED INTRACRANIAL MICRODIALYSIS BY REDUCTION OF TRAUMATIC PENETRATION INJURY AT THE PROBE TRACK

Dr. Andrea Jaquins-Gerstl contributed the immunohistochemistry and fluorescence microscopy work presented in this chapter.

3.1 INTRODUCTION

Microdialysis is a powerful and popular approach for intracranial chemical monitoring.[1-4] There are several reasons for this. The probes sample a broad array of interesting substances, limited mainly by the molecular weight cutoff of the dialysis membrane. Because the dialysate samples are free of macromolecules, blood, and cellular debris, they are suitable for near real-time analysis by online methods without further sample preparation. Brain dialysate is compatible with a variety of high-performance analytical methods, including HPLC, capillary electrophoresis, and mass spectrometry. Recent enhancements of such methods have produced substantial gains in temporal resolution.[8, 9, 11] The power and utility of microdialysis has spawned

a vast literature on intracranial monitoring in awake, freely moving animals and in human patients with brain injury.[1-4, 8, 9, 11, 16]

Nevertheless, implanting a microdialysis probe causes a traumatic penetration injury in the brain tissue that triggers ischemia, opens the blood–brain barrier, activates astrocytes and microglia, damages neurons, axons and terminals, and leads to scar formation at the probe track.[25-28, 31, 33, 34] This scenario is not unique to microdialysis, as the tissue response also confronts brain–machine interfaces.[42, 47] The penetration injury significantly perturbs the neurochemistry of the tissue from which the dialysate samples are obtained[24, 33, 34, 57] and contributes to the loss in probe patency over time following implantation.[36-40] Thus, our objective is to reduce, if not eventually eliminate, the penetration injury and its deleterious effects on neurochemical monitoring.

Herein, we show that combining a 5-day postimplantation wait period with the continuous retrodialysis of a low-micromolar concentration of dexamethasone vastly reduces both the voltammetric and histological signs of the penetration injury. Dexamethasone (DEX) is a glucocorticoid anti-inflammatory agent. We have previously documented that continuous DEX retrodialysis (DEX$_{retro}$) diminishes the effects of the penetration injury at 4 and 24 h after probe implantation.[33, 34] However, we now show that at 5-days after probe implantation DEX$_{retro}$ reinstates normal evoked dopamine (DA) release activity in the tissue adjacent to the probe, facilitates robust detection of evoked DA release at the probe outlet (i.e., without the aid of a DA uptake inhibitor), establishes quantitative agreement between evoked DA measured simultaneously at the probe outlet and in the tissue next to the probe, reinstates normal immunoreactivity for tyrosine hydroxylase (TH) and the dopamine transporter (DAT) near the probe, and prevents glial scarring at the probe track. Our findings support the conclusion that the

beneficial effects of DEX in this application may be attributed to its actions as an anti-inflammatory agent.

3.2   RESULTS AND DISCUSSION

3.2.1   Experimental Design

Microdialysis probes were implanted unilaterally into the striatum of rats and perfused continuously for 5 days with or without DEX_{retro}. As before,[31] we perfused the probes with 10 μM DEX for the first 24 h after probe implantation and then switched to 2 μM DEX thereafter. Five days after probe implantation, the rats were reanesthetized and returned to a stereotaxic frame, where they remained for the duration of the measurements reported below. A stimulating electrode was placed in the medial forebrain bundle ipsilateral to the microdialysis probe, and a carbon fiber electrode was placed in the striatum at a location 1.0 or 1.5 mm from the microdialysis probe, as specified below. The outlet capillary of the microdialysis probe was threaded into a detection chamber and interfaced to a second carbon fiber microelectrode (Figure 3-1). This setup permits evoked DA responses to be recorded by fast scan cyclic voltammetry (FSCV) simultaneously at the probe outlet and in the tissue adjacent to the probe. The stimulations were applied for 25 s at 45 Hz unless noted otherwise. The 25-s stimulus duration was selected, based on prior work, to match the response time of the microdialysis probes (see Figure 6 of ref 23).
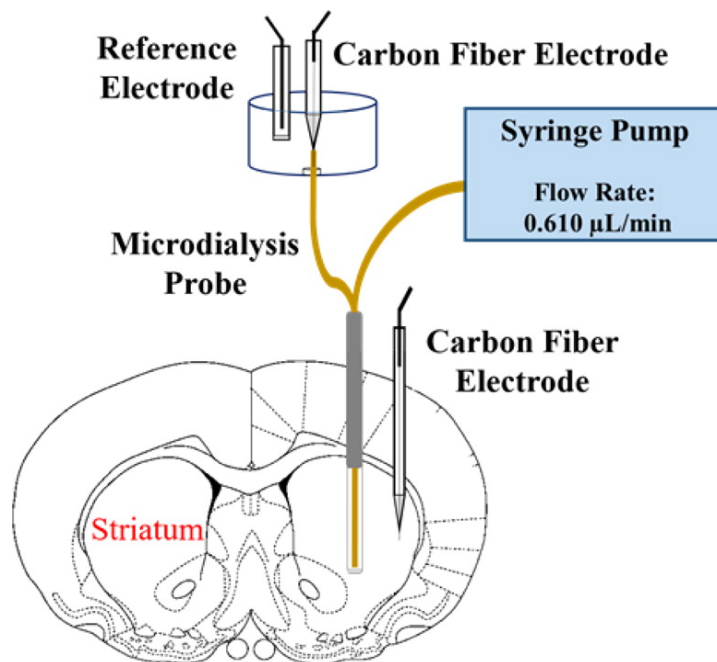
Figure 3-1.
Five days after implanting a microdialysis probe into the striatum, a carbon fiber electrode was placed 1.5 mm from the probe. The outlet of the microdialysis probe was threaded into a detection chamber and interfaced to a second carbon fiber electrode. This arrangement allows simultaneous recordings of evoked DA release at the probe outlet and in the tissue next to the probe.

In the figures that follow, the time axes for responses recorded at the probe outlet are corrected to account for the time required for the dialysate to travel the length of the outlet capillary. DA concentrations recorded at the probe outlet have not been corrected for probe recovery. DEX_{retro} had no significant effect on evoked DA responses recorded in the striatal tissue 1.5 mm from the microdialysis probes (Figure 3-S1).

3.2.2   Evoked DA Responses Recorded at the Probe Outlet

Figure 3-2 compares evoked DA responses recorded at the probe outlet 5-days after implantation with (red) or without (blue) continuous DEX_{retro}. Without DEX_{retro}, there was no

response (0 responses from 6 rats). With DEX_{retro}, however, the response was both robust and reproducible (6 responses from 6 rats).

In our view, the evoked response recorded at the probe outlet after 5 days of DEX_{retro} (Figure 3-2, red) represents a major step forward in our efforts to reduce, if not eventually eliminate, the effects of the penetration injury. During our prior studies at 4 and 24 h after probe implantation,[23, 34, 40, 58] we have never observed a pre-nomifensine response by voltammetry at the probe outlet, either with or with DEX_{retro}. The requirement for uptake inhibition stems from the tissue response, which abolishes evoked DA release in the tissue adjacent to the probe.[24, 33, 34, 57] Figure 3-2 is the first of several observations reported herein indicating a vast reduction in the

penetration injury by the combination of DEX retrodialysis and a sufficient postimplantation wait interval.

To permit comparisons with evoked responses previously measured at 4 and 24 h after probe implantation,[34] we recorded additional responses at the probe outlet after treating rats first with nomifensine (20 mg/kg i.p.), a DAT inhibitor, and then with raclopride (2 mg/kg i.p.), a dopamine D2 receptor antagonist (Figure 3-3 A,B). Figures 3-3 C and D summarize the maximum amplitude and the area under the curve (AUC) of the evoked responses. We performed the AUC analysis because the temporal profile of the outlet responses was somewhat altered after the 5-day wait interval (see Figures 3-S2 and 3-S3). The amplitude of the pre-nomifensine response with DEX$_{retro}$ is significant (one-tailed t test). DEX$_{retro}$ significantly increased the post-nomifensine and post-nomifensine/raclopride amplitudes and AUCs (ANOVA; details are in the figure legend).
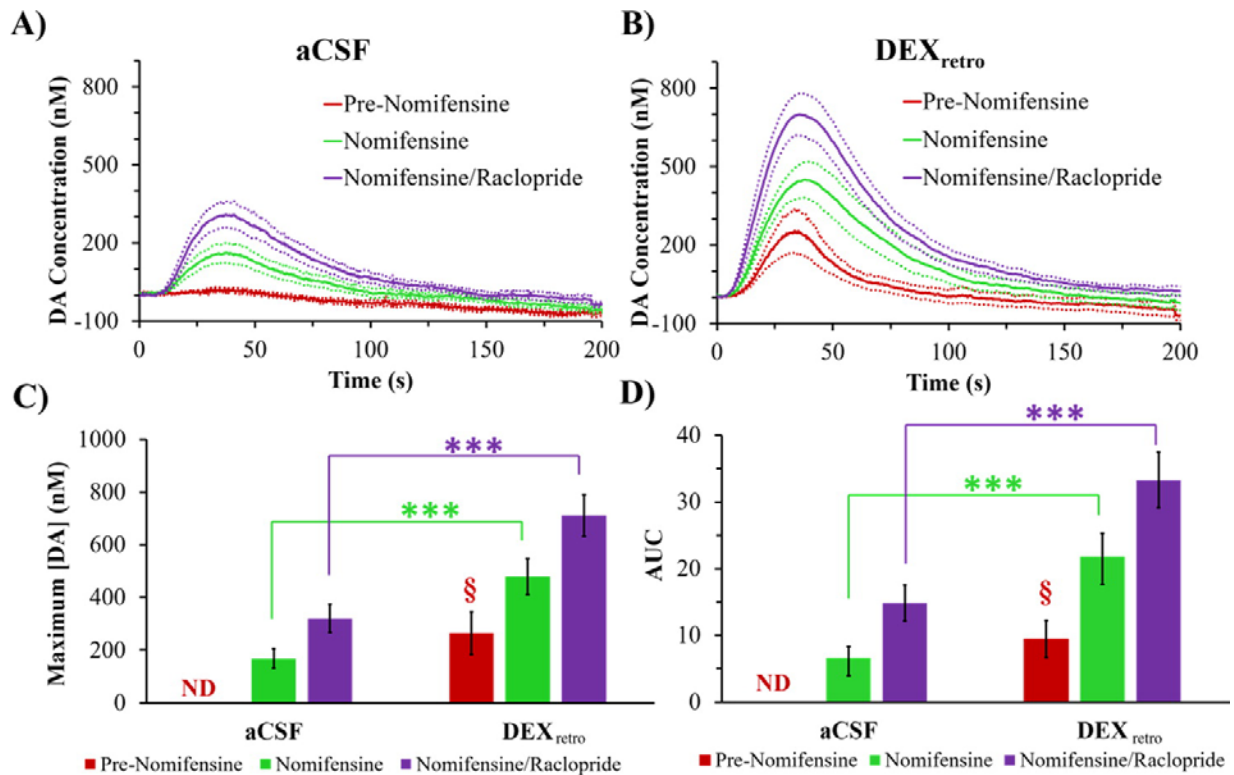
Figure 3-3.
Evoked DA responses (mean ± SEM, n = 6 per group) measured at the outlet of microdialysis probes perfused with (A) aCSF or (B) DEX. DA was measured before nomifensine (red), after nomifensine (green), and then again after raclopride (purple). The amplitudes and AUCs are analyzed in C and D, respectively (ND = not detected). The 5 day DEX_{retro} pre-nomifensine responses are significant when compared to zero (amplitude, $t(5) = 3.27$; AUC, $t(5) = 3.40$; one-tailed t test); § = $p < 0.05$. The amplitude and AUC results underwent 2-way ANOVA with treatment (aCSF, DEX) and drug (nomifensine and nomifensine/raclopride; repeated measurements) as factors. (C) Treatment ($F(1,10) = 19.93$, $p < 0.005$) and drug ($F(1,10) = 26.96$, $p < 0.001$) are significant factors: no significant interaction. (D) Treatment ($F(1,10) = 18.25$, $p < 0.005$) and drug ($F(1,10) = 21.96$, $p < 0.001$) are significant factors: no significant interaction. Asterisks report posthoc pairwise comparisons. ***$p < 0.005$.

Without DEX_{retro}, evoked responses at the outlet of probes implanted in animals treated with nomifensine and then with raclopride exhibited significant decreases in amplitude and AUC between 4 and 24 h after implantation and showed no tendency to rebound after 5 days (Figure 3-4). However, with DEX_{retro} there were no such declines (Figure 3-4). Instead, DEX_{retro} stabilized the postdrug responses, which exhibited only minor differences among the 4 h, 24 h,

and 5 day time points. It is important to emphasize that different groups of animals were used for each time point and for each condition (aCSF and DEX).
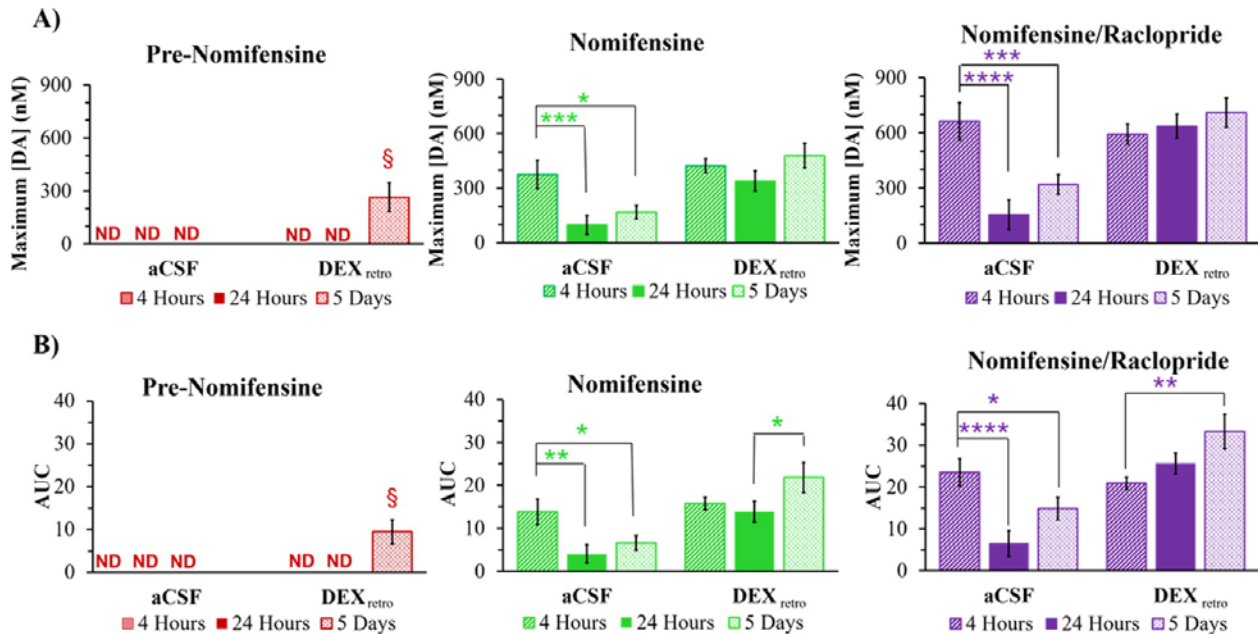
Figure 3-4.
(A) Amplitude and (B) AUC (mean ± SEM, n = 6 per group) of evoked DA responses detected at the probe outlet (ND = not detected). The data at 4 h, 24 h, and 5 days are from separate groups of rats. The data at 4 and 24 h are from a prior study.[34] The 5 day DEX$_{retro}$ pre-nomifensine responses are statistically significant compared to zero (amplitude, t(5) = 3.27; AUC, t(5) = 3.40; one-tailed t test, § = p < 0.05). Statistical analysis of the nomifensine and nomifensine/raclopride panels was by three-way ANOVA with time (4 h, 24 h, and 5 days), treatment (aCSF and DEX), and drug (nomifensine and nomifensine/raclopride; repeated measurements). Time (amp F(2,30) = 5.69, p < 0.01, AUC F(2,30) = 4.66, p < 0.05), treatment (amp F(1,30) = 21.8, p < 0.001, AUC F(1,30) = 28.1, p < 0.001), and drug (amp F(1,30) = 100, p < 0.001, AUC F(1,30) = 57.2, p < 0.001) are significant factors. Interactions are significant. Asterisks indicate posthoc pairwise comparisons. *p < 0.05, **p < 0.01, ***p < 0.005, and ****p < 0.001.

3.2.3   Comparison of Outlet and In Vivo Responses

Figure 3-5 compares the amplitudes of responses recorded at the probe outlet after 5 days of continuous DEX$_{retro}$ (Figure 3-5A) to the amplitudes of in vivo responses recorded in the tissue adjacent to the probe (the probe–electrode separation was 1.5 mm, Figure 3-5B).

Responses at the outlet are in the 200–700 nM range, whereas the in vivo responses are in the 5–20 µM range. Thus, the in vivo recovery ratio of evoked DA is on the order of 5%.
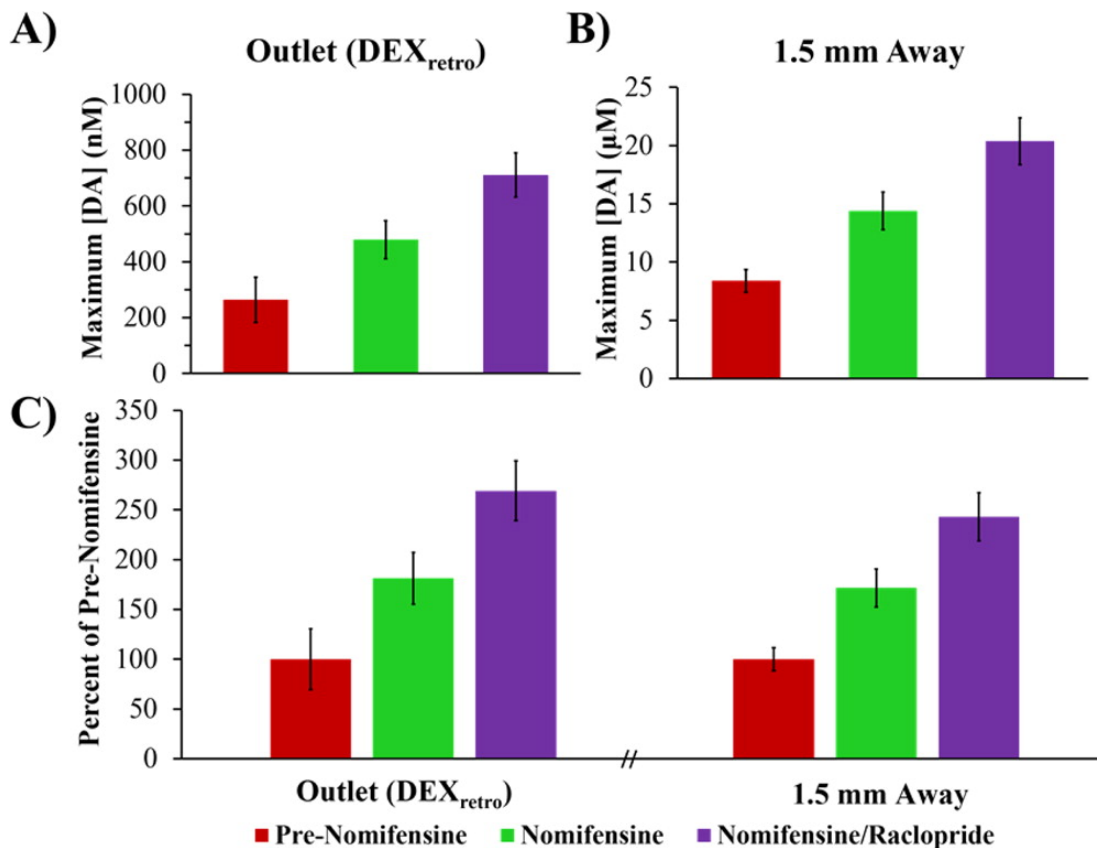
Figure 3-5.
Evoked DA (mean ± SEM) measured (A) at the probe outlet after 5 days of DEX_{retro} (n = 6, data from Figure 3-3C) and (B) directly in the striatal tissue (n = 18: Figure 3-S1 data combined). (C) Response amplitudes normalized with respect to the pre-nomifensine amplitude. Statistical analysis was by a two-way ANOVA for location (outlet, tissue) and drug (nomifensine, nomifensine/raclopride; repeated measurements). Only the drug was a significant factor $(F(1,22) = 16.99, p < 0.001)$: neither location nor interaction were significant.

Because of our new ability to record outlet responses without the aid of nomifensine, it is now possible to report the amplitude of both the outlet and in vivo responses normalized with respect to their pre-nomifensine amplitudes (Figure 3-5C). We found no significant differences between the normalized outlet and normalized in vivo responses (statistical details are in the

figure legend). Thus, Figure 3-5C indicates essentially perfect quantitative agreement between the outlet and in vivo responses.

Figure 3-5C represents the first occasion upon which we have been able to report near-perfect quantitative agreement between evoked responses recorded at the outlet of probes and in the tissue adjacent to the probes. Prior studies have consistently found that uptake inhibition increases the in vivo recovery of DA.[11, 22-24, 34, 40, 58, 119, 138] On theoretical grounds, we suggested that the impact of DAT inhibition on the in vivo recovery of DA is indicative of the presence of a zone of disrupted tissue adjacent to the probe wherein DA uptake exceeds DA release.[58-60] Figure 3-5 strongly suggests that this zone of disrupted tissue is no longer present under the conditions of these measurements, strongly suggesting that the combination of a 5-day postimplantation interval with continuous retrodialysis of DEX vastly reduces the effects of the penetration injury.

3.2.4   In Vivo Voltammetry Next to the Probe

A second series of experiments was performed to directly assess the impact of DEX_{retro} on evoked DA release activity in the tissue surrounding the probe. Five days after probe implantation, evoked DA responses were recorded in vivo with two carbon fiber microelectrodes. As in a prior study,[34] one electrode was placed 1 mm from the probe, and the other was placed 100 μm from the probe (Figure 3-6A and C). Without DEX_{retro}, the evoked responses 100 μm from the probe were either abolished or significantly reduced (Figure 3-S4), consistent with prior observations at 4 and 24 h after implantation.[34] However, with DEX_{retro} there were no significant differences between the response amplitudes measured 1 mm and 100 μm from the probe (Figure 3-6B).
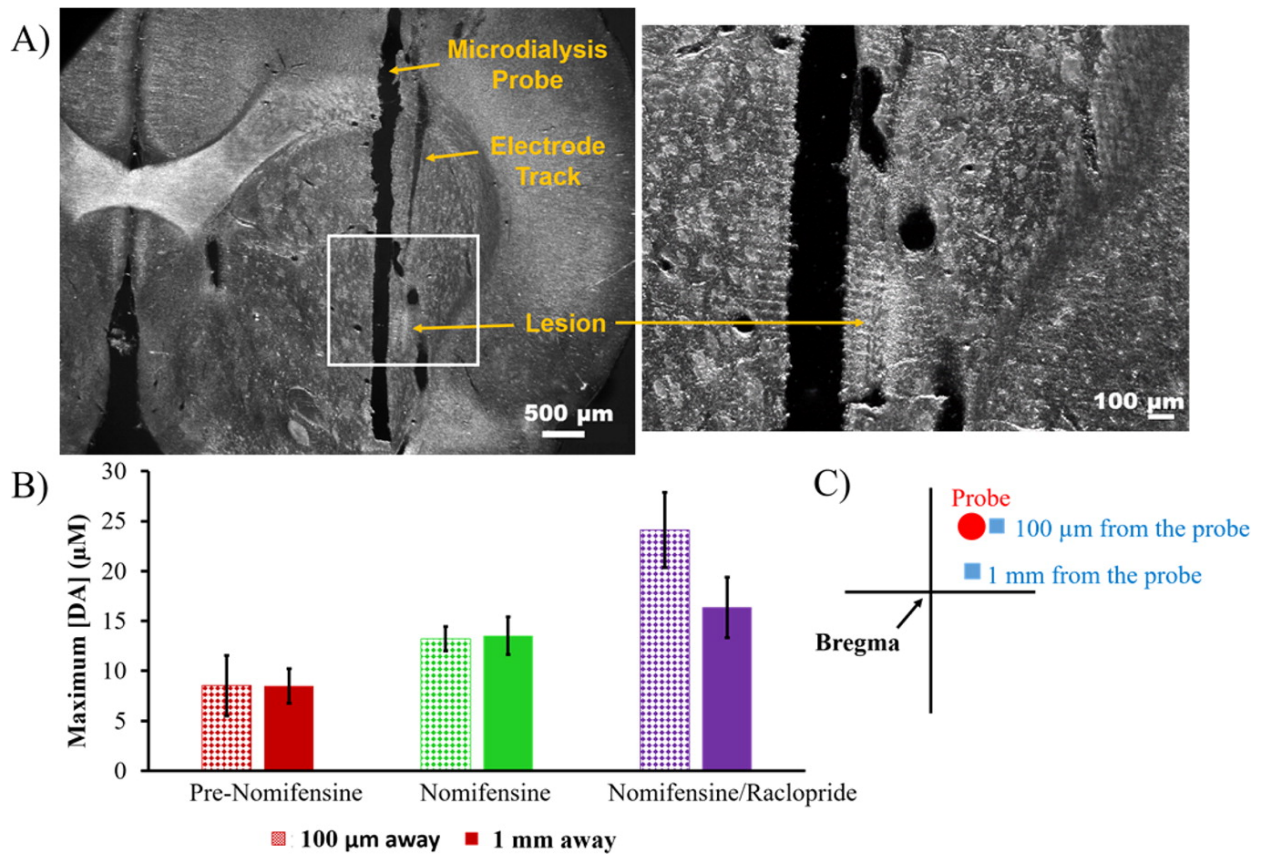
Figure 3-6.
(A) Electrolytic lesion confirmed the placement of a carbon fiber electrode 100 μm from the microdialysis probe by applying a current of 20 μA for 5 s to the electrode. The white box in the left image is magnified on the right. Scale bars are 500 μm (left) and 100 μm (right). (B) Evoked release (mean ± SEM, n = 4 per group) measured 100 μm (pattern) and 1 mm (solid) away from the probe after 5 days of DEX_{retro} (responses in Figure 3-S4). Statistical analysis was by two-way ANOVA for the drug (pre-nomifensine, nomifensine, and nomifensine/raclopride; repeated measurements) and location (100 μm, 1 mm). The drug was significant ($F(1,6) = 23.02$, $p < 0.005$), while the location and the interaction were not significant factors. (C) Schematic of voltammetry next to the probe with the electrodes represented by blue boxes and the probe by a red circle. The adjacent electrode was implanted at a 5° angle to allow the tip of the electrode to be placed 100 μm from the probe.

In our prior study at 4 and 24 h after probe implantation,[34] evoked responses in close proximity to probes perfused with DEX (probe–electrode separation of 100 μm) were detectable but significantly lower in amplitude than normal. Thus, Figure 3-6 clearly indicates that combining a 5-day postimplantation wait time with continuous DEX_{retro} leads to a reinstatement of normal evoked DA activity in close proximity to the probe.

3.2.5   DA Kinetic Analysis

Additional responses were recorded 1 mm and 100 μm from the probe using a 3-s stimulus delivered at 60 Hz. The responses underwent kinetic analysis with the numerical model of Walters et al.[139] The model provides excellent fits to responses recorded 100 μm away with DEX$_{retro}$ and to responses 1 mm away either with or without DEX$_{retro}$ (Figure 3-7). Moreover, there were no significant differences between the kinetic parameters providing best fits to these responses (Table 3-S1). Thus, after 5 days of continuous DEX$_{retro}$, we detect no significant alterations in the kinetics of DA release, uptake, or transport in close proximity to the microdialysis probes.
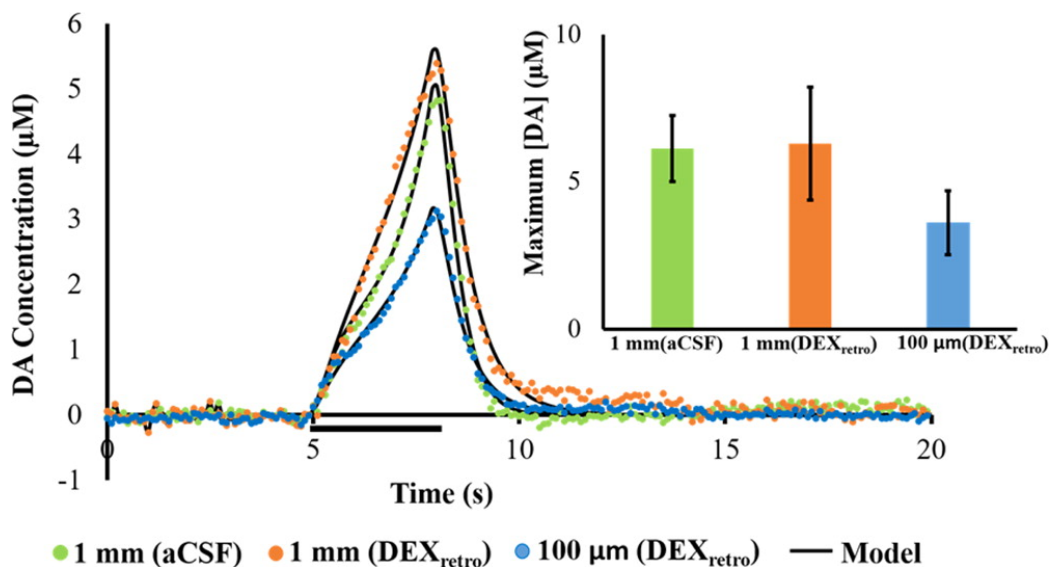
Figure 3-7.
Evoked release (mean, n = 4 per group) measured 1 mm away without (green) and with (orange) DEX$_{retro}$, and 100 μm from the probe with DEX$_{retro}$ (blue): error bars are omitted for clarity. The stimulus in this case was for 3 s (marked by the horizontal black bar) at 60 Hz. The black lines report the average of the model fits to each individual response. The average values of the kinetic parameters (see Table 3-S1) exhibited no significant differences (multivariate ANOVA, Pillai's Trace). The inset shows the response amplitudes, which are not statistically different (one-way ANOVA).

3.2.6 Immunohistochemistry

Horizontal tissue sections (35 μm thick) containing the probe tracks were immunolabeled for TH and DAT, two widely accepted markers of DA terminals (Figures 3-S5 and 3-S6), and for ED-1, a marker of microglia and macrophages.[140, 141] The images were quantified by the pixel counting routines built into Metamorph (see Methods).

Images of TH and DAT immunoreactivity in tissues surrounding the tracks of probes perfused for 5 days with or without DEX_{retro} were indistinguishable from each other and from images of nonimplanted control tissue (Figure 3-8). All images exhibited extensive immunoreactivity except in locations corresponding to myelinated axon bundles, blood vessels, and the probe tracks: all such features were clearly visible in DIC images of the same tissues. Quantitative image analysis produced no significant differences among these images (ANOVA details are in the figure legend). Images at higher magnification (40, 60, and 100×) indicate punctate TH labeling up to the very edge of the probe tracks (Figure 3-S7).
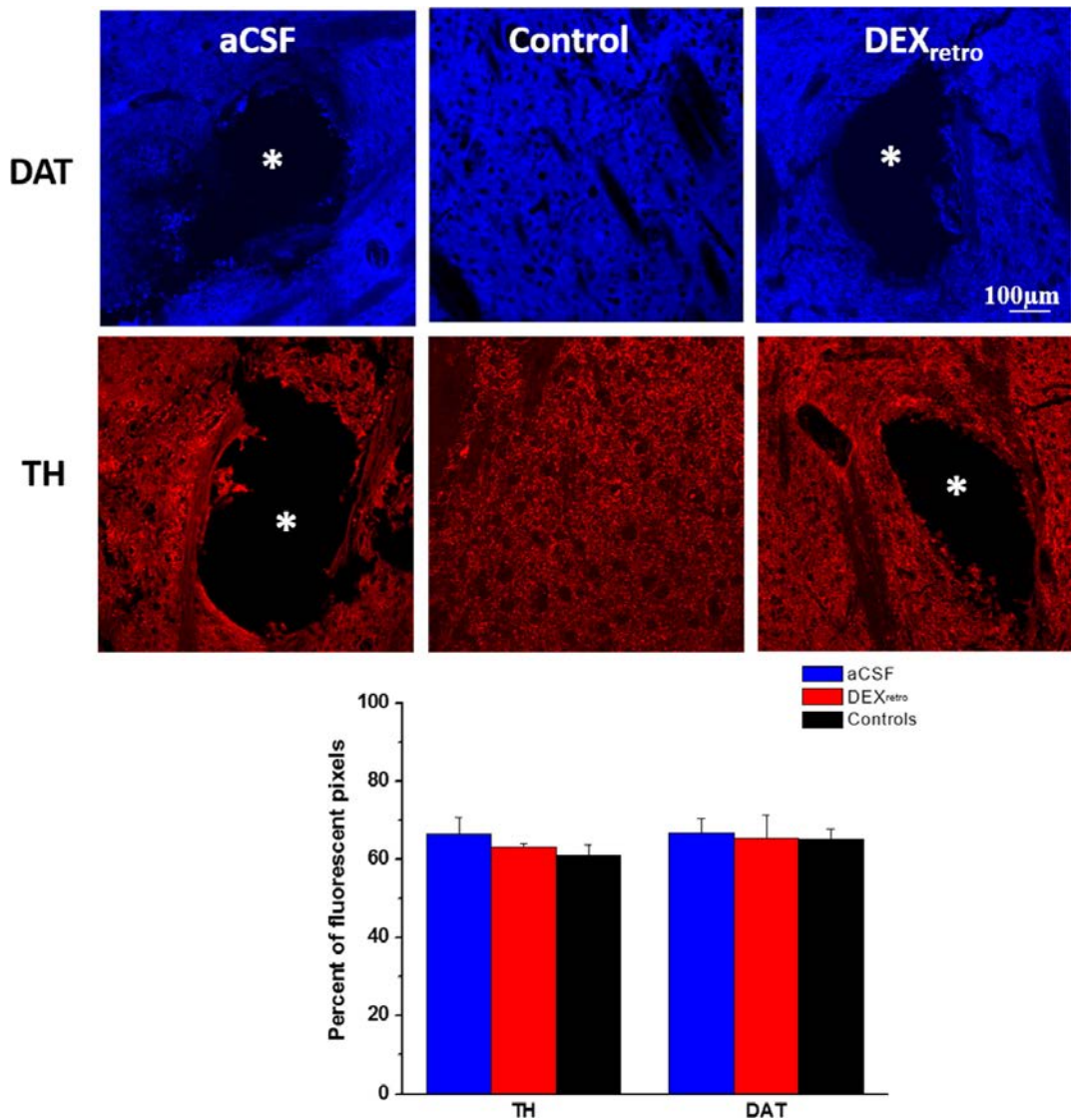
Figure 3-8.
DAT (blue) and TH (red) immunoreactivity in tissue sections containing tracks of probes perfused without (left) and with (right) DEX$_{retro}$ for 5 days and in sections of nonimplanted control tissue (center). Asterisks mark the center of the probe tracks. Scale bar = 100 μm. The bottom graph shows the quantification of the fluorescent pixels for each marker: the probe tracks were excluded from the regions of interest. In a 2-way ANOVA of treatment (aCSF, DEX, and control) and antibody (TH and DAT), neither the treatment nor the antibody was a significant factor.

These findings stand in stark contrast to our observations of marked disruptions of TH immunoreactivity near probe tracks at 4 and 24 h after implantation, especially when DEX$_{retro}$ was absent.[33, 34] The reinstatement of normal TH and DAT immunoreactivity appears to be in excellent agreement with the reinstatement of evoked DA activity in close proximity to the

probes (Figures 3-2 through 3-6). However, images of TH and DAT immunoreactivity near probes perfused without DEX also appear similarly normal, which comes as a surprise because evoked DA release adjacent to and at the outlet of these probes show major disruptions (Figure 3-2 and 3-S4). Thus, the ability of 5 days of DEX$_{retro}$ to reinstate normal evoked DA release activity cannot be attributed solely to the reinstatement of normal TH and DAT immunoreactivity.

During previous work, we showed that 5 days of DEX$_{retro}$ is highly effective at suppressing the activation of astrocytes and preventing the formation of a glial scar at the probe track[31] (see also Figure 3-S8). Here, we document that DEX$_{retro}$ is likewise highly effective at suppressing the activation of microglia (Figure 3-9). Thus, our histochemical findings suggest that the reinstatement of normal TH and DAT immunoreactivity in close proximity to the probes is necessary but not sufficient for reinstatement of evoked DA release activity, as suppression of gliosis and scar formation is also critical.
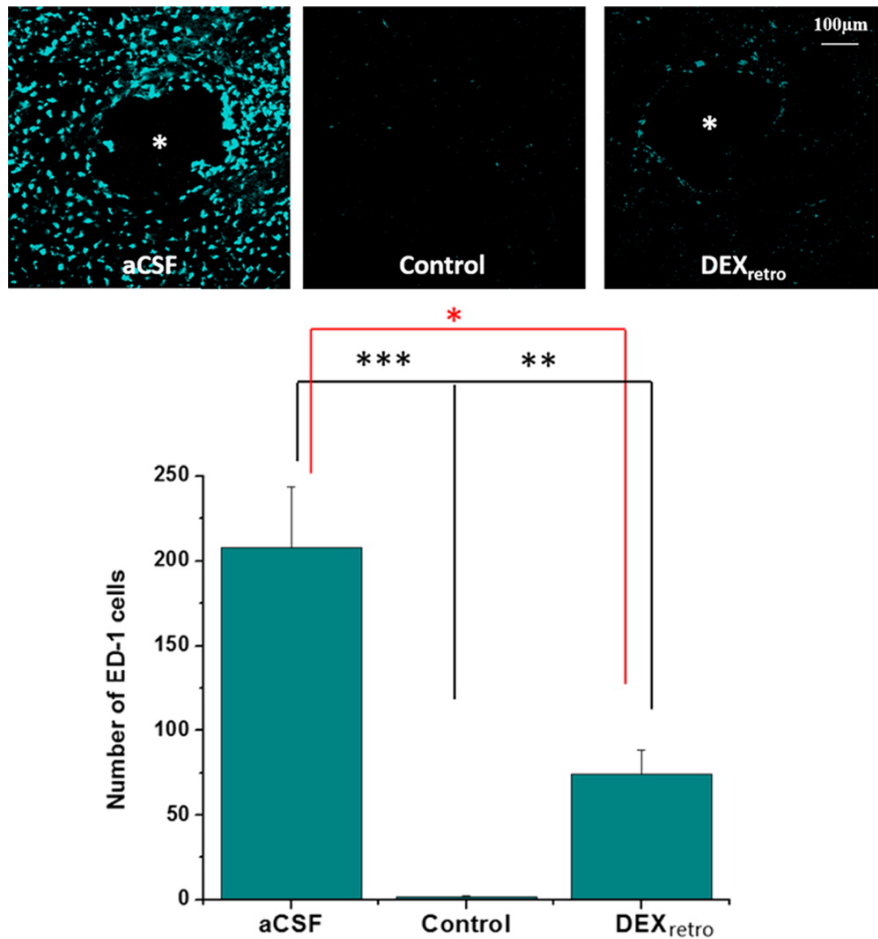
Figure 3-9.
Immunoreactivity for ED-1 in sections containing the tracks of probes without (left) or with DEX$_{retro}$ (right) and sections from nonimplanted control tissue (center) (asterisks represent the center of the probe track, scale bar = 100 μm). The bottom graph compares counts of ED-1 positive cells in area matched sections of aCSF, DEX$_{retro}$, and control tissue. Statistical analysis was by one-way ANOVA, $F(2,22) = 21.560$, $p < 0.001$. Asterisks report the posthoc tests (Games–Howell). $*p < 0.05$, $**p < 0.01$, and $***p < 0.005$.

3.3   CONCLUSIONS

Our findings confirm that combining a 5-day postimplantation wait period with concurrent and continuous DEX$_{retro}$ vastly reduces the effects of the penetration injury at the microdialysis probe track. This enables the recording of robust and reproducible evoked DA responses at the probe outlet, which can be attributed to a reinstatement of normal evoked DA

activity in the tissues in close proximity to the probes. Furthermore, the reinstatement of normal evoked DA activity adjacent to the probes blocked nomifensine's ability to alter the in vivo microdialysis recovery of DA, a phenomenon previously attributed to a zone of disrupted tissue at the probe track.[58-60] Overall, combining a 5-day postimplant interval with DEX$_{retro}$ brings evoked DA responses at the probe outlet into excellent quantitative agreement with in vivo responses. In our line of investigation into these matters, this is the first occasion upon which we have observed such excellent agreement. The efficacy of DEX in this work appears to be due to its anti-inflammatory actions, as markers of DA terminals appear normal upon histochemical examination after 5 days regardless of whether DEX$_{retro}$ was performed. Thus, the reinstatement of normal TH and DAT immunoreactivity, accepted markers of DA terminals, at the probe track is necessary but not sufficient for the reinstatement of normal evoked DA release activity, as suppression of gliosis and scarring is also critical.

Our conclusion that the postimplantation wait period is an important contributor to the reinstatement of DA function in close proximity to the probe concurs with the work of Di Chiara and colleagues.[142-144] In their work, histology after several weeks of repetitive probe insertions through a guide cannula shows the presence of TH-positive varicosities and no signs of necrosis.[142-144] This concurs with our finding (Figure 3-8) that DA terminals appear normal as early as 5 days after probe implantation. However, our findings show that gliosis is also an important consideration.

The choice of dexamethasone as an anti-inflammatory agent raises some potentially contentious issues as steroids have their own neurochemical actions.[145] During this work, we found no evidence that dexamethasone altered evoked DA release, which is consistent with a body of literature indicating that DA systems are not highly sensitive to steroids.[146-150] Thus, the

effects of DEX described above appear to reflect anti-inflammatory rather than neurochemical mechanisms. However, DEX might prove unsuitable in some microdialysis investigations of other neurochemical systems that exhibit greater sensitivity to steroids. In this light, it is relevant to mention that alternatives to DEX are available, including nonsteroidal anti-inflammatory drugs. It is also worth mentioning that retrodialysis, even over extended time periods, involves truly minuscule quantities of drug: the total amount of dexamethasone delivered via retrodialysis during the experiments reported here is less 20 nanomoles. While alternative anti-inflammatory strategies (agent, dose, duration, etc.) remain to be explored, we believe that this work clearly establishes the overall principle of anti-inflammatory enhanced microdialysis.

3.4   METHODS

All use of animals was approved by the University of Pittsburgh Institutional Animal Care and Use Committee. Some of the methods and procedures employed for the present study have been previously described.[11, 34]

3.4.1   Reagents and Solutions

All solutions were prepared with ultrapure water (Nanopure; Barnstead, Dubuque, IA). Artificial cerebrospinal fluid (aCSF: 142 mM NaCl, 1.2 mM $CaCl_2$, 2.7 mM KCl, 1.0 mM $MgCl_2$, and 2.0 mM NaH_2PO_4, pH 7.4) was used for voltammetric DA calibration and as the perfusion fluid of the microdialysis probe. Dexamethasone sodium phosphate (APP Pharmaceuticals LLC, Schaumburg, IL) was diluted in aCSF. The perfusion fluids for

48

microdialysis were filtered with Nalgene sterile filter units (Fisher, Pittsburgh, PA; PES 0.2 μm pores). Nomifensine maleate and S(−)raclopride (+)-tartrate (Sigma-Aldrich, St. Louis, MO) were dissolved in phosphate-buffered saline (PBS: 137 mM NaCl, 2.7 mM KCl, 1.47 mM KH$_2$PO$_4$, and 10 mM Na$_2$HPO$_4$, pH 7.4) and administered at 20 mg/kg and 2 mg/kg (i.p.), respectively. DA (Sigma-Aldrich, St. Louis, MO) standards were prepared in N$_2$-purged aCSF for electrode calibration.

3.4.2 Microdialysis Probes and DEX$_{retro}$

Concentric-style microdialysis probes (300 μm in diameter, 4 mm membrane length) were built in-house (13 kDa MWCO Spectra/Por hollow fiber, Spectrum Laboratories Inc. Rancho, Dominquez, CA). Fused silica capillaries (75 μm I.D., 150 μm O.D., Polymicro Technologies, Phoenix, AZ) were used for the inlet and outlet lines. The probe inlet was connected to a syringe pump (Harvard Apparatus, Holliston, MA) running at 0.610 μL/min. The outlet capillary was 10 cm long. Prior to use, the probes were soaked in 70% ethanol and then immersed in and flushed with filtered perfusion fluid for several hours before implantation (aCSF or aCSF with DEX). During procedures involving DEX$_{retro}$, the probe was perfused first with 10 μM DEX for 24 h and thereafter with 2 μM DEX, as previously described.[31] When DEX was used, it was added to the perfusion fluid prior to probe implantation.

3.4.3 Voltammetry

Carbon fiber electrodes were constructed by placing a single carbon fiber (7 μm diameter, T650, Cytec Carbon Fibers LLC., Piedmont, SC) in a borosilicate capillary (0.58 mm I.D., 1.0

mm O.D., Sutter Instruments, Novato, CA), pulling the capillary to a fine tip (Narishing Tokyo, Japan), sealing the tip with a low viscosity epoxy (Spurr Epoxy, Polysciences Inc., Warrington, PA), and trimming the exposed fiber to 400 or 800 μm for in vivo and outlet recordings, respectively. FSCV was performed with a potentiostat (EI-400, Ensman Instruments, Bloomington, IN) and CV Tarheel software (version 4.3, Michael Heien, University of Arizona, Tucson AZ). The waveform began at the rest potential of 0 V, scanned to +1.0 V, then to −0.5 V, and back to the rest potential at 400 V/s: potentials are vs Ag/AgCl. Scans were performed at 2.5 Hz during the 25-s stimulations and 10 Hz for the 3-s stimulations. The 800 μm outlet electrodes were pretreated (0–2 at 200 V/s for 3 s) 10 min before each stimulus or calibration procedure. This pretreatment improves sensitivity but also causes some drift in the FSCV background signal, which is noticeable at low DA concentrations (~20–30 nM).[23] To minimize the drift, the pretreatment was followed by application of the FSCV waveform at 60 Hz for 120 s.

3.4.4 Voltammetry at the Microdialysis Probe Outlet

The outlet capillary was passed through the floor of a Plexiglas electrochemical cell. The microelectrode for FSCV at the outlet was inserted into the capillary end with a miniature micromanipulator (Fine Science Tools, Foster City, CA). To confirm the performance of the probe and the electrode, calibration was performed by exposing the probe to a 10 μM DA solution for 30 s prior to animal use.

3.4.5   Surgical and Stimulation Procedures

Prior to surgery, rats (male Sprague–Dawley, 250–350 g, Charles River, Raleigh, NC) were acclimated overnight to a Raturn Microdialysis Bowl (MD-1404, BASI, West Lafayette, IN). The next day, the rats were anesthetized with isoflurane (5% induction, 2.5% maintenance) and implanted with microdialysis probes following aseptic stereotaxic surgical technique. Using flat skull coordinates,[151] the probes were slowly lowered into the striatum (1.6 mm anterior, 2.5 mm lateral from bregma, and 7.0 mm below the dura) at 5 μm/s using a micropositioner (David Kopf Instruments, Tujunga, CA). Probes were secured with bone screws and acrylic cement and the incision was closed with sutures (there was no guide cannula). Anesthesia was removed and animals were returned to the Raturn system and given free access to food and water.

After 5 days, the rats were reanesthetized and returned to the stereotaxic frame, where they remained for the duration of all procedures. A reference electrode was contacted to the brain surface with a salt bridge, a carbon fiber microelectrode was inserted into the striatum 1.5 mm away from the probe (0.45 mm anterior to bregma, 3.5 mm lateral from bregma, and 5.0 mm below dura), and a bipolar stimulating electrode was lowered into the medial forebrain bundle ipsilateral to the probe and carbon fiber microelectrode (4.3 mm posterior from bregma, 1.2 mm lateral from midline, and 7.2 mm below the dura). The stimulus waveform was a biphasic, square wave with constant current pulses (300 μA pulse height and 4 ms pulse width). The waveform was delivered for 25 s at 45 Hz or 3 s at 60 Hz. Nomifensine and raclopride were sequentially administered (i.p.), and evoked DA responses were recorded 20 min after each drug administration. A second series of evoked responses were recorded in the tissue next to the probes with carbon fiber electrodes placed 1 mm and 100 μm from the probes, as previously described.[34]

At the end of the experiment, while the rats were deeply anesthetized, the locations of the carbon fiber electrodes were marked with a current lesion (20 μA for 5 s) just before the rats were perfused through the heart to preserve the brain for subsequent analysis.[31]

3.4.6   Area under the Curve (AUC) Analysis

The responses measured at the probe outlet (black line, Figure 3-S3) underwent an AUC analysis. If the response exhibited baseline drift, as discussed above, the drift was measured and subtracted (purple line, Figure 3-S3). Next, we applied the "hang-up" correction described elsewhere[139] (green line, Figure 3-S3). The AUC was determined with MATLAB's trapezoidal integration function in units of micromolar and seconds.

3.4.7   Immunohistochemistry

Horizontal tissue sections (35 μm thick) were prepared in a cryostat and stored at −20 °C until further use. Tissue sections were hydrated in PBS, blocked with 20% normal goat serum, 1% bovine serum albumin, and 0.3% Triton X (Sigma) in PBS (2.5 h). Sections were then incubated with primary antibodies for TH (1.5:1000, Millipore, Temecula, CA), DAT (1:400, Synaptic Systems, Göttingen, Germany), or ED-1 (for activated microglia/macrophages, CD68, 1:100, AbD Serotec, Raleigh, NC). Secondary antibodies were goat anti-rabbit IgG, CY3 (Invitrogen, USA) for TH, while ED-1 and DAT used goat anti-rabbit IgG Cy5 (Invitrogen, USA). Secondary antibodies were diluted 1:1000 in blocking solution. Sections were rinsed in PBS (3 × 5 min) and coverslips added with Fluoromount-G (Southern Biotechnology Associates, Birmingham, Alabama).

3.4.8 Fluorescence Microscopy and Image Analysis

Fluorescence microscopy (Olympus BX61, Olympus; Melville, NY) was performed with a 20, 40, 60, and 100× objective using appropriate filter sets (Chroma Technology; Rockingham, VT). The Metamorph/Fluor 7.1 software package (Universal Imaging Corporation; Molecular Devices) was used to collect, threshold, analyze, and quantify the images. The numbers of ED-1 positive cells in the section of the tissue surrounding the microdialysis track were counted. The number of fluorescent pixels in the TH and DAT images was expressed as a percent of pixels in the region of interest, which excluded the probe track. A minimum of 3 animals per group with 3 slices per brain were used for the statistical analysis.

3.4.9 Statistics

IBM Statistical Package for the Social Sciences (SPSS) 22 software was used for all statistical analysis. For ANOVA, SPSS was used to check for parameter normality and equality of variance. For statistical significance, $p < 0.05$ was used for all tests.

3.5   SUPPORTING INFORMATION
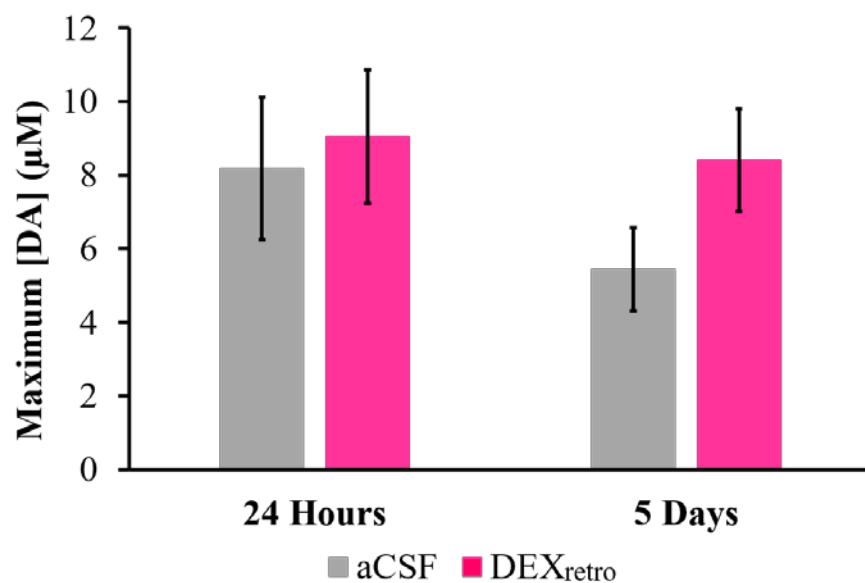
Figure 3-S1.
Amplitude (mean ± SEM, n = 6 per group) of evoked responses measured with FSCV at microelectrodes placed in the striatum 1.5 mm away from the microdialysis probes. A two-way ANOVA was performed with time (24 hr, 5 days) and treatment (aCSF, DEX) as the classifications: time, treatment, and interaction were not significant factors ($p > 0.05$).
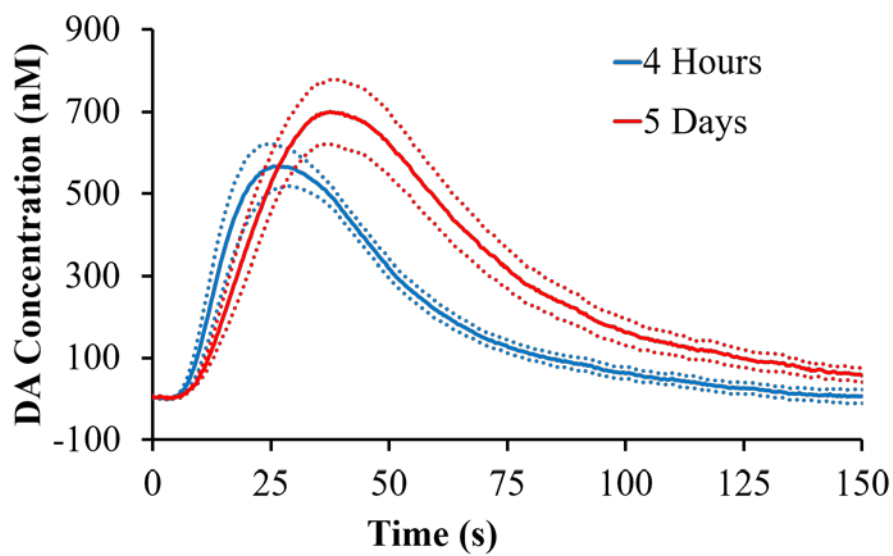
Figure 3-S2.
Evoked responses (mean ± SEM, n = 6 per group) measured after administration of nomifensine and raclopride at the microdialysis probe outlet 4 hr (blue) and 5 days (red) after probe implantation. This data is a representation of the notably broader responses observed after 5 days. The exact reasons underlying the changes in the temporal features of the response over time are unknown.
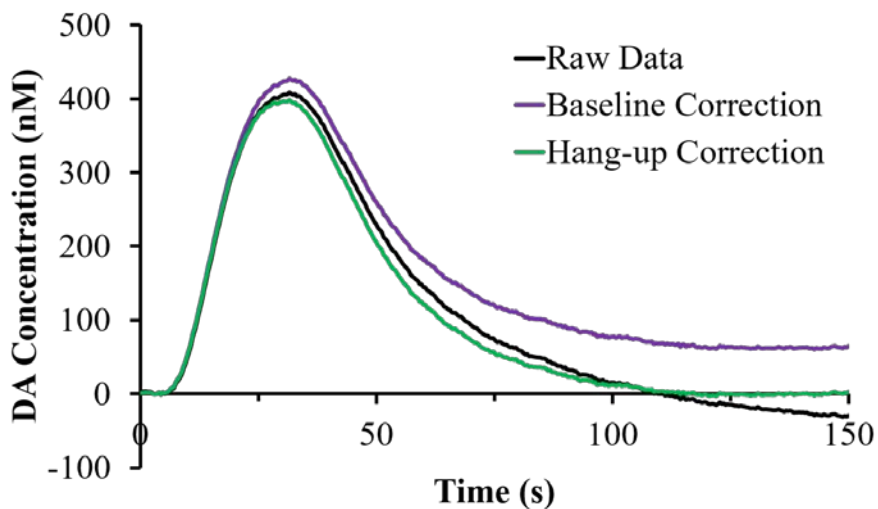
Figure 3-S3.
A representative data set to illustrate the area-under-the-curve procedure explained in the methods section. The raw data (black) exhibits baseline drift, which is corrected by subtraction (purple). The hang-up correction procedure[139] is applied after the baseline subtraction (green). The area under the green curve is determined by numerical integration.
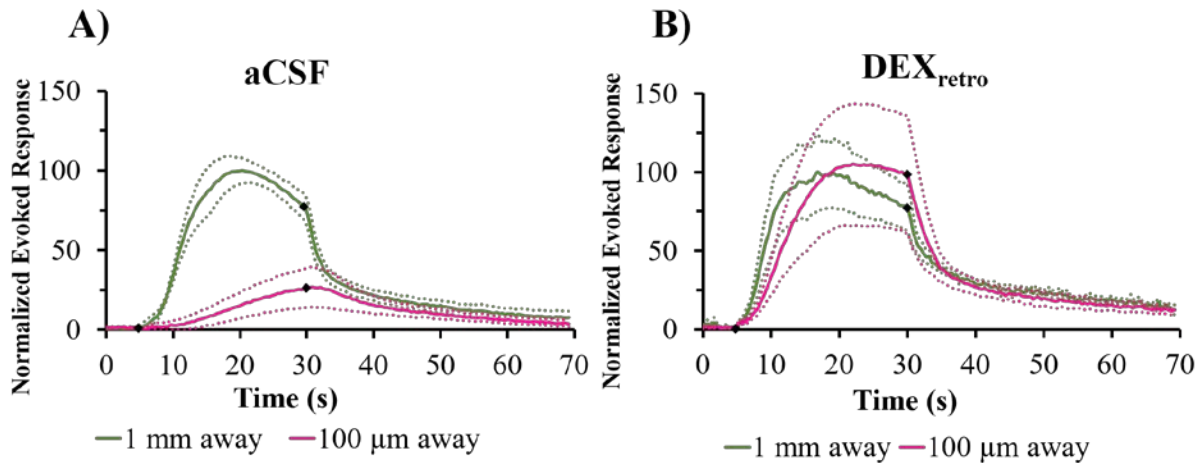
Figure 3-S4.

Evoked responses (mean ± SEM, n=4 per group) to a pre-nomifensine stimulation measured simultaneously at two carbon fiber electrodes in the striatum. Black diamonds mark the start and end of stimulation. The curves are represented as percentage of the 1 mm away response (green line) for both A) aCSF and B) DEX$_{retro}$ treated rats. With DEX$_{retro}$ the responses were comparable (see Figure 3-6B). However, without DEX$_{retro}$ evoked dopamine was either abolished (3 of 4 rats) or significantly reduced (1 of 4 rats) adjacent to the probe (pink line) (t(5)=0.347, p<0.005). In 1 of the 4 animals without DEX$_{retro}$ the response was reduced but measurable adjacent to the probe, and in this case the lesion confirmed the electrode was placed slightly further from the probe.
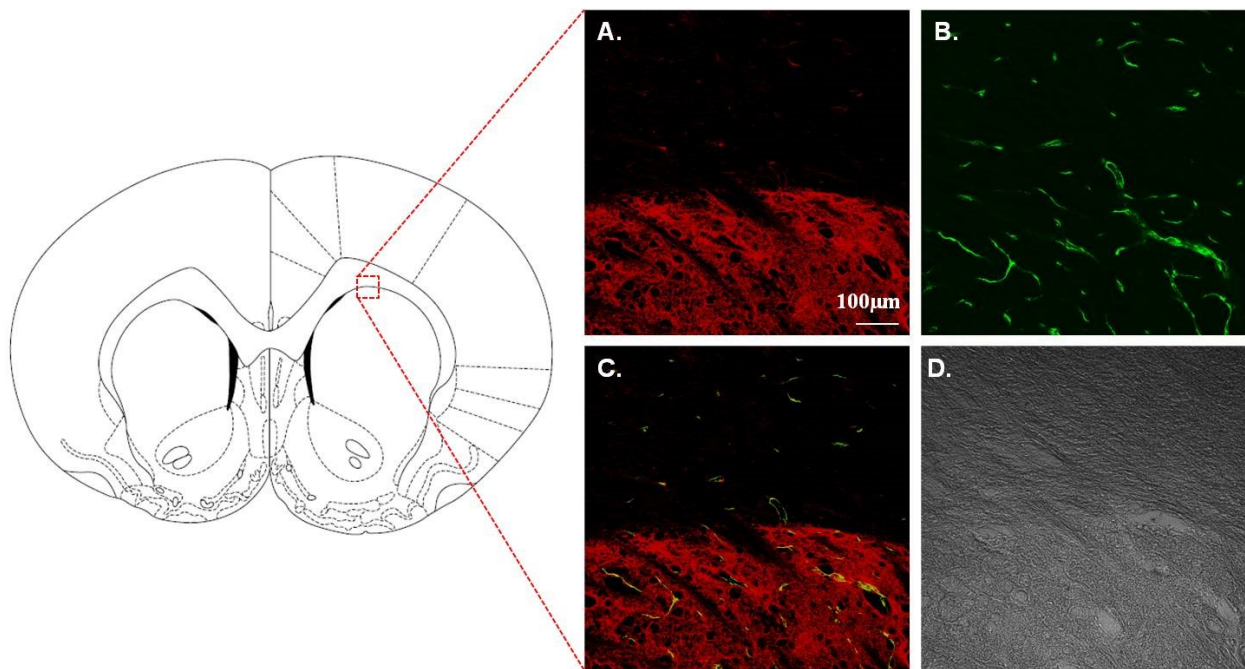
Figure 3-S5.

Striatal tissue labeled with TH. A) This image of TH labeling at the edge of the striatum shows that only the striatal portion of the section is labeled. B) This is an image of nanobeads in blood vessels. C) This image is the overlay of the TH and the nanobead images from A and B. D) This is the corresponding DIC image. Similar images were obtained for DAT labeling. Scale bar is 100 μm.
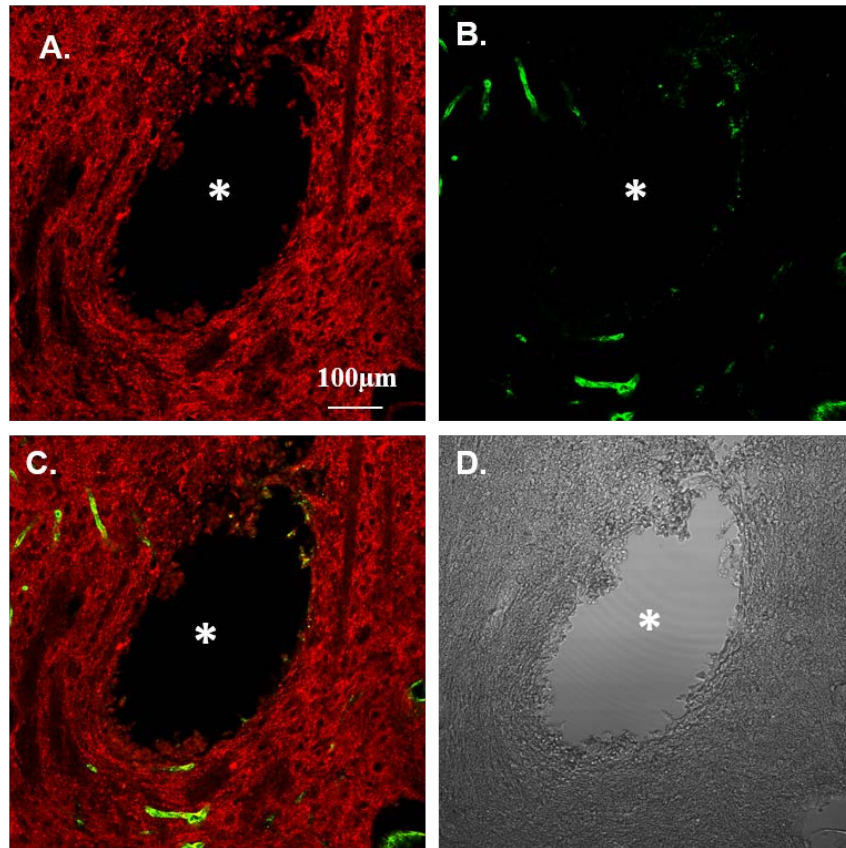
Figure 3-S6.
Images of a horizontal tissue section (35 μm thick) containing a probe track labeled for TH immunoreactivity (red, A) and for blood vessels (green, B). The overlay image (C) shows TH and blood vessels in close proximity to the probe track. D) is the DIC image of the same section.
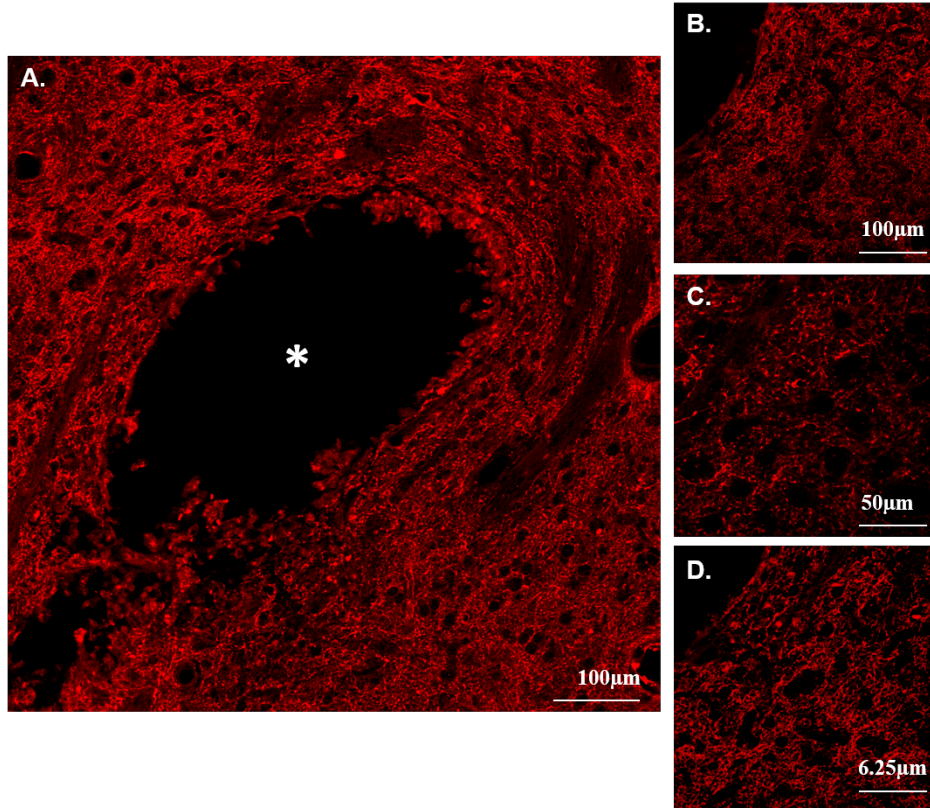
Figure 3-S7.
Fluorescence microscopy of TH labeling around a probe track (A) at three magnifications (B, C, and D). Punctate labeling near the probe track is visible at the higher magnifications.
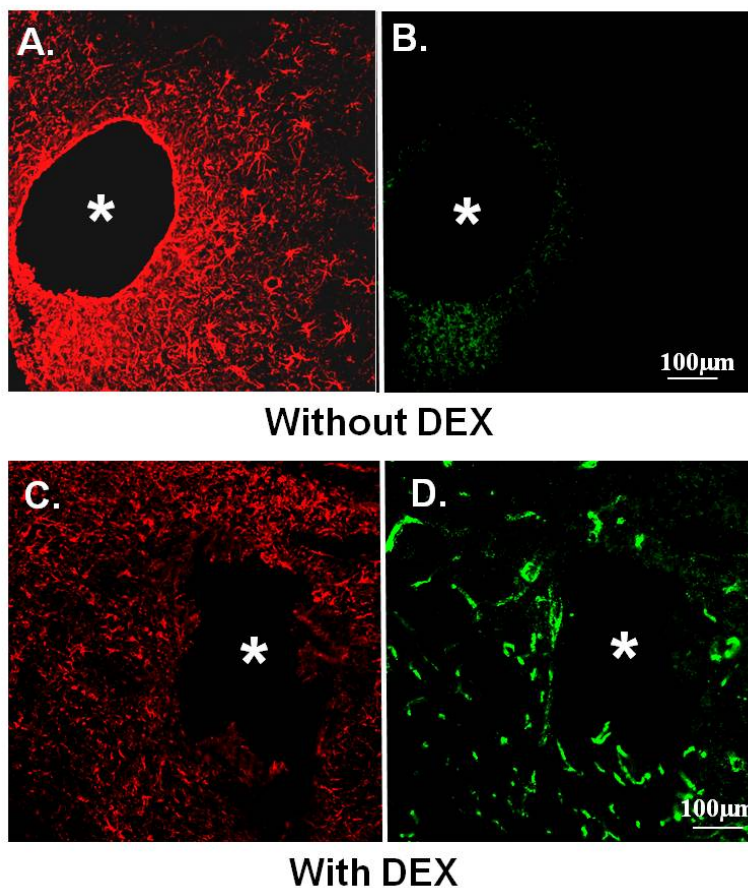
Figure 3-S8.
Fluorescence microscopy of tissue perfused for 5 days without DEX$_{retro}$ (top) and with DEXr$_{etro}$ (bottom). Sections were labeled with GFAP (A and C) and nanobeads (B and D). Asterisks represent the center of the probe track. Scale bar = 100μm.

	R_p (zmol)	k_U (s^{-1})	k_T (s^{-1})	k_R (s^{-1})
1 mm (aCSF)	1.33 ± 0.91	3.68 ± 0.49	3.02 ± 0.23	-0.79 ± 0.28
1 mm (DEX$_{retro}$)	3.06 ± 1.80	5.10 ± 0.68	1.43 ± 0.24	-0.53 ± 0.13
100 μm (DEX$_{retro}$)	2.72 ± 2.19	5.68 ± 1.91	1.80 ± 0.51	-0.53 ± 0.18

Table 3-S1.
Four adjustable parameters obtained through fitting the data in Figure 3-7 with the restricted diffusion model previously described.1 The parameters are R_p for the kinetics of DA release, k_U for the kinetics of uptake, k_T represents mass transport (restricted diffusion), and k_R is a short term plasticity factor modifying the rate of release. Through analysis of the four parameters there was no significant difference in the model fits of the three curves (multivariate ANOVA: Pillai's Trace, F $(8,14)=1.021$, p>0.05).

4.0 ENHANCING CONTINUOUS ONLINE MICRODIALYSIS USING DEXAMETHASONE: MEASUREMENT OF DYNAMIC NEUROMETABOLIC CHANGES DURING SPREADING DEPOLARIZATION

Dr. Andrea Jaquins-Gerstl contributed the immunohistochemistry and fluorescence microscopy work presented in this chapter. The Boutelle group designed the K^+ and glucose detection systems and Dr. Chi Leng Leong trained Andrea and I on the systems.

4.1 INTRODUCTION

The high incidence of traumatic brain injury (TBI) is a significant health crisis, described recently as a "silent epidemic".[61, 62] In the United States, 1.7 million brain injuries per year lead to 275 000 hospitalizations and 52 000 deaths.[63] The heart of the problem is secondary brain injury, which can cause death many days after the primary TBI even though the patient is under intensive care. Secondary injury occurs when the so-called penumbra is subjected to secondary insults, such as high intracranial pressure, transient ischemia, seizures, and spreading

60

depolarization (SD). Neuromonitoring after severe TBI detects SD[64-66, 152-154] in approximately 60% of patients.[68-71] SD is a pathological mechanism for secondary injury that drives expansion of the brain lesion into the penumbra.[66-71, 155] Incidence of SD is significantly correlated with poor patient outcomes, including death, vegetative state, and severe disability.[64-66] SD disrupts the concentration gradients of ions and molecules between intra- and extracellular spaces, and repolarization after SD requires vast amounts of energy. [64-66] Clusters of SD impose particularly severe energy demands on the injured brain.[16, 67, 72, 73]

Microdialysis is well-established for real time intracranial chemical monitoring.[3, 4] Clinical microdialysis facilitates monitoring of the local metabolic status of brain tissue in patients with TBI.[16, 17, 75, 77, 78, 156, 157] Boutelle and co-workers developed a rapid sampling microdialysis (rsMD) system that monitors glucose with 30 s temporal resolution.[75] By the combination of rsMD with an online ion selective electrode (ISE), simultaneous rapid monitoring of glucose and K^+ is now possible.[76-78]

Nevertheless, inserting a microdialysis probe into brain tissue causes a penetration injury.[25-28, 31-34] The brain wound response produces a barrier of abnormal tissue that surrounds the microdialysis probe, thereby impairing microdialysis sampling.[22, 31, 35-39] Emerging evidence suggests that retrodialysis of dexamethasone (DEX), a glucocorticoid anti-inflammatory steroid, is a simple yet effective strategy for mitigating the probe penetration injury. Recent work on the microdialysis of dopamine in the rat striatum shows that DEX reduces ischemia, suppresses glial activation, protects neurons and neuronal terminals, prevents the formation of a glial barrier, and reinstates normal dopamine activity in the tissues surrounding microdialysis probes.[31-35]

Here, we report that DEX offers similar benefits to the microdialysis monitoring of SD-induced glucose and K^+ transients in the rat cortex. We inserted microdialysis probes, with and

without retrodialysis of DEX, and monitored SD-induced glucose and K^+ transients 2 h, 5 days, or 10 days later. Retrodialysis of DEX improved the detection of SD-induced transients at all three time points. In our 10-day studies, DEX retrodialysis was performed only during the first 5 days, confirming that continuous DEX delivery for the entire 10-day time window is not required. Finally, after retrodialysis of DEX, histochemical inspection of probe tracks found no signs of ischemia or gliosis 10 days after insertion. Our findings confirm that DEX enhances the performance of microdialysis for monitoring SD-induced glucose and K^+ transients in the rat cortex for at least 10 days after probe insertion.

4.2   RESULTS AND DISCUSSION

4.2.1   Experimental Design

Microdialysis probes were inserted into the rat cortex and used to monitor K^+ and glucose in response to SD triggered by needle pricks 2 h, 5 days, or 10 days later. Due to the design of the experiments, different animals were used at each time point. For observations at 2 h after probe insertion, the animals were anesthetized for probe insertion and remained anesthetized for the duration of the experiment. For observations at 5 and 10 days after probe insertion, the animals were anesthetized for probe insertion, allowed to recover from anesthesia, housed in a Raturn system, and then reanesthetized for the measurements. The anesthetic was isoflurane. Once inserted, all probes were perfused continuously at 1.67 μL/min, with only occasional brief interruptions to refill the perfusion syringe. The probes were perfused with artificial

62

cerebrospinal fluid (aCSF) either with or without DEX. The concentration of DEX was 10 μM for the first day of perfusion, 2 μM for days 1–5, and zero for days 5–10.[31, 35]

Glucose and K^+ were monitored with rsMD and an online ISE, respectively, as previously described (Figure 4-1).[76] In vitro probe recovery was 64.0 ± 1.5% for K^+ and 10.1 ± 0.6% for glucose (mean ± SE). The higher recovery for K^+ is due to its small size compared to glucose. Probe recovery was constant when probes were stored in aCSF for 10 days (Table 4-S1). Dialysate concentrations reported herein have not been corrected for probe recovery.
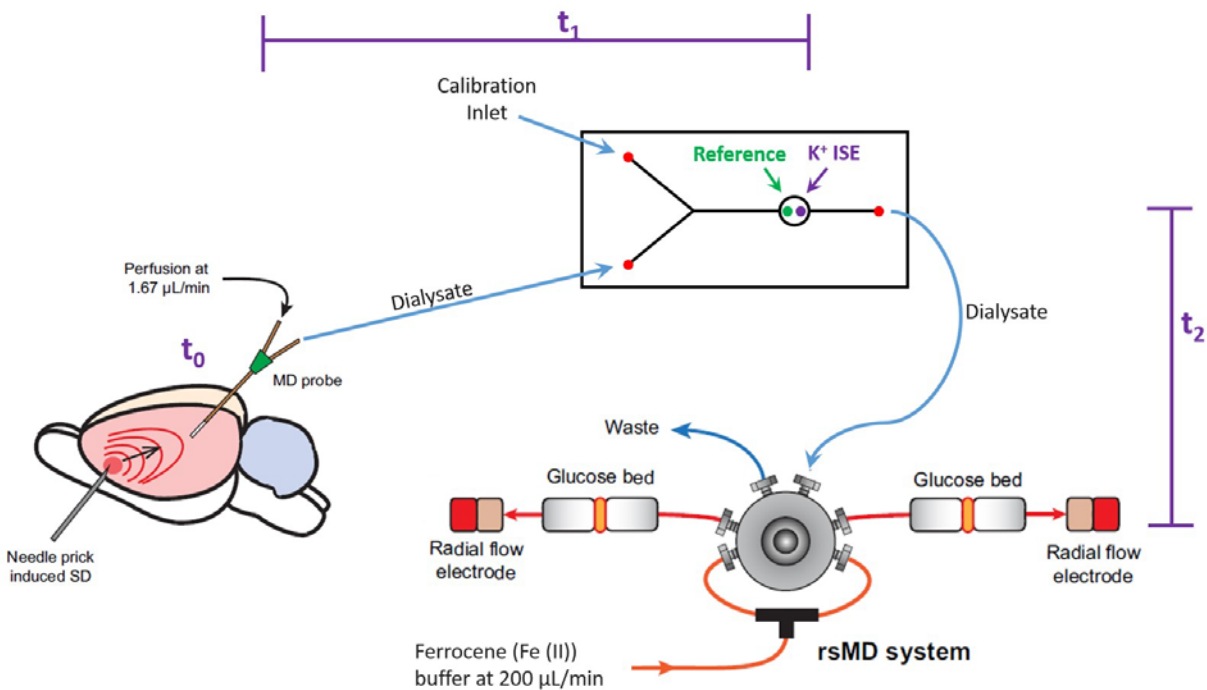
Figure 4-1.
Experimental design. SD was induced by needle pricks in the cortex. The SD arrives at the microdialysis probe at t_0: intervals between the needle pricks and t_0 were typically less than 1 min. Next, the sample travels to the K^+ ISE in approximately 4 min, t_1. Finally, the sample travels to the glucose detector in approximately 7 min, t_2. Recordings of K^+ and glucose in Figures 4-2 through 4-6 are time-adjusted to account for t_1 and t_2.

4.2.2 Probe Insertion and Representative Observations

Figure 4-2 shows an example of a complete recording of K^+ and glucose from an acute experiment in a single rat. Prior to probe insertion the dialysate K^+ and glucose concentrations, 2.7 mM and zero, respectively, derive from the perfusion fluid. In Figure 4-2, and all subsequent figures, the K^+ and glucose traces are time-adjusted according to t_1 and t_2 (see Figure 4-1) so that the transients are aligned in time with each other and with the needle pricks. The vertical black lines show when the needle pricks were performed. The delay time between the needle pricks and the time-adjusted K^+ transients, which begin at t_0 (Figure 4-1), was typically less than 1 min. Each needle prick induced a clear K^+ spike and a clear glucose dip. The spike in K^+ is a hallmark feature of SD and the glucose dip is indicative of the energy consumed as the tissue repolarizes after SD.
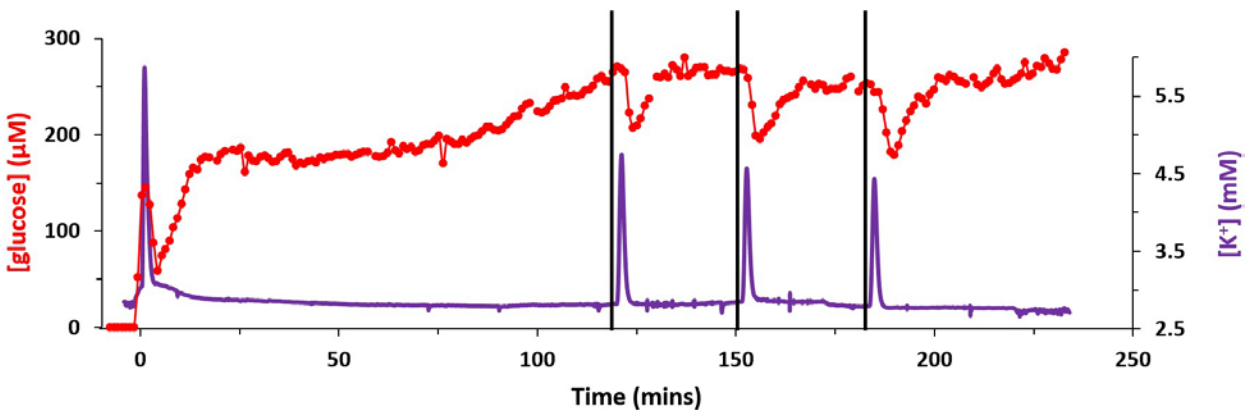
Figure 4-2.
Representative complete recording of K^+ (purple) and glucose (red) from an acute experiment performed in one rat. The microdialysis probe was inserted at time 0 with DEX perfusion. Then, 2 h later, three needle pricks were performed 30 min apart (black lines mark when the needle pricks occurred). The K^+ and glucose traces have been time-adjusted to account for t_1 and t_2 (defined in Figure 4-1).

A prominent K^+ spike also occurred just after the microdialysis probe was inserted into the cortex (Figure 4-2). A few moments later, the glucose signal, which had been initially increasing toward a basal level, also dipped. This initial K^+ spike and glucose dip, which we attribute to SD triggered by the penetration injury during probe insertion,[22, 25-28, 31-39] were observed in all animals regardless of whether or not the perfusion fluid contained DEX (Figure 4-3).
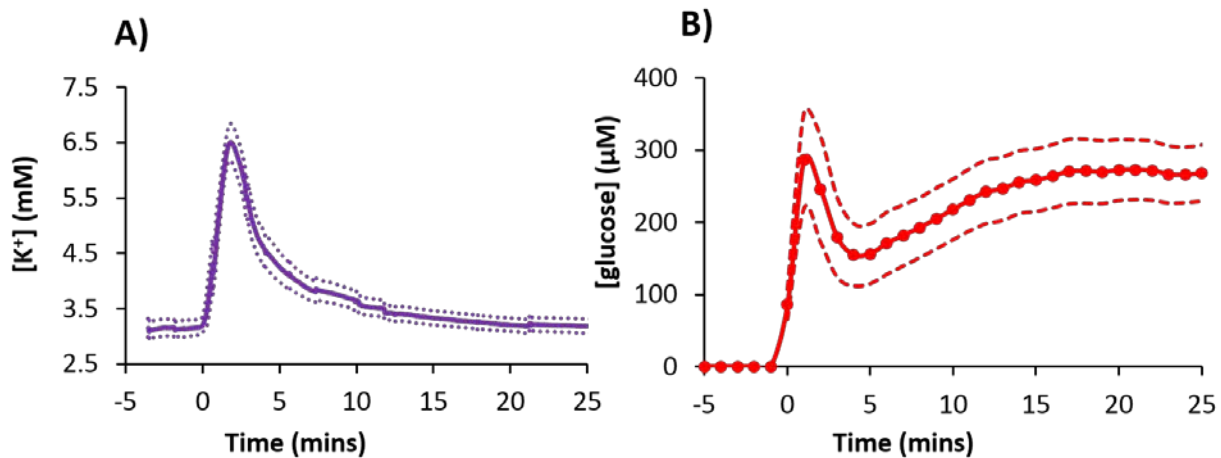
Figure 4-3.
Probe insertion SD in the rat cortex characterized by (A) an increase in K^+ (K^+ spike) and (B) a decrease in glucose (glucose dip) time-aligned to the probe insertion at time zero (mean ± SEM, n = 16 rats). In this figure, t = 0 is the time at which probe insertion was completed: note, however, that recovery of K^+ and glucose begins as soon as the probe contacts brain tissue.

In the case of Figure 4-2, after the insertion SD the dialysate glucose concentration increased quickly at first, stabilized, and then increased slowly but continuously until the needle pricks began. All animals exhibited some combination of drift and noise in the glucose baseline but there were no consistent trends between animals prior to the needle pricks.

Two additional examples of complete recordings of K^+ and glucose from single animals are provided in the Supporting Information. Figure 4-S1 is an example with needle pricks that

65

produced neither a K^+ spike nor a glucose dip. Of the 104 needle pricks performed during this work, only 11 (~11%) produced neither a K^+ spike nor a glucose dip. We assume that the needle prick either did not induce SD or that SD did not reach the location of the microdialysis probe. When this occurred, extra pricks were performed so that three SD responses were recorded from each animal. In Figure 4-S1, the needle pricks triggered a slow decline in the basal glucose level in addition to the glucose dips. A similar event was noted in 65% of the animals included in this study. Previous studies have a reported similar observations.[16, 17]

Figure 4-S2 shows a unique adverse event: in this one animal, the needle prick induced a long-lasting elevation in K^+ and a long-lasting decline in glucose. The rat died about 1 h later. This unique event resembles a phenomenon called spreading ischemia,[158] although without direct measurement of blood flow this cannot be confirmed.

4.2.3   SD-Induced Transients 2 h after Probe Insertion

Three needle pricks were performed at 30 min intervals beginning 2 h after insertion of microdialysis probes into the rat cortex. DEX increased the amplitudes of the SD-induced K^+ spikes and glucose dips by 127% and 86% (averages of the three responses), respectively, compared to those observed without DEX (Figure 4-4: DEX also significantly increased the areas-under-the-curves, see Figure 4-S3). The amplitudes of the K^+ spikes and the glucose dips consistently decreased upon each consecutive needle prick (Figure 4-4) but this trend did not reach statistical significance (see the figure legend for the ANOVA details). We speculate this decreasing trend is a consequence of repetitively pricking the same cortical location.

Figure 4-4.
Cortical responses to three needle pricks recorded 2 h after probe insertion with (A) aCSF or (B) DEX (mean ± SEM, n = 8 rats (24 needle pricks) per group). Maximum changes in (C) K^+ and (D) glucose were analyzed with two-way ANOVAs with group (aCSF, DEX) and needle prick (1, 2, 3; repeated measures) as the factors. The needle prick and interactions were not significant, but group was significant for both K^+ ($F_{(1,14)} = 13.422$) and glucose ($F_{(1,14)} = 6.253$). **$p < 0.005$, *$p < 0.05$.

4.2.4 SD-Induced Transients 5 Days after Probe Insertion

Probes were inserted and perfused with aCSF or DEX for 5 days. Then, rats were reanesthetized 1 h before the first needle prick. If a needle prick produced neither a K^+ spike nor a glucose dip, an extra needle prick was performed, as explained above. In some cases, however, the needle prick produced a K^+ spike but no detectable glucose dip (11 of 15 with aCSF and 3 of 15 with DEX). Such needle pricks were not repeated: instead, the glucose dip was rated as nondetectable. All needle pricks that induced a K^+ spike were included in the data analysis explained below.

Glucose dips were rated as nondetectable if their amplitude did not exceed 3× the baseline noise. The baseline noise was determined from the standard deviation of the glucose concentrations measured over the 10 min interval prior to each needle prick (Figure 4-S4). By this procedure, the average glucose detection limit for the five groups in this study was 37 ± 16 μM (mean ± SE): this value exceeds the rsMD detection limit of 25 μM reported previously.[159] Thus, the limit of detection in this work is determined by the noise in the glucose baseline rather than the noise in the rsMD detector.

After microdialysis probes were perfused with aCSF for 5 days, the K^+ spikes were of low amplitude and the glucose dips were essentially nondetectable (Figure 4-5A). Fifteen K^+ spikes were observed (5 animals, 3 responses each), but only 4 were accompanied by glucose dips with amplitudes greater than 3× the baseline noise. As observed at 2 h, the amplitude of the consecutive K^+ spikes decreased upon each consecutive needle prick (Figure 4-5C), presumably due to repetitively pricking the same cortical location. Our previous work shows that microdialysis probes are surrounded by a barrier of abnormal tissue by 5 days after insertion,[31, 35]

thus we attribute the low amplitudes of these K^+ and glucose transients to the presence of such a barrier.
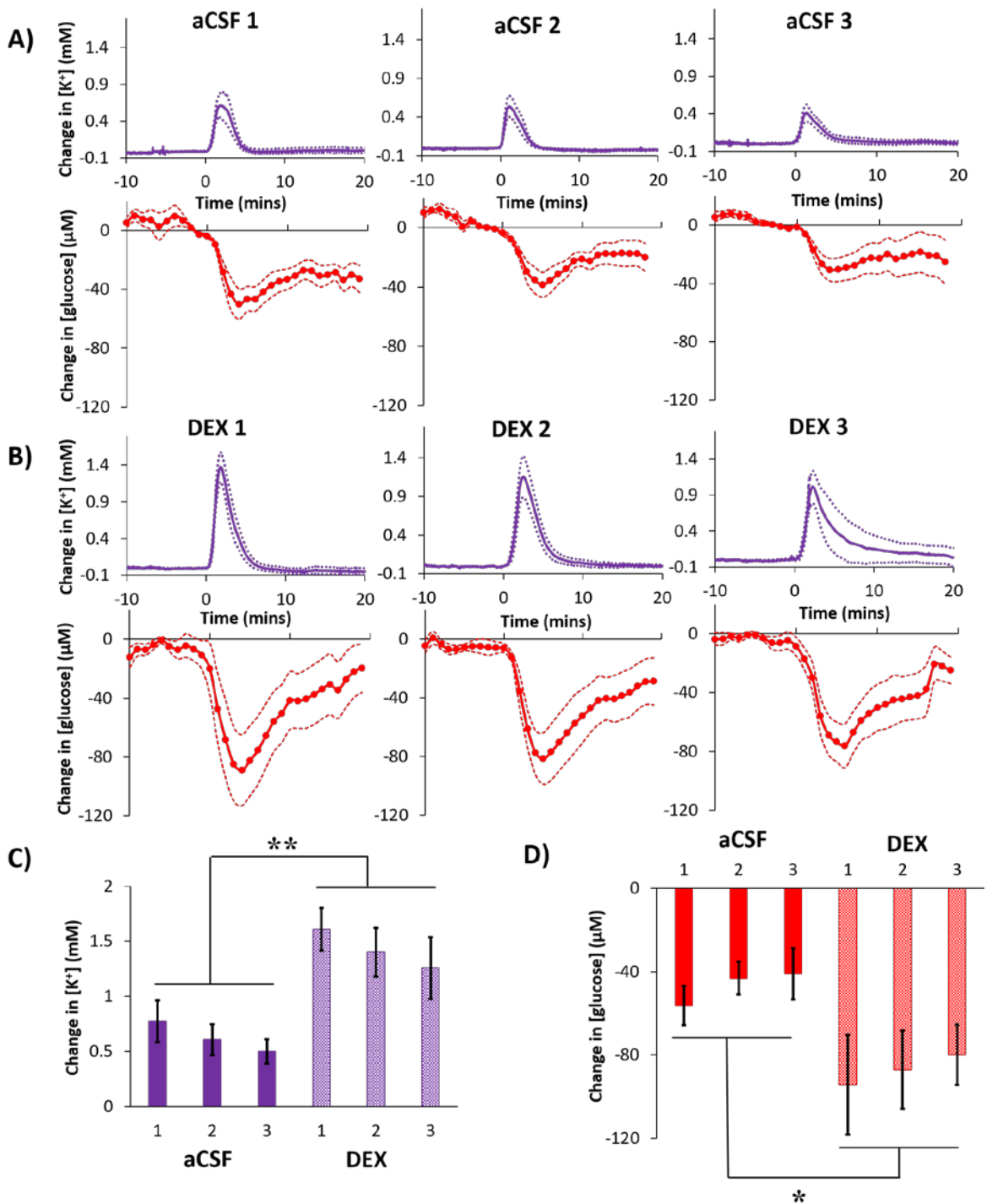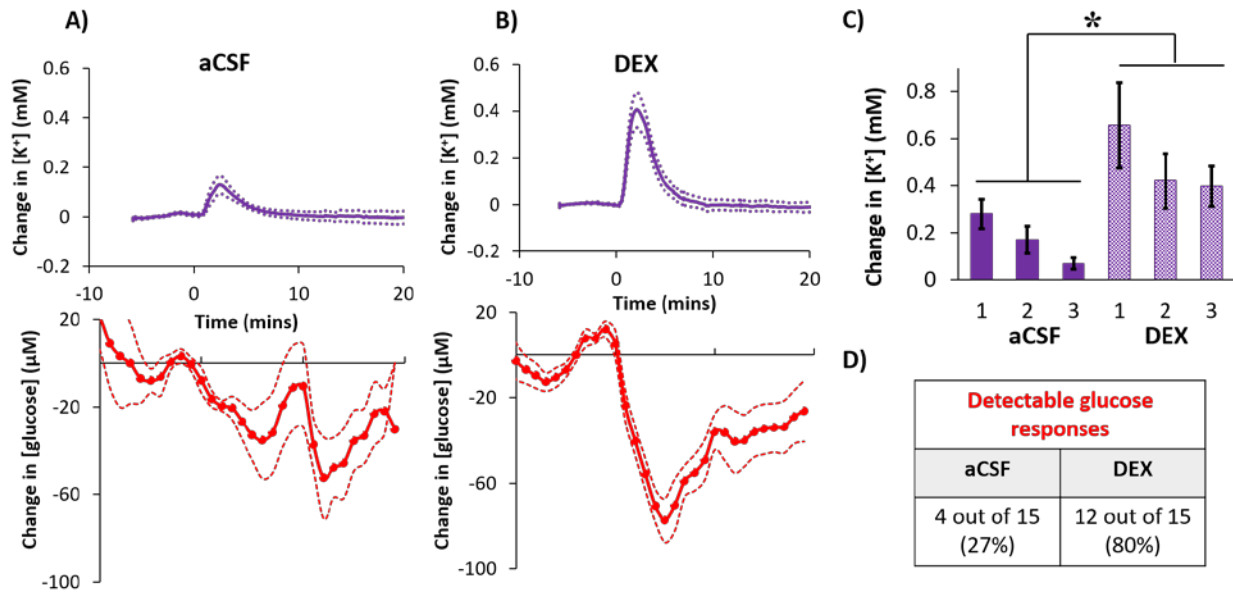

Figure 4-5.
Average cortical response to needle pricks recorded 5 days after probe insertion with (A) aCSF or (B) DEX (mean ± SEM, n = 5 rats (15 needle pricks) per group). (C) Changes in K^+ to the three needle pricks were analyzed with a two-way ANOVA with group (aCSF, DEX) and needle prick (1, 2, 3; repeated measures) as the factors. Group ($F_{(1,8)}$ = 5.844, p < 0.05) and needle prick ($F_{(2,16)}$ = 12.689, p < 0.001) are significant, interaction is not significant. (D) Only detectable glucose responses are represented in (A) and (B); see Table 4-1 and Figure 4-S4 for details. *p < 0.05.

After microdialysis probes were perfused with DEX for 5 days, needle pricks induced robust K^+ spikes and robust glucose dips (Figure 4-5B). We observed 15 K^+ spikes and 12 (80%) of these were accompanied by quantifiable glucose dips. Averaging over the three consecutive needle pricks, the amplitudes of K^+ spikes measured with DEX were 184% larger than those measured without DEX (Figure 4-5C). The effect of DEX was significant (ANOVA details in the legend of Figure 4-5: statistical analysis of the glucose responses were not possible because those measured without DEX were not quantifiable, see Figure 4-5D). We attribute DEX's

ability to enhance the detection of SD-induced transients to its ability to prevent the formation of a barrier of abnormal tissue at the probe track, as previously demonstrated.[31-35]

4.2.5 SD-Induced Transients 10 Days after Probe Insertion

Microdialysis probes were inserted into the rat cortex and responses to needle pricks were recorded 10 days later. DEX retrodialysis was performed only during the first 5 days. On the fifth day the perfusion fluid was switched from DEX to aCSF, which was perfused through the probes for the remainder of the experiments. There were two principal reasons for adopting this protocol. First, DEX is an exogenous agent. In most instances, whether working in animals or patients, it is preferable to use a minimum sufficient quantity of such an exogenous agent. Second, prior work on neuroprosthetic devices suggests that continuous delivery of DEX might not be necessary for long-term benefits.[42, 46, 47]

Needle pricks performed 10 days after probe insertion induced robust K^+ spikes and corresponding glucose dips (Figure 4-6): 87% of the 15 K^+ spikes were accompanied by a quantifiable glucose dip (Table 4-1). As observed at 2 h and 5 days, there was a decreasing trend in the amplitude of the K^+ spikes on each consecutive needle prick. However, no such trend appeared in the glucose responses, which exhibited consistent amplitudes. Figure 4-6 confirms the benefits of DEX retrodialysis for monitoring SD-induced K^+ and glucose transients outlast the duration of the DEX retrodialysis itself. Figure 4-6 is our first report of DEX-enhanced microdialysis at 10 days after probe insertion. Previously, we showed that 5 days of DEX retrodialysis reinstated normal dopamine neurochemical activity near the probe.[35] Here we extend that work not only to 10 days after probe insertion, a clinically relevant time window, but also to include the enhancement of monitoring K^+ and glucose transients in the context of SD.
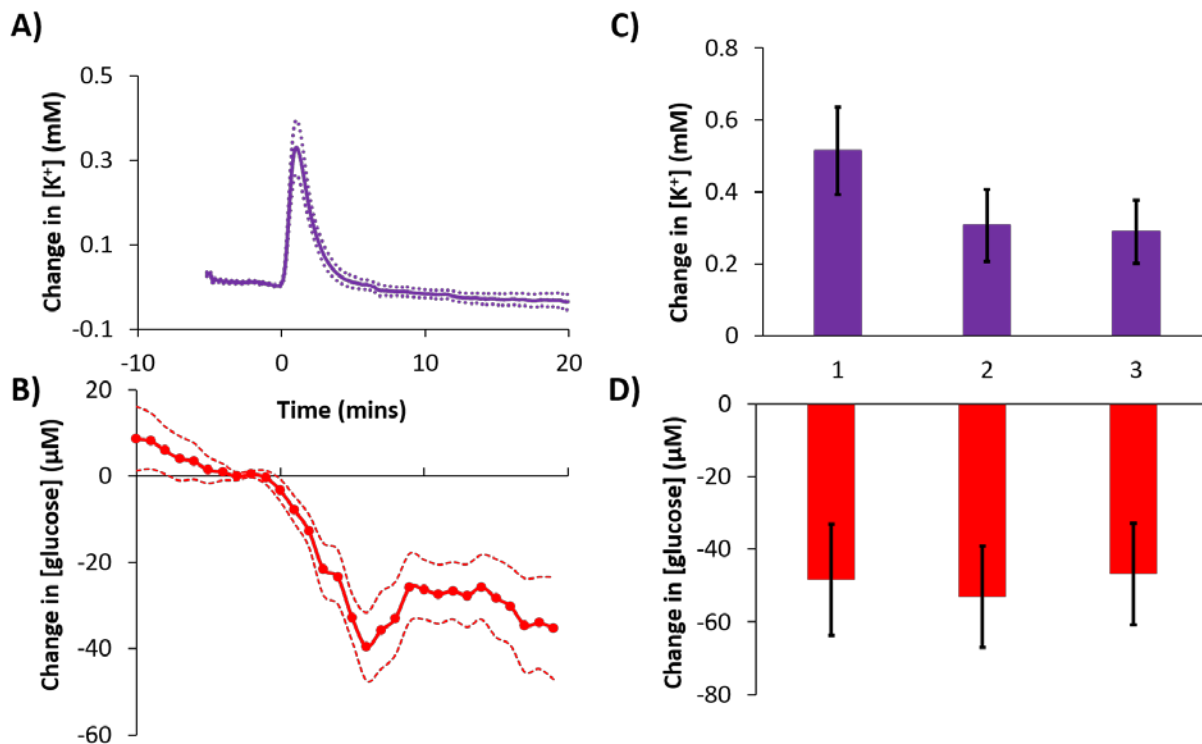
Figure 4-6.
(A) K^+ and (B) glucose response (mean $\pm$ SEM) to needle pricks performed 10 days after probe insertion (n = 5 rats, 15 needle pricks). (C) and (D) provide the changes in K^+ and glucose, respectively, to each of the three needle pricks. Needle prick number was not a significant factor for either K^+ or glucose (1-way ANOVAs, repeated measures). The microdialysis probe was perfused with DEX for days 1–5 and then aCSF for days 5–10.

	Total changes in [K$^+$]	Quantifiable changes in [glucose]
2 h DEX	24	24 (100%)
2 h aCSF	24	21 (88%)
5 d DEX	15	12 (80%)
5 d aCSF	15	4 (27%)
10 d DEX	15	13 (87%)

Table 4-1.
Observation of a K^+ spike confirmed SD in the vicinity of the probe. In every case, except for 5 days aCSF, the majority of the K^+ spikes were accompanied by a quantifiable glucose dip. Only the quantifiable glucose dips are included in Figures 4-4 through 4-7. The noise in a 10 min glucose baseline prior to each needle prick was used to create a threshold quantifiable glucose value (see text and Figure 4-S4 for details).

4.2.6 Quantitative Comparisons

In the presence of DEX, the amplitudes of the K$^+$ spikes were significantly larger at 2 h compared to 5 and 10 days (Figure 4-7A). In contrast, there were no significant differences between the amplitudes of the glucose dips at the three time points (Figure 4-7B). In the presence of DEX, the fraction of K$^+$ spikes accompanied by quantifiable glucose dips was relatively constant across the three time points (Table 4-1). In the absence of DEX, glucose dips were essentially nondetectable 5 days after probe insertion (Table 4-1).
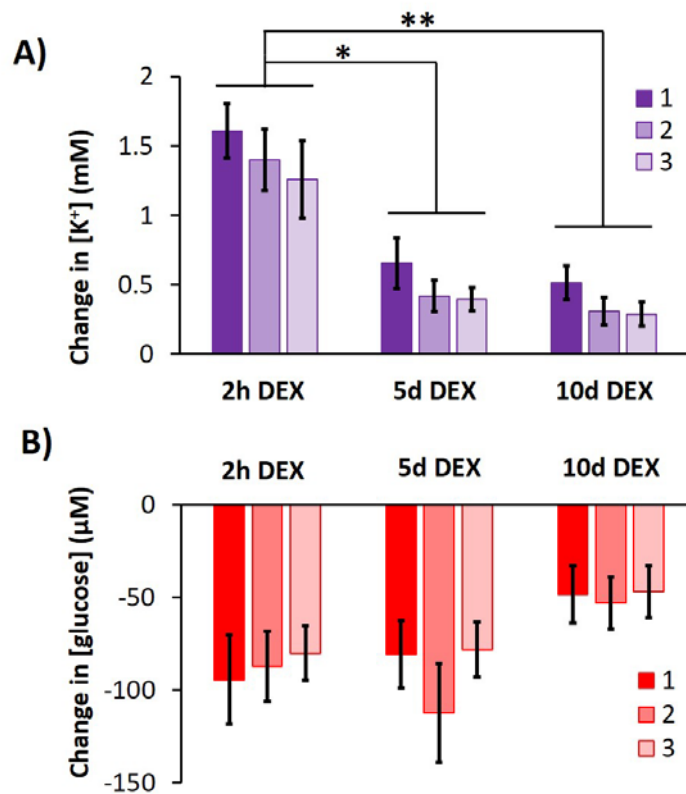
Figure 4-7.
Summary comparison (mean ± SEM) of the amplitudes of (A) K$^+$ spikes and (B) glucose dips in response to three needle pricks recorded 2 h, 5 days, and 10 days after probe insertion in the presence of DEX. Data were analyzed with two-way ANOVAs with time (2 h, 5 days, 10 days) and needle prick (1, 2, 3; repeated measures) as the factors. K$^+$: time is significant (F$(2,15)$ = 15.878, p < 0.0005 while needle prick and the interaction are not significant. Glucose: neither factor was significant. Stars represent Games-Howell posthoc tests, **p < 0.001 and *p < 0.005.

Prior to the start of the needle pricks the basal K^+ and glucose concentrations were 3.1 ± 0.1 mM and 374 ± 36 µM, respectively (mean ± SE, n = 31 animals). There were no significant differences between the basal levels of the 5 groups analyzed in this study (one-way ANOVAs). This confirms that none of the probes failed during this study, including those perfused for 5 days without DEX.

4.2.7   Immunohistochemistry

We used fluorescence microscopy to examine thin sagittal sections of brain tissue containing the tracks of probes implanted for 10 days. Nonimplanted control tissues from the contralateral hemisphere were used for comparison. When probes were perfused with DEX for 5 days after probe insertion, immunohistochemistry showed no evidence of ischemia (lack of nanobeads) or gliosis (GFAP) 10 days after probe insertion (Figure 4-8). When the percent of fluorescent pixels in images of probe tracks were compared to images of nonimplanted control tissue, there were no significant differences between either the blood flow or gliosis images (Figure 4-8D,H: during the analysis the probe tracks were excluded from the regions of interest). Figure 4-8 extends our previous reports that DEX prevents ischemia and gliosis.[31, 33]

Figure 4-8 is our first report that DEX prevents ischemia and gliosis near probes inserted into the rat cortex, that the benefits of DEX last for 10 days after insertion, and that the benefits of DEX retrodialysis long outlast the DEX retrodialysis itself.
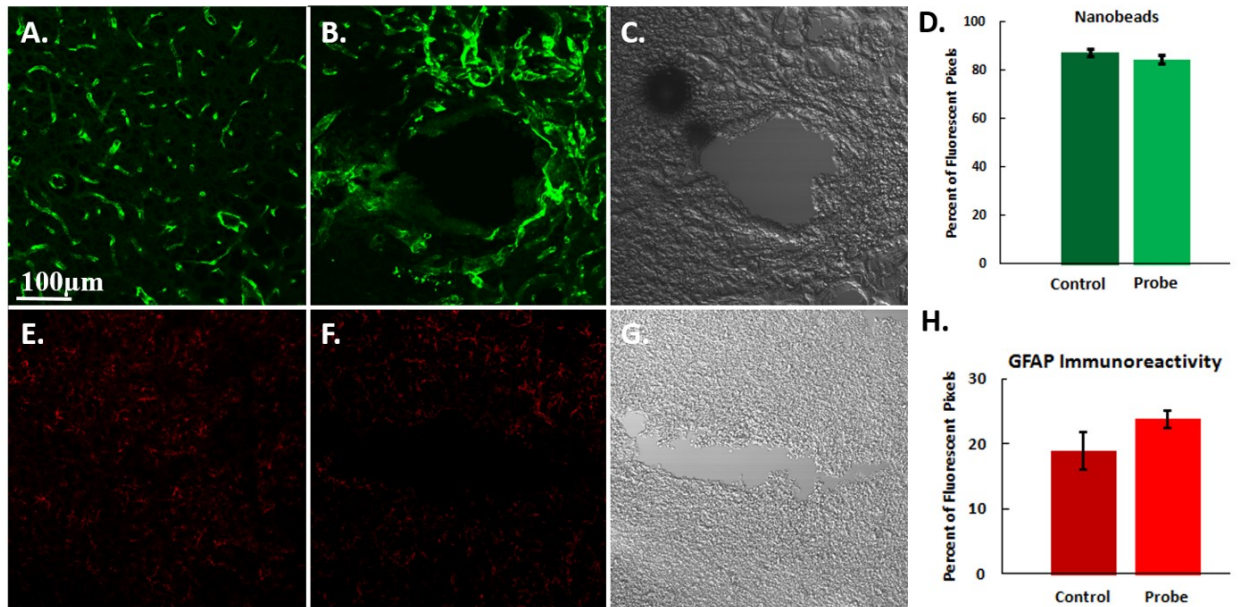
Figure 4-8.
Representative fluorescent microscopy images of the probe tracks after 10 days. The cortex is labeled for (A,B) blood flow (fluorescent nanobeads) and (E,F) GFAP immunoreactivity. The left column (A,E) is control, nonimplanted cortex tissue from the contralateral hemisphere. The center column (B,F) is tissue surrounding the microdialysis probe 10 days after probe implantation (5 days of DEX). The DIC images (C,G) are provided to identify the location of the microdialysis probe tracks in (B) and (F). Graphs comparing the (D) blood flow and (H) GFAP immunoreactivity in the areas of interest in both the ipsilateral and contralateral hemispheres. There is no significant difference between probe tracks and control tissue for either nanobeads or GFAP (t tests). Results are reported as the percent of fluorescent pixels (mean ± SEM). Scale bar is 100 μm.

4.3   CONCLUSIONS

Our findings confirm that DEX retrodialysis enhances the microdialysis detection of SD-induced K^+ and glucose transients for at least 10 days after probe insertion. We observed an insertion SD (Figures 4-2 and 4-3), supplementing prior evidence that insertion causes a penetration injury.[22, 25-28, 31-39] Despite the penetration injury, brain microdialysis is well tolerated by animals and human patients alike, presumably because only a small volume of tissue is

74

affected. The issue at hand, however, is the impact of the penetration injury-induced ischemia, cell loss, gliosis, and glial barrier formation on the outcome of brain microdialysis sampling.[25-28, 31-35] Thus, our objective is to promote the recovery of normal brain function and activity at the probe site. Retrodialysis of DEX is emerging as a simple yet effective strategy for achieving this objective.

Without DEX, SD-induced transients became difficult to monitor 5 days after probe insertion. K^+ transients exhibited a significant decrease in amplitude and glucose transients became too small to reliably quantify: 11 of 15 detected K^+ spikes were not accompanied by any detectable glucose dip. These observations are consistent with the idea that a tissue barrier prevents SD-induced transient detection by microdialysis.

With the retrodialysis of DEX, SD-induced K^+ and glucose transients were reliably quantified 2 h, 5 days, and 10 days after probe insertion (Figures 4-4 through 4-6). This work is our first extension of DEX enhanced microdialysis to K^+ and glucose transients, to the rat cortex, and to 10 days after probe insertion. We attribute the enhanced transient detection to DEX's ability to prevent ischemia, cell loss, gliosis, and barrier formation at the probe track. A key finding of the present study is that the beneficial effects of DEX persisted to 10 days after probe insertion even though we stopped retrodialysis of DEX on day 5.

With the retrodialysis of DEX, however, the amplitude of the K^+ transients decreased systematically day-to-day (Figure 4-7). First, the amplitudes decreased in response to each consecutive needle prick: as mentioned above, this is likely because we repetitively pricked the same cortical location. Second, there was a statistically significant decrease from 2 h to 5 days; however, there was no further significant decrease from 5 to 10 days. The amplitude of the glucose transients exhibited similar declining trends but these were not statistically significant

75

(Figure 4-7). Overall, these day-to-day declines might be an indication that the tissue next to the probe becomes more tolerant of SD over time. Brain tissue depends on the vasculature for moment-to-moment delivery of glucose and oxygen to meet the energy demands of repolarization after SD.[64] Retrodialysis with DEX reinstates blood flow to the probe track at 5 days following insertion[31] and Figure 4-8 documents that this persists to 10 days. We speculate, therefore, that the declining response amplitudes, especially of the K^+ transients, reflect an improvement in the health status of the tissue at the probe track.

Furthermore, we found no evidence of inherent probe failure during this work. During a 10-day in vitro test, recovery for K^+ and glucose remained constant (Table 4-S1). During in vivo procedures, all probes maintained consistent flow without evidence of clogging, increased flow resistance, or other flow problems. Moreover, there were no statistically significant differences among the basal glucose and K^+ levels, measured just prior to the onset of the needle prick procedures, regardless of postinsertion time or inclusion of DEX. For this reason, we conclude that the key factor determining the ability to detect SD-induced transients by microdialysis is the status of the tissue adjacent to the probe: the probes themselves show no signs of failure over the course of our 10 day studies.

Although this work was conducted in animals, our eventual goal is clinical translation. We hypothesize that the combination of rsMD with DEX-enhanced microdialysis has the potential to impact clinical microdialysis in important ways. Traditional clinical microdialysis has been previously performed in TBI patients for 10 days with a microdialysis sampling time of 1 h and without DEX or any other strategy to mitigate the consequences of the probe insertion.[156, 157] A correlation was found between dialysate glucose levels during the first 50 h of microdialysis and patient outcome.[157] However, no correlation was found 2–10 days after probe

insertion. This latter observation is perplexing, because ECoG detects SD in TBI patients well beyond 50 h.[16, 69, 73, 155] Although it remains to be seen, we are hopeful that the combination of rsMD with DEX retrodialysis will offer enhanced microdialysis monitoring capabilities for patients at risk of secondary injury by SD.

4.4   METHODS

4.4.1   Reagents and Solutions

All solutions were prepared with ultrapure water (Nanopure; Barnstead, Dubuque, IA). Artificial cerebrospinal fluid (aCSF) contained 142 mM NaCl, 1.2 mM $CaCl_2$, 2.7 mM KCl, 1.0 mM $MgCl_2$, and 2.0 mM NaH_2PO_4, adjusted to a pH 7.4. Dexamethasone sodium phosphate (APP Fresenius Kabi USA, LLC, Lake Zurich IL) was diluted in aCSF. The microdialysis perfusion fluids were filtered with Nalgene sterile filter units (Fisher, Pittsburgh, PA; PES 0.2 μm pores). Glucose oxidase (GOx, 100–200 units/mg) and horseradish peroxidase (HRP, ≥250 units/mg) were obtained from Sigma-Aldrich. The ferrocene solution contained 1.5 mM ferrocenecarboxylic acid, 1 mM EDTA, 150 mM sodium chloride and 100 mM sodium citrate and was filtered before use with 0.1 and 0.02 μm pore size filters.

4.4.2   Microdialysis Probes, Surgical Procedures, and Experimental Protocol

Concentric style microdialysis probes were built in-house with hollow fiber membranes (13 kDa MWCO, Specta/Por RC, Spectrum, Ranco Dominguez, CA), 4 mm in length and 280

μm in outer diameter. Fused silica capillaries (75 μm I.D., 150 μm O.D., Polymicro Technologies, Phoenix, AZ) were used for the inlet and outlet lines. Prior to use, probes were soaked in 70% ethanol and then flushed and immersed in aCSF (or aCSF with DEX) for several hours prior to implantation into the brain. Prior to insertion, the probe inlet was connected to a 1 mL gastight syringe driven by a microliter syringe pump (Harvard Apparatus, Holliston, MA) at a perfusion rate of 1.67 μL/min. The probe outlet (50 cm long) was connected to the K^+ ISE detector.

Rats (male, Sprague–Dawley, 250–350g, Charles River, Raleigh, NC) were anesthetized with isoflurane (5% induction, 2.5% maintenance), placed in a stereotaxic frame (David Kopf Instruments, Tujunga, CA), and adjusted to flat skull[151] for probe insertion. Aseptic technique was used throughout. The microdialysis probe was lowered at a 51° angle into the cortex using the coordinates 4.2 mm posterior to bregma, 1.5 mm lateral to midline, and 4 mm below dura: the entire active portion of the probe came to rest in the cortex. For the 2 h study, the rats (n = 8 per group) remained under anesthesia for the duration of the experiment and responses to needle pricks were monitored beginning 2 h after probe insertion. To perform the needle pricks, a second hole was drilled through the skull ipsilateral to the probe, just anterior to bregma (approximately 4.5 mm from the probe). The surface of the cortex was manually pricked with the tip of an 18-gauge hypodermic needle. Three pricks, 30 min apart, were performed per animal. For the 5 and 10 day experiments (n = 5 per group), the probes were inserted as described above and secured with bone screws and acrylic cement. The incision was closed with sutures, anesthesia was removed, and the rats were housed in a Raturn Microdialysis Bowl (MD-1404, BASI, West Lafayette, IN) with continuous perfusion of the microdialysis probe at 1.67 μL/min. When used, the concentration of DEX was 10 μM for the first 24 h and then 2 μM for the next 5

days.[31, 35] After 5 or 10 days the rats were reanesthetized 1 h prior to recording responses to needle pricks.

4.4.3 Potassium and Glucose Detection

The K^+ ISE electrode and poly(dimethyl)siloxane (PDMS) microfluidic system have been described previously.[77] Briefly, a miniaturized K^+ ISE was made in-house. A membrane containing 2 mg potassium ionophore, 0.2 mg potassium tetrakis(4-chlorophenyl)borate, 150.0 mg bis(2-ethylhexyl) sebacate, and 66 mg poly(vinyl chloride) (PVC) dissolved in tetrahydrofuran (reagents from Sigma-Aldrich) was cast over a segment of perfluoroalkoxyalkane tubing (PFA, IDEX Health Sciences, 360 μm O.D. and 150 μm I.D.). The electrode was assembled with an internal Ag/AgCl reference and aCSF filling solution. The potential of the K^+ ISE was measured against an external Ag/AgCl reference electrode using custom electronics built in-house. The K^+ ISE and external reference electrode were inserted into a PDMS chip fabricated with soft lithography, as shown in Figure 4-1. The total internal volume of the PDMS chip is approximately 700 nL. Connections to and from the PDMS chip were made with 0.15 mm and 0.13 mm ID FEP tubing, respectively.

The rapid sampling microdialysis (rsMD) system has been described previously.[75] Briefly, the dialysate enters a custom built sampling valve (Valco, Switzerland) with two 100 nL internal sampling loops. A standard HPLC pump (flow rate: 200 μL/min) mixed ferrocene solution with the dialysate and injected the mixture at 30 s intervals into one of two paths, both of which contain dual enzyme reactors in-line with a 3 mm glassy carbon disk electrode. The enzyme reactor contained two 6 mm-diameter membranes (0.025 μm pores, Millipore) loaded with glucose oxidase (1 mg/mL) or horseradish peroxidase (0.5 mg/mL). The reduction of the

79

ferrocenium ion was measured at 0 V with a three-electrode system with a Ag/AgCl reference electrode (UniJet, BASi, USA) and custom-built electronics.

4.4.4   Data Analysis

The rsMD data were analyzed with previously published algorithms[159] and converted to concentration with postexperiment calibrations. In Figures 4-2 through 4-6, the K^+ and glucose recordings were time-aligned to t_0 (Figure 4-1) to account for the travel time to and between the sensors. At the 1.67 μL/min flow rate it takes approximately 4 min, t_1, for the sample to travel to the K^+ sensor and an additional 7 min, t_2, to travel to the glucose detector (Figure 4-1). The K^+ spikes were used to confirm SD at the probe site: if there was no K^+ spike the needle prick was repeated (see discussion of Figure 4-S1). A 10 min baseline prior to the expected glucose response was used to calculate a threshold for a detectable glucose signal, defined as 3× the noise of the 10 min baseline. If the glucose level dropped below the threshold in the next 15 min it was included as a detectable response (see Figure 4-S4). Only detectable glucose responses were included in the data analysis and figures. A K^+ threshold was calculated in a similar manner using the signal recorded for 2 min prior to needle pricks.

4.4.5   Immunohistochemistry and Fluorescence Microscopy

The procedures for immunohistochemistry and fluorescence microscopy are described in our previous papers.[30, 31, 105] Rats were deeply anesthetized with isoflurane (2.5% by volume O_2) and perfused transcardially with 200 mL 0.01 M phosphate-buffered saline (PBS), pH 7.4, followed by 160 mL of 4% paraformaldehyde, and then with 50 mL of a solution containing

commercially available (Molecular Probes) 100 nm fluorescent beads (1:1000 dilution PBS). The entire brain was quickly removed and further fixed in 4% paraformaldehyde for 24 h at 4 °C before being equilibrated in a 30% sucrose solution at 4 °C for 24 h. The brain was then frozen in 2-methylbutane in a bath of liquid nitrogen to prevent freeze fracturing. The tissue containing the probe track was cut to 20-μm sagittal sections (n = 3, 3 slides per animal). Free floating sections were rinsed in PBS, three times (10 min each), then blocked with 5% goat serum in PBS containing 0.1% Triton X-100 for 1 h at room temperature and subjected to immunohistochemical staining. The sections were incubated overnight at 4 °C with the primary antibody antiglial fibrillary acidic protein (GFAP; 1:100; #Z033401, DAKO Agilent Technologies). As a negative control, PBS was used instead of the primary antibody. Sections were then washed with PBS (5 min) and incubated in a secondary solution consisting of 5% goat serum, 0.1% Triton X-100, and antibody (1:500 goat anti-rabbit Alexa 568, Invitrogen, Carlsbad CA) for 2 h at room temperature. Sections were then rinsed with PBS for 10 min before being coverslipped with Fluoromount-G (Southern Biotech, Birmingham AL). Sections were imaged using fluorescent microscopy (FluoView 1000, Olympus, Inc., Tokyo, Japan) at 20× magnification.

Tissue images were processed and analyzed with the Metamorph/Fluor 7.1 software package (Universal Imaging Corporation; Molecular Devices). Quantitative analysis was based on individual sections containing the microdialysis probe track in the ipsilateral region. Sections from the contralateral region (nonimplanted control tissue) were treated in identical fashion to the ipsilateral region. The fluorescence intensities of GFAP and blood flow were determined by setting threshold values; the total number of pixels was expressed as the percent of fluorescence in the region of interest.[33] Samples were compared to a nonimplanted region of the tissue slice.

4.4.6   Statistics

IBM Statistical Package for the Social Sciences (SPSS) 22 software was used for all statistical analysis. For all tests, a $p < 0.05$ was used for statistical significance.

4.5   SUPPORTING INFORMATION

	K⁺ Probe Recovery (%)	Glucose Probe Recovery (%)
Day 0 (4 hours)	67.6 ± 1.5	11.6 ± 0.6
Day 5	66.8 ± 0.2	12.7 ± 0.7
Day 10	69.1 ± 1.1	11.4 ± 0.5

Table 4-S1.
In vitro probe recovery (mean ± S.E.) was consistent when probes were continually perfused and stored in aCSF for 10 days (n = 3 probes). There is no significant difference between the three time points for either K⁺ or glucose (ANOVA, repeated measures).
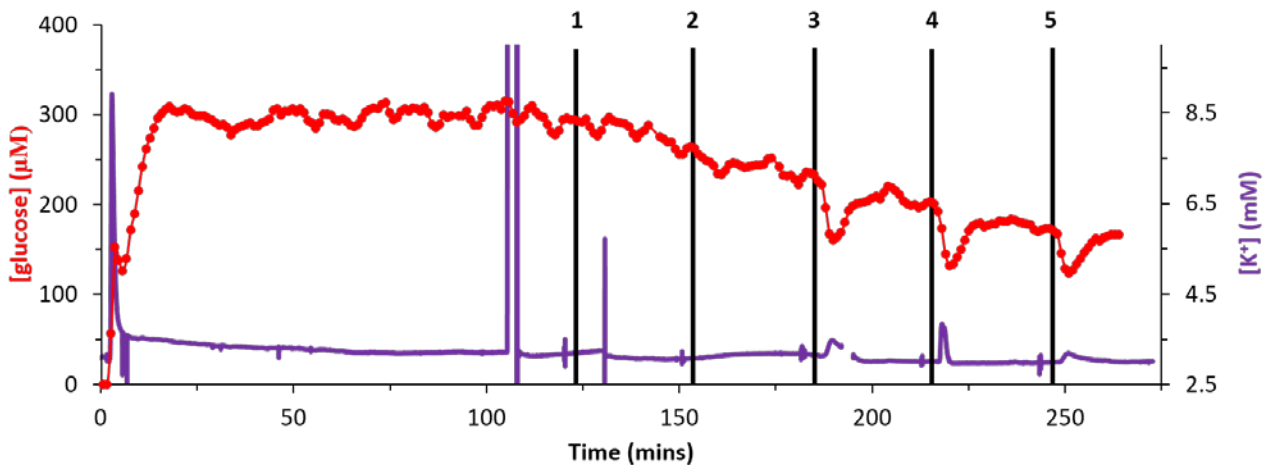
Figure 4-S1.
Representative data showing SD induction with no K⁺ spike or glucose dip. The probe was inserted at time 0. The vertical black lines mark 5 SD inductions. Both 1 and 2 were not detected, meaning no change in K⁺. Approximately 11% of SD inductions were not detected by the microdialysis probe and thus were not included in the data analysis.

Needle pricks 3, 4, and 5 were measured by the probe. An additional feature that was commonly observed is the decline in basal glucose following multiple SD. Note there are noise spikes in the K^+ signal prior to and after the first needle prick and also in the middle of the third SD. The noise spike during the third SD was removed for clarity of the corresponding glucose dip.
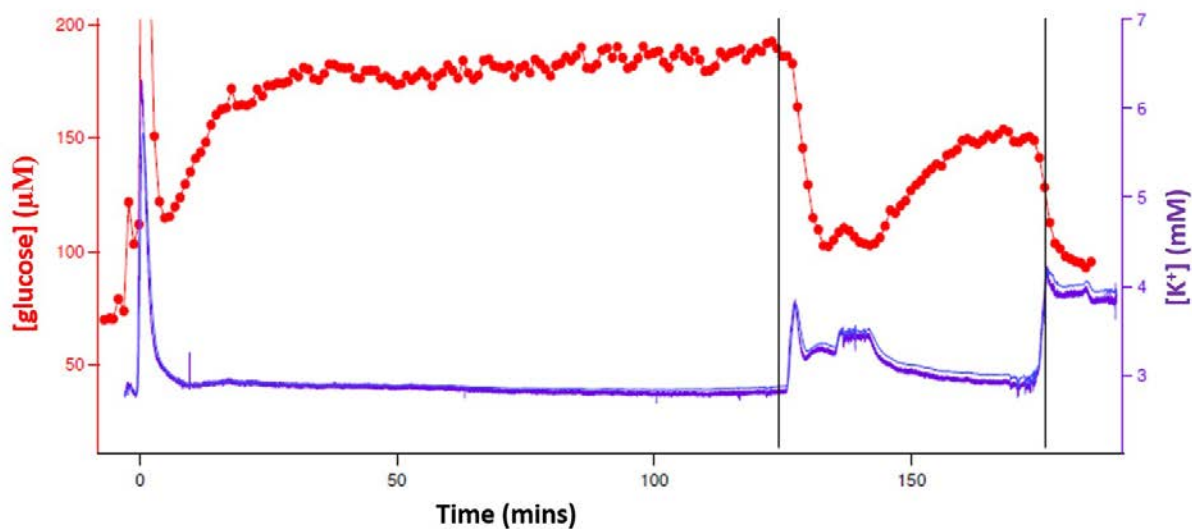
Figure 4-S2.
Overall trace of an acute study in which the rat died approximately 1 hr after the first needle prick. The first vertical black line represents the needle prick. The second vertical black line marks the sudden death of the animal. Probe inserted at time zero.
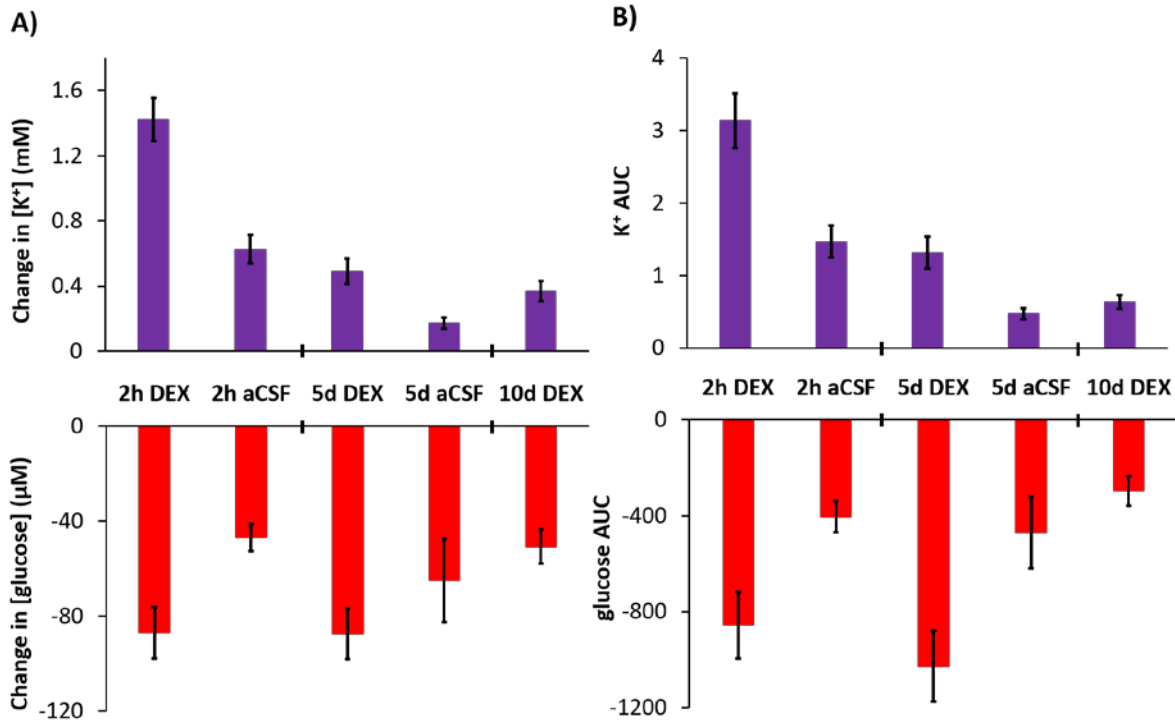
Figure 4-S3.
Data presented in the manuscript are depicted as changes in K^+ and glucose. The area under the curve (AUC) was also analyzed for each SD response. The A) maximum changes in concentration and B) AUC have similar trends for the 5 groups analyzed.
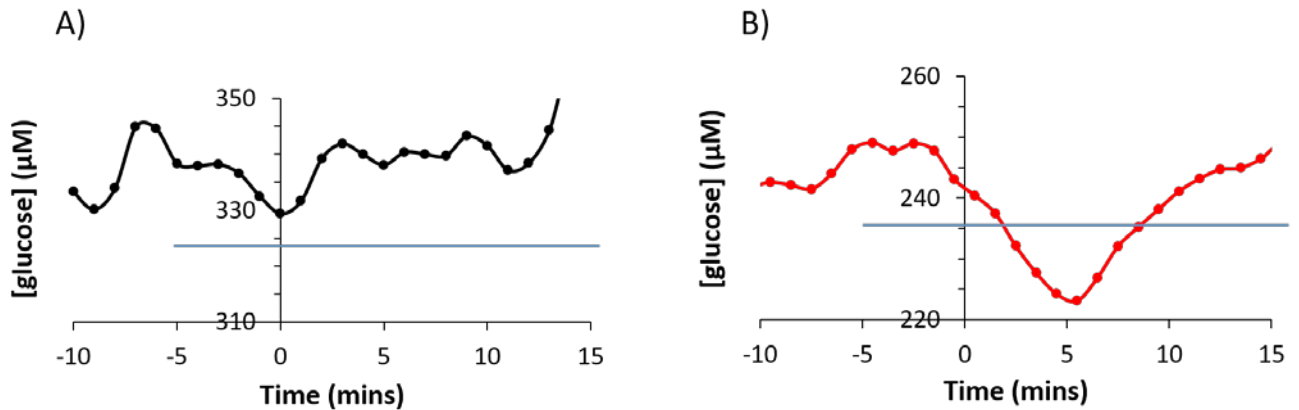
Figure 4-S4.
Characterization of a significant change in glucose. A 10 minute baseline was established prior to the SD (time zero). The baseline was used to create a threshold signal to noise ratio, defined as three times the baseline noise level. If the glucose signal drops below the threshold (blue line above) in the 15 minutes post SD it was included as a detectable glucose signal and was used in the figures and calculations. Figure A is an example of an undetectable signal, obtained from the first needle prick of a probe perfused with aCSF for 5 days. Figure B is an example of a detectable signal, obtained from the third needle prick of a probe perfused with DEX for 10 days (days 1-5 were DEX and days 5-10 were aCSF).

5.0   CONCLUSIONS

The results presented in this dissertation confirm dexamethasone retrodialysis mitigates the tissue response to the probe insertion and enhances long-term neurochemical sampling from the rat brain.

Our studies agree with previous observations that inserting a microdialysis probe into the brain tissue results in a penetration injury and ensuing tissue response.[22-35] The progression of the tissue response creates a time-dependent neurochemical disruption in the surrounding area.[36-40] This disruption hinders the ability of the probe to provide an accurate representation of the chemical changes occurring in the undisturbed tissue.

Our studies show that perfusing dexamethasone (DEX), a glucocorticoid anti-inflammatory agent, through the microdialysis probe mitigates the tissue response and preserves the neurochemical sampling for up to 10 days after probe insertion. The efficacy of DEX appears to be due to its anti-inflammatory actions rather than any direct neurochemical impact. Histochemical analysis confirmed DEX suppresses microglia activation, reinstated blood flow, and prevented the formation of a glial barrier around the microdialysis probe track.[35] Additionally, histochemical markers for dopamine terminals appeared normal at both 24 h and 5 days after probe insertion regardless of the perfusion fluid containing DEX or not.[34, 35]

We first evaluated the benefits of DEX retrodialysis by using fast scan cyclic voltammetry to measure evoked dopamine release in the rat striatum next to and at the outlet of

85

microdialysis probes. The probe insertion injury created a gradient of dopamine release around the microdialysis probe, resulting in evoked responses being undetectable at the probe outlet without the aid of an uptake inhibitor. However, combining DEX retrodialysis with a 5-day postimplantation wait period reinstated normal evoked dopamine activity next to the probe and brought the responses at the probe outlet into quantitative agreement with the in vivo responses. Previous studies found that uptake inhibition increased the in vivo probe recovery of dopamine due to a zone of disrupted tissue adjacent to the probe.[22-24, 40, 58, 119, 60, 59] The quantitative agreement between the responses in the dialysate and responses next to the probe after 5 days with DEX suggests the zone of disrupted tissue is no longer present.

Our second study confirmed the microdialysis enhancement achieved with DEX is transferable to the rat cortex, to monitoring K^+ and glucose transients following induced spreading depolarization, and to 10 days after probe insertion. The initial insertion of the microdialysis probe caused a spreading depolarization, supporting prior evidence of the tissue disruption during probe insertion. When comparing responses 2 h and 5 days after probe insertion, without DEX the K^+ responses decreased and the glucose responses became essentially undetectable after 5 days. However with DEX glucose transients were quantifiable at 2 h, 5 days, and 10 days after probe insertion. In the 10 day study DEX was removed from the perfusion fluid after 5 days, thus the benefits of DEX outlast the retrodialysis itself. This is significant as it is ideal to use the minimum amount of an exogenous agent while still maintaining the anti-inflammatory effects. While our studies have established the anti-inflammatory enhancement of microdialysis using DEX, it is important to note that other strategies including the choice of the anti-inflammatory agent, dose, and duration are available for future studies.

5.1   FUTURE DIRECTIONS

The future of dexamethasone enhanced microdialysis has the potential to significantly impact long-term microdialysis studies for both animal models and human patients. Mitigating the tissue response with the retrodialysis of an anti-inflammatory agent is a simple and effective method that can be easily translated to other microdialysis studies. Microdialysis is an exceptionally versatile technique, thus enhancing microdialysis with dexamethasone extends beyond the analytes and research areas investigated thus far.

The work presented herein focused on using dexamethasone as the anti-inflammatory agent to mitigate the tissue response to the microdialysis probe insertion. We did not encounter any neurochemical perturbations associated with the use of a steroidal anti-inflammatory agent. However, steroids are known to be active in the brain, thus depending on the application, future investigations may be interested in non-steroidal alternatives.

The use of microdialysis in animal models has vastly contributed to our understanding of the neurochemistry in the living brain. Currently, most microdialysis studies rely on repeated probe insertions or multiple animals to evaluate the neurochemical changes that occur over time. Using dexamethasone enhanced microdialysis will provide future investigations with extended monitoring from a single animal. Our observations have shown that 5 days of dexamethasone retrodialysis enhances microdialysis sampling for up to 10 days after probe insertion. It will be important for future investigations to extend this time frame and explore the mitigation of the initial tissue response with 5 days of dexamethasone and its impact on microdialysis studies weeks or months after the initial probe insertion.

In addition to animal models, microdialysis is exceptionally beneficial for clinical applications. Microdialysis is currently used to monitor patients with traumatic brain injury to

identify episodes of spreading depolarization, a form of secondary brain injury. Clinical microdialysis studies are currently research based, thus the data obtained are not used for patient diagnosis or care. However, investigators are interested in using microdialysis not only to identify the frequency and duration of spreading depolarization, but also to develop targeted treatment methods. Events of spreading depolarization occur in approximately 60% of traumatic brain injured patients, contributing to the heterogeneity of this disease. Real time monitoring of spreading depolarization would allow not only for personalized treatment plans but also evaluation of the therapeutic effect during treatment. Our work has shown that dexamethasone enhances the microdialysis sampling K^+ and glucose transients following spreading depolarization in an animal model for up to 10 days after probe insertion. Translating this work into clinical applications will improve the identification of spreading depolarization, and aid in the understanding and treatment of this complex disease.

BIBLIOGRAPHY

[1] Robinson, T. E., and Justice, J. B., Eds (1991) *Techniques in the Behavioral and Neural Sciences*, Vol. *7: Microdialysis in the Neurosciences*, Elsevier, Amsterdam.

[2] Davies, M. I., Cooper, J. D., Desmond, S. S., Lunte, C. E., and Lunte, S. M. (2000) Analytical considerations for microdialysis sampling, *Adv. Drug Delivery Rev. 45*, 169-188.

[3] Watson, C. J., Venton, B. J., and Kennedy, R. T. (2006) In Vivo Measurements of Neurotransmitters by Microdialysis Sampling, *Anal. Chem. 78*, 1391-1399.

[4] Westerink, B. H., and Cremers, T. I. F. H., Eds (2007) *Handbook of Microdilaysis: Methods, Applications and Perspectivies*, Academic Press, London.

[5] Matzneller, P., and Brunner, M. (2011) Recent advances in clinical microdialysis, *TrAC Trends Anal. Chem. 30*, 1497-1504.

[6] Kennedy, R. T. (2013) Emerging trends in in vivo neurochemical monitoring by microdialysis, *Curr. Opin. Chem. Biol. 17*, 860-867.

[7] Ganesana, M., Lee, S. T., Wang, Y., and Venton, B. J. (2017) Analytical Techniques in Neuroscience: Recent Advances in Imaging, Separation, and Electrochemical Methods, *Anal. Chem. 89*, 314-341.

[8] Yang, H., Thompson, A. B., McIntosh, B. J., Altieri, S. C., and Andrews, A. M. (2013) Physiologically Relevant Changes in Serotonin Resolved by Fast Microdialysis, *ACS Chem. Neurosci. 4*, 790-798.

[9] Vander Weele, C. M., Porter-Stransky, K. A., Mabrouk, O. S., Lovic, V., Singer, B. F., Kennedy, R. T., and Aragona, B. J. (2014) Rapid dopamine transmission within the nucleus accumbens: dramatic difference between morphine and oxycodone delivery, *Eur. J. Neurosci. 40*, 3041-3054.

[10] Wang, M., Slaney, T., Mabrouk, O., and Kennedy, R. T. (2010) Collection of nanoliter microdialysate fractions in plugs for off-line in vivo chemical monitoring with up to 2 s temporal resolution, *J. Neurosci. Methods. 190*, 39-48.

[11] Gu, H., Varner, E. L., Groskreutz, S. R., Michael, A. C., and Weber, S. G. (2015) In Vivo Monitoring of Dopamine by Microdialysis with 1 min Temporal Resolution Using Online Capillary Liquid Chromatography with Electrochemical Detection, *Anal. Chem. 87*, 6088-6094.

[12] Zhang, J., Jaquins-Gerstl, A., Nesbitt, K. M., Rutan, S. C., Michael, A. C., and Weber, S. G. (2013) In vivo monitoring of serotonin in the striatum of freely moving rats with one minute temporal resolution by online microdialysis-capillary high-performance liquid chromatography at elevated temperature and pressure, *Anal. Chem. 85*, 9889-9897.

[13] Nandi, P., Scott, D. E., Desai, D., and Lunte, S. M. (2013) Development and optimization of an integrated PDMS based-microdialysis microchip electrophoresis device with on-chip derivatization for continuous monitoring of primary amines, *Electrophoresis. 34*, 895-902.

[14] Pitz, M. W., Desai, A., Grossman, S. A., and Blakeley, J. O. (2011) Tissue concentration of systemically administered antineoplastic agents in human brain tumors, *J. Neurooncol. 104*, 629-638.

[15] Lam, H. A., Wu, N., Cely, I., Kelly, R. L., Hean, S., Richter, F., Magen, I., Cepeda, C., Ackerson, L. C., Walwyn, W., Masliah, E., Chesselet, M. F., Levine, M. S., and Maidment, N. T. (2011) Elevated tonic extracellular dopamine concentration and altered dopamine modulation of synaptic activity precede dopamine loss in the striatum of mice overexpressing human alpha-synuclein, *J. Neurosci. Res. 89*, 1091-1102.

[16] Feuerstein, D., Manning, A., Hashemi, P., Bhatia, R., Fabricius, M., Tolias, C., Pahl, C., Ervine, M., Strong, A. J., and Boutelle, M. G. (2010) Dynamic metabolic response to multiple spreading depolarizations in patients with acute brain injury: an online microdialysis study, *J. Cereb. Blood Flow Metab. 30*, 1343-1355.

[17] Parkin, M., Hopwood, S., Jones, D. A., Hashemi, P., Landolt, H., Fabricius, M., Lauritzen, M., Boutelle, M. G., and Strong, A. J. (2005) Dynamic changes in brain glucose and lactate in pericontusional areas of the human cerebral cortex, monitored with rapid sampling on-line microdialysis: relationship with depolarisation-like events, *J. Cereb. Blood Flow Metab. 25*, 402-413.

[18] Justice, J. B., Jr. (1993) Quantitative microdialysis of neurotransmitters, *J. Neurosci. Methods. 48*, 263-276.

[19] Lonnroth, P., Jansson, P. A., and Smith, U. (1987) A microdialysis method allowing characterization of intercellular water space in humans, *Am. J. Physiol. 253*, E228-231.

[20] Stenken, J. A. (1999) Methods and issues in microdialysis calibration, *Anal. Chim. Acta. 379*, 337-358.

[21] Hershey, N. D., and Kennedy, R. T. (2013) In Vivo Calibration of Microdialysis Using Infusion of Stable-Isotope Labeled Neurotransmitters, *ACS Chem. Neurosci. 4*, 729-736.

[22] Bungay, P. M., Newton-Vinson, P., Isele, W., Garris, P. A., and Justice, J. B. (2003) Microdialysis of dopamine interpreted with quantitative model incorporating probe implantation trauma, *J. Neurochem. 86*, 932-946.

[23] Lu, Y., Peters, J. L., and Michael, A. C. (1998) Direct comparison of the response of voltammetry and microdialysis to electrically evoked release of striatal dopamine, *J. Neurochem. 70*, 584-593.

[24] Borland, L. M., Shi, G., Yang, H., and Michael, A. C. (2005) Voltammetric study of extracellular dopamine near microdialysis probes acutely implanted in the striatum of the anesthetized rat, *J. Neurosci. Methods. 146*, 149-158.

[25] Benveniste, H., and Diemer, N. H. (1987) Cellular reactions to implantation of a microdialysis tube in the rat hippocampus, *Acta Neuropathol. 74*, 234-238.

[26] Clapp-Lilly, K. L., Roberts, R. C., Duffy, L. K., Irons, K. P., Hu, Y., and Drew, K. L. (1999) An ultrastructural analysis of tissue surrounding a microdialysis probe, *J. Neurosci. Methods. 90*, 129-142.

[27] Hascup, E. R., af Bjerken, S., Hascup, K. N., Pomerleau, F., Huettl, P., Stromberg, I., and Gerhardt, G. A. (2009) Histological studies of the effects of chronic implantation of ceramic-based microelectrode arrays and microdialysis probes in rat prefrontal cortex, *Brain Res. 1291*, 12-20.

[28] Zhou, F., Zhu, X., Castellani, R. J., Stimmelmayr, R., Perry, G., Smith, M. A., and Drew, K. L. (2001) Hibernation, a model of neuroprotection, *Am. J Pathol. 158*, 2145-2151.

[29] Cepeda, D. E., Hains, L., Li, D., Bull, J., Lentz, S. I., and Kennedy, R. T. (2015) Experimental evaluation and computational modeling of tissue damage from low-flow push-pull perfusion sampling in vivo, *J. Neurosci. Methods. 242*, 97-105.

[30] Jaquins-Gerstl, A., and Michael, A. C. (2009) Comparison of the brain penetration injury associated with microdialysis and voltammetry, *J. Neurosci. Methods. 183*, 127-135.

[31] Jaquins-Gerstl, A., Shu, Z., Zhang, J., Liu, Y., Weber, S. G., and Michael, A. C. (2011) Effect of dexamethasone on gliosis, ischemia, and dopamine extraction during microdialysis sampling in brain tissue, *Anal. Chem. 83*, 7662-7667.

[32] Kozai, T. D., Jaquins-Gerstl, A. S., Vazquez, A. L., Michael, A. C., and Cui, X. T. (2016) Dexamethasone retrodialysis attenuates microglial response to implanted probes in vivo, *Biomaterials. 87*, 157-169.

[33] Nesbitt, K. M., Jaquins-Gerstl, A., Skoda, E. M., Wipf, P., and Michael, A. C. (2013) Pharmacological Mitigation of Tissue Damage during Brain Microdialysis, *Anal. Chem. 85*, 8173-8179.

[34] Nesbitt, K. M., Varner, E. L., Jaquins-Gerstl, A., and Michael, A. C. (2015) Microdialysis in the Rat Striatum: Effects of 24 h Dexamethasone Retrodialysis on Evoked Dopamine Release and Penetration Injury, *ACS Chem. Neurosci. 6*, 163-173.

[35] Varner, E. L., Jaquins-Gerstl, A., and Michael, A. C. (2016) Enhanced Intracranial Microdialysis by Reduction of Traumatic Penetration Injury at the Probe Track, *ACS Chem. Neurosci. 7*, 728-736.

[36] Robinson, T. E., and Camp, D. M. (1991) The effects of four days of continuous striatal microdialysis on indices of dopamine and serotonin neurotransmission in rats, *J. Neurosci. Methods. 40*, 211-222.

[37] Holson, R. R., Bowyer, J. F., Clausing, P., and Gough, B. (1996) Methamphetamine-stimulated striatal dopamine release declines rapidly over time following microdialysis probe insertion, *Brain Res. 739*, 301-307.

[38] Holson, R. R., Gazzara, R. A., and Gough, B. (1998) Declines in stimulated striatal dopamine release over the first 32 h following microdialysis probe insertion: generalization across releasing mechanisms, *Brain Res. 808*, 182-189.

[39] Sharp, T., Ljungberg, T., Zetterstrom, T., and Ungerstedt, U. (1986) Intracerebral dialysis coupled to a novel activity box--a method to monitor dopamine release during behaviour, *Pharmacol. Biochem. Behav. 24*, 1755-1759.

[40] Yang, H., and Michael, A. C. (2007) In Vivo Fast-Scan Cyclic Voltammetry of Dopamine near Microdialysis Probes, In *Electrochemical Methods for Neuroscience* (Michael, A. C., and Borland, L. M. Eds.), CRC Press, Boca Raton (FL).

[41] Westerink, B. H. C., and De Vries, J. B. (1988) Characterization of In Vivo Dopamine Release as Determined by Brain Microdialysis After Acute and Subchronic Implantations: Methodological Aspects, *J. Neurochem. 51*, 683-687.

[42] Groothuis, J., Ramsey, N. F., Ramakers, G. M., and van der Plasse, G. (2014) Physiological challenges for intracortical electrodes, *Brain Stimul. 7*, 1-6.

[43] Grill, W. M., Norman, S. E., and Bellamkonda, R. V. (2009) Implanted neural interfaces: biochallenges and engineered solutions, *Annu. Rev. Biomed. Eng. 11*, 1-24.

[44] Polikov, V. S., Tresco, P. A., and Reichert, W. M. (2005) Response of brain tissue to chronically implanted neural electrodes, *J. Neurosci. Methods. 148*, 1-18.

[45] Keeler, G. D., Durdik, J. M., and Stenken, J. A. (2015) Localized delivery of dexamethasone-21-phosphate via microdialysis implants in rat induces M(GC) macrophage polarization and alters CCL2 concentrations, *Acta Biomater. 12*, 11-20.

[46] Spataro, L., Dilgen, J., Retterer, S., Spence, A. J., Isaacson, M., Turner, J. N., and Shain, W. (2005) Dexamethasone treatment reduces astroglia responses to inserted neuroprosthetic devices in rat neocortex, *Exp. Neurol. 194*, 289-300.

[47] Zhong, Y., and Bellamkonda, R. V. (2007) Dexamethasone-coated neural probes elicit attenuated inflammatory response and neuronal loss compared to uncoated neural probes, *Brain Res. 1148*, 15-27.

[48] Phillips, P. E., Stuber, G. D., Heien, M. L., Wightman, R. M., and Carelli, R. M. (2003) Subsecond dopamine release promotes cocaine seeking, *Nature 422*, 614-618.

[49] Lotharius, J., and Brundin, P. (2002) Pathogenesis of Parkinson's disease: dopamine, vesicles and alpha-synuclein, *Nature Rev. Neurosci. 3*, 932-942.

[50] Brisch, R., Saniotis, A., Wolf, R., Bielau, H., Bernstein, H.-G., Steiner, J., Bogerts, B., Braun, K., Jankowski, Z., Kumaratilake, J., Henneberg, M., and Gos, T. (2014) The Role of Dopamine in Schizophrenia from a Neurobiological and Evolutionary Perspective: Old Fashioned, but Still in Vogue, *Front. Psychiatry. 5*, 47.

[51] Schultz, W. (2007) Multiple dopamine functions at different time courses, *Annu. Rev. Neurosci. 30*, 259-288.

[52] Ford, C. P. (2014) The Role of D2-Autoreceptors in Regulating Dopamine Neuron Activity and Transmission, *Neuroscience. 282*, 13-22.

[53] Garris, P. A., and Mark Wightman, R. (1995) Regional Differences in Dopamine Release, Uptake, and Diffusion Measured by Fast-Scan Cyclic Voltammetry, In *Voltammetric Methods in Brain Systems* (Boulton, A. A., Baker, G. B., and Adams, R. N. Eds.), pp 179-220, Humana Press, Totowa, NJ.

[54] Robinson, D. L., Venton, B. J., Heien, M. L., and Wightman, R. M. (2003) Detecting subsecond dopamine release with fast-scan cyclic voltammetry in vivo, *Clin. Chem. 49*, 1763-1773.

[55] Michael, A. C., and Borland, L., Eds. (2006) *Electrochemical Methods for Neuroscience*, CRC Press, Boca Raton, FL.

[56] Howell, J. O., Kuhr, W. G., Ensman, R. E., and Mark Wightman, R. (1986) Background subtraction for rapid scan voltammetry, *J. Electroanal. Chem. Interfacial Electrochem. 209*, 77-90.

[57] Wang, Y., and Michael, A. C. (2012) Microdialysis probes alter presynaptic regulation of dopamine terminals in rat striatum, *J. Neurosci. Methods. 208*, 34-39.

[58] Yang, H., Peters, J. L., and Michael, A. C. (1998) Coupled effects of mass transfer and uptake kinetics on in vivo microdialysis of dopamine, *J. Neurochem. 71*, 684-692.

[59] Yang, H., Peters, J. L., Allen, C., Chern, S. S., Coalson, R. D., and Michael, A. C. (2000) A theoretical description of microdialysis with mass transport coupled to chemical events, *Anal. Chem. 72*, 2042-2049.

[60] Peters, J. L., and Michael, A. C. (1998) Modeling voltammetry and microdialysis of striatal extracellular dopamine: the impact of dopamine uptake on extraction and recovery ratios, *J. Neurochem. 70*, 594-603.

[61] Langlois, J. A., Rutland-Brown, W., and Wald, M. M. (2006) The epidemiology and impact of traumatic brain injury: a brief overview, *J. Head Trauma Rehabil. 21*, 375-378.

[62] The Lancet Neurology (2010) Traumatic brain injury: time to end the silence, *Lancet Neurol. 9*, 331.

[63] Faul M, X. L., Wald MM, Conrodado V. (2010) Traumatic brain injury in the United States: Emergency Department Visits, Hospitalizations and Deaths 2002-2006, *Centers for Disease Control and Prevention, National Center for Injury Prevention and Control, Atlanta, GA.*

[64] Ayata, C., and Lauritzen, M. (2015) Spreading Depression, Spreading Depolarizations, and the Cerebral Vasculature, *Physiol. Rev. 95*, 953-993.

[65] Dreier, J. P. (2011) The role of spreading depression, spreading depolarization and spreading ischemia in neurological disease, *Nat. Med. 17*, 439-447.

[66] Dreier, J. P. (2016) Recording, analysis, and interpretation of spreading depolarizations in neurointensive care: Review and recommendations of the COSBID research group, *J. Cereb. Blood Flow Metab*. 37, 1595-1625.

[67] Nakamura, H., Strong, A. J., Dohmen, C., Sakowitz, O. W., Vollmar, S., Sué, M., Kracht, L., Hashemi, P., Bhatia, R., Yoshimine, T., Dreier, J. P., Dunn, A. K., and Graf, R. (2010) Spreading depolarizations cycle around and enlarge focal ischaemic brain lesions, *Brain 133*, 1994.

[68] Lauritzen, M., Dreier, J. P., Fabricius, M., Hartings, J. A., Graf, R., and Strong, A. J. (2011) Clinical relevance of cortical spreading depression in neurological disorders: migraine, malignant stroke, subarachnoid and intracranial hemorrhage, and traumatic brain injury, *J. Cereb. Blood Flow Metab. 31*, 17-35.

[69] Hartings, J. A., Bullock, M. R., Okonkwo, D. O., Murray, L. S., Murray, G. D., Fabricius, M., Maas, A. I., Woitzik, J., Sakowitz, O., Mathern, B., Roozenbeek, B., Lingsma, H., Dreier, J. P., Puccio, A. M., Shutter, L. A., Pahl, C., and Strong, A. J. (2011) Spreading depolarisations and outcome after traumatic brain injury: a prospective observational study, *Lancet Neurol. 10*, 1058-1064.

[70] Hartings, J. A., Watanabe, T., Bullock, M. R., Okonkwo, D. O., Fabricius, M., Woitzik, J., Dreier, J. P., Puccio, A., Shutter, L. A., Pahl, C., and Strong, A. J. (2011) Spreading depolarizations have prolonged direct current shifts and are associated with poor outcome in brain trauma, *Brain 134*, 1529.

[71] Hartings, J. A., Strong, A. J., Fabricius, M., Manning, A., Bhatia, R., Dreier, J. P., Mazzeo, A. T., Tortella, F. C., and Bullock, M. R. (2009) Spreading depolarizations and late secondary insults after traumatic brain injury, *J. Neurotrauma 26*, 1857-1866.

[72] Dreier, J. P., Woitzik, J., Fabricius, M., Bhatia, R., Major, S., Drenckhahn, C., Lehmann, T. N., Sarrafzadeh, A., Willumsen, L., Hartings, J. A., Sakowitz, O. W., Seemann, J. H., Thieme, A., Lauritzen, M., and Strong, A. J. (2006) Delayed ischaemic neurological deficits after subarachnoid haemorrhage are associated with clusters of spreading depolarizations, *Brain 129*, 3224-3237.

[73] Fabricius, M., Fuhr, S., Bhatia, R., Boutelle, M., Hashemi, P., Strong, A. J., and Lauritzen, M. (2006) Cortical spreading depression and peri-infarct depolarization in acutely injured human cerebral cortex, *Brain 129*, 778-790.

[74] Osier, N. D., and Dixon, C. E. (2016) The Controlled Cortical Impact Model: Applications, Considerations for Researchers, and Future Directions, *Front. Neurol. 7*. 134

[75] Jones, D. A., Parkin, M. C., Langemann, H., Landolt, H., Hopwood, S. E., Strong, A. J., and Boutelle, M. G. (2002) On-line monitoring in neurointensive care: Enzyme-based electrochemical assay for simultaneous, continuous monitoring of glucose and lactate from critical care patients, *J. Electroanal. Chem. 538–539*, 243-252.

[76] Rogers, M. L., Feuerstein, D., Leong, C. L., Takagaki, M., Niu, X., Graf, R., and Boutelle, M. G. (2013) Continuous Online Microdialysis Using Microfluidic Sensors: Dynamic Neurometabolic Changes during Spreading Depolarization, *ACS Chem. Neurosci. 4*, 799-807.

[77] Papadimitriou, K. I., Wang, C., Rogers, M. L., Gowers, S. A., Leong, C. L., Boutelle, M. G., and Drakakis, E. M. (2016) High-Performance Bioinstrumentation for Real-Time Neuroelectrochemical Traumatic Brain Injury Monitoring, *Front. Hum. Neurosci. 10*, 212.

[78] Rogers, M. L., Leong, C. L., Gowers, S. A., Samper, I. C., Jewell, S. L., Khan, A., McCarthy, L., Pahl, C., Tolias, C. M., Walsh, D. C., Strong, A. J., and Boutelle, M. G. (2016) Simultaneous monitoring of potassium, glucose and lactate during spreading

depolarisation in the injured human brain - Proof of principle of a novel real-time neurochemical analysis system, continuous online microdialysis, *J. Cereb. Blood Flow Metab.37, 1883.*

[79] Ungerstedt, U. (1984) Measurement of neurotransmitter release by intracranial dialysis, In *In Measurement of Neurotransmitter Release In Vivo* (Marsden, C. A., Ed.), pp 81-105, John Wiley & Sons, New York.

[80] Badiani, A., Oates, M. M., Day, H. E., Watson, S. J., Akil, H., and Robinson, T. E. (1998) Amphetamine-induced behavior, dopamine release, and c-fos mRNA expression: modulation by environmental novelty, *J. Neurosci. 18*, 10579-10593.

[81] El Arfani, A., Bentea, E., Aourz, N., Ampe, B., De Deurwaerdere, P., Van Eeckhaut, A., Massie, A., Sarre, S., Smolders, I., and Michotte, Y. (2014) NMDA receptor antagonism potentiates the L-DOPA-induced extracellular dopamine release in the subthalamic nucleus of hemi-parkinson rats, *Neuropharmacol. 85*, 198-205.

[82] Sharp, T., Maidment, N. T., Brazell, M. P., Zetterström, T., Ungerstedt, U., Bennett, G. W., and Marsden, C. A. (1984) Changes in monoamine metabolites measured by simultaneous in vivo differential pulse voltammetry and intracerebral dialysis, *Neuroscience. 12*, 1213-1221.

[83] Sharp, T., Zetterstrom, T., Ljungberg, T., and Ungerstedt, U. (1987) A direct comparison of amphetamine-induced behaviours and regional brain dopamine release in the rat using intracerebral dialysis, *Brain Res. 401*, 322-330.

[84] Di Chiara, G., Tanda, G., and Carboni, E. (1996) Estimation of in-vivo neurotransmitter release by brain microdialysis: the issue of validity, *Behav. Pharmacol. 7*, 640-657.

[85] Bosche, B., Dohmen, C., Graf, R., Neveling, M., Staub, F., Kracht, L., Sobesky, J., Lehnhardt, F.-G., and Heiss, W.-D. (2003) Extracellular Concentrations of Non–Transmitter Amino Acids in Peri-Infarct Tissue of Patients Predict Malignant Middle Cerebral Artery Infarction, *Stroke. 34*, 2908-2913.

[86] Tossman, U., Eriksson, S., Delin, A., Hagenfeldt, L., Law, D., and Ungerstedt, U. (1983) Brain amino acids measured by intracerebral dialysis in portacaval shunted rats, *J. Neurochem. 41*, 1046-1051.

[87] Wright, I. K., Upton, N., and Marsden, C. A. (1992) Effect of established and putative anxiolytics on extracellular 5-HT and 5-HIAA in the ventral hippocampus of rats during behaviour on the elevated X-maze, *Psychopharm. 109*, 338-346.

[88] Westerink, B. H. C. (1995) Brain microdialysis and its application for the study of animal behaviour, *Behav. Brain Res. 70*, 103-124.

[89] Carboni, E., Spielewoy, C., Vacca, C., Nosten-Bertrand, M., Giros, B., and Di Chiara, G. (2001) Cocaine and amphetamine increase extracellular dopamine in the nucleus accumbens of mice lacking the dopamine transporter gene, *J. Neurosci. 21*, Rc141: 141-144.

[90] Di Chiara, G., and Imperato, A. (1988) Drugs abused by humans preferentially increase synaptic dopamine concentrations in the mesolimbic system of freely moving rats, *Proc. Natl. Acad. Sci. U. S. A. 85*, 5274-5278.

[91] Arbuthnott, G. W., Fairbrother, I. S., and Butcher, S. P. (1990) Brain microdialysis studies on the control of dopamine release and metabolism in vivo, *J. Neurosci. Methods. 34*, 73-81.

[92] Zetterström, T., Sharp, T., Marsden, C. A., and Ungerstedt, U. (1983) In Vivo Measurement of Dopamine and Its Metabolites by Intracerebral Dialysis: Changes After d-Amphetamine, *J. Neurochem. 41*, 1769-1773.

[93] Abercrombie, E. D., and Zigmond, M. J. (1989) Partial injury to central noradrenergic neurons: reduction of tissue norepinephrine content is greater than reduction of extracellular norepinephrine measured by microdialysis, *J. Neurosci. 9*, 4062-4067.

[94] Kehr, J. (2006) Chapter 2.1 New methodological aspects of microdialysis, In *Handbook of Behavioral Neuroscience* (Ben, H. C. W., and Thomas, I. F. H. C., Eds.), pp 111-129, Elsevier.

[95] Chefer, V. I., Thompson, A. C., Zapata, A., and Shippenberg, T. S. (2009) Overview of brain microdialysis, *Current Protocols in Neuroscience;* John wiley & Sons, Inc. New York.

[96] Lee, W. H., Slaney, T. R., Hower, R. W., and Kennedy, R. T. (2013) Microfabricated Sampling Probes for in Vivo Monitoring of Neurotransmitters, *Anal. Chem. 85*, 3828-3831.

[97] Shou, M., Ferrario, C. R., Schultz, K. N., Robinson, T. E., and Kennedy, R. T. (2006) Monitoring Dopamine in Vivo by Microdialysis Sampling and On-Line CE-Laser-Induced Fluorescence, *Anal. Chem. 78*, 6717-6725.

[98] Emmett, M. R., Andrén, P. E., and Caprioli, R. M. (1995) Specific molecular mass detection of endogenously released neuropeptides using in vivo microdialysis/mass spectrometry, *J. Neurosci. Methods. 62*, 141-147.

[99] Scott, D. E., Grigsby, R. J., and Lunte, S. M. (2013) Microdialysis Sampling Coupled to Microchip Electrophoresis with Integrated Amperometric Detection on an All-Glass Substrate, *Chem-PhysChem 14*, 2288-2294.

[100] Bert, L., Parrot, S., Robert, F., Desvignes, C., Denoroy, L., Suaud-Chagny, M. F., and Renaud, B. (2002) In vivo temporal sequence of rat striatal glutamate, aspartate and dopamine efflux during apomorphine, nomifensine, NMDA and PDC in situ administration, *Neuropharmacol. 43*, 825-835.

[101] Santiago, M., and Westerink, B. H. (1990) Characterization of the in vivo release of dopamine as recorded by different types of intracerebral microdialysis probes, *Naunyn-Schmiedeberg's Arch. Pharmacol. 342*, 407-414.

[102] Parrot, S., Bert, L., Mouly-Badina, L., Sauvinet, V., Colussi-Mas, J., Lambas-Senas, L., Robert, F., Bouilloux, J. P., Suaud-Chagny, M. F., Denoroy, L., and Renaud, B. (2003) Microdialysis monitoring of catecholamines and excitatory amino acids in the rat and mouse brain: recent developments based on capillary electrophoresis with laser-induced fluorescence detection--a mini-review, *Cell. Mol. Neurobiol. 23*, 793-804.

[103] Li, Q., Zubieta, J.-K., and Kennedy, R. T. (2009) Practical Aspects of in Vivo Detection of Neuropeptides by Microdialysis Coupled Off-Line to Capillary LC with Multistage MS, *Anal. Chem. 81*, 2242-2250.

[104] Hopwood, S. E., Parkin, M. C., Bezzina, E. L., Boutelle, M. G., and Strong, A. J. (2005) Transient changes in cortical glucose and lactate levels associated with peri-infarct depolarisations, studied with rapid-sampling microdialysis, *J. Cereb. Blood Flow Metab. 25*, 391-401.

[105] Mitala, C. M., Wang, Y., Borland, L. M., Jung, M., Shand, S., Watkins, S., Weber, S. G., and Michael, A. C. (2008) Impact of microdialysis probes on vasculature and dopamine in the rat striatum: a combined fluorescence and voltammetric study, *J. Neurosci. Methods. 174*, 177-185.

[106] Major, O., Shdanova, T., Duffek, L., and Nagy, Z. (1990) Continuous monitoring of blood-brain barrier opening to Cr51-EDTA by microdialysis following probe injury, *Acta Neurochir. Suppl. (Wien) 51*, 46-48.

[107] Planas, A. M., Justicia, C., Sole, S., Friguls, B., Cervera, A., Adell, A., and Chamorro, A. (2002) Certain forms of matrix metalloproteinase-9 accumulate in the extracellular space after microdialysis probe implantation and middle cerebral artery occlusion/reperfusion, *J. Cereb. Blood Flow Metab. 22*, 918-925.

[108] Kadota, E., Nonaka, K., Karasuno, M., Nishi, K., Nakamura, Y., Namikawa, K., Okazaki, Y., Teramura, K., and Hashimoto, S. (1994) Experimental quantitative evaluation of transvascular removal of unnecessary substances in brain edema fluid, *Acta Neurochir. Suppl. (Wien) 60*, 162-164.

[109] Benveniste, H., Drejer, J., Schousboe, A., and Diemer, N. H. (1987) Regional cerebral glucose phosphorylation and blood flow after insertion of a microdialysis fiber through the dorsal hippocampus in the rat, *J. Neurochem. 49*, 729-734.

[110] Davalos, D., Grutzendler, J., Yang, G., Kim, J. V., Zuo, Y., Jung, S., Littman, D. R., Dustin, M. L., and Gan, W. B. (2005) ATP mediates rapid microglial response to local brain injury in vivo, *Nat. Neurosci. 8*, 752-758.

[111] Bungay, P. M., Morrison, P. F., and Dedrick, R. L. (1990) Steady-state theory for quantitative microdialysis of solutes and water in vivo and in vitro, *Life Sci. 46*, 105-119.

[112] Tang, A., Bungay, P. M., and Gonzales, R. A. (2003) Characterization of probe and tissue factors that influence interpretation of quantitative microdialysis experiments for dopamine, *J. Neurosci. Methods. 126*, 1-11.

[113] Tang, A., Bungay, P. M., and Gonzales, R. A. (2003) Characterization of probe and tissue factors that influence interpretation of quantitative microdialysis experiments for dopamine, *J. Neurosci. Methods*. *126*, 1-11.

[114] Westerink, B. H., and Tuinte, M. H. (1986) Chronic use of intracerebral dialysis for the in vivo measurement of 3,4-dihydroxyphenylethylamine and its metabolite 3,4-dihydroxyphenylacetic acid, *J. Neurochem. 46*, 181-185.

[115] Imperato, A., and Di Chiara, G. (1985) Dopamine release and metabolism in awake rats after systemic neuroleptics as studied by trans-striatal dialysis, *J. Neurosci. 5*, 297-306.

[116] Church, W. H., Justice, J. B., Jr., and Byrd, L. D. (1987) Extracellular dopamine in rat striatum following uptake inhibition by cocaine, nomifensine and benztropine, *Eur. J. Pharmacol. 139*, 345-348.

[117] Pontieri, F. E., Tanda, G., and Di Chiara, G. (1995) Intravenous cocaine, morphine, and amphetamine preferentially increase extracellular dopamine in the "shell" as compared with the "core" of the rat nucleus accumbens, *Pro. Natl. Acad. Sci. U. S. A. 92*, 12304-12308.

[118] Rahman, S., Zhang, J., Engleman, E. A., and Corrigall, W. A. (2004) Neuroadaptive changes in the mesoaccumbens dopamine system after chronic nicotine self-administration: a microdialysis study, *Neuroscience. 129*, 415-424.

[119] Floresco, S. B., West, A. R., Ash, B., Moore, H., and Grace, A. A. (2003) Afferent modulation of dopamine neuron firing differentially regulates tonic and phasic dopamine transmission, *Nat. Neurosci. 6*, 968-973.

[120] Garris, P. A., Christensen, J. R., Rebec, G. V., and Wightman, R. M. (1997) Real-time measurement of electrically evoked extracellular dopamine in the striatum of freely moving rats, *J. Neurochem. 68*, 152-161.

[121] Moquin, K. F., and Michael, A. C. (2009) Tonic autoinhibition contributes to the heterogeneity of evoked dopamine release in the rat striatum, *J. Neurochem. 110*, 1491-1501.

[122] Chang, S. Y., Kimble, C. J., Kim, I, Paek, S. B., Kressin, K. R., Boesche, J. B., Whitlock, S. V., Eaker, D. R., Kasasbeh, A., Horne, A. E., Blaha, C. D., Bennet, K. E., and Lee, K. H. (2013) Development of the Mayo Investigational Neuromodulation Control System: toward a closed-loop electrochemical feedback system for deep brain stimulation, *J. Neurosurg. 119*, 1556-1565.

[123] Amos, A. N., Roberts, J. G., Qi, L., Sombers, L. A., and McCarty, G. S. (2014) Reducing the Sampling Rate of Biochemical Measurements Using Fast-Scan Cyclic Voltammetry for In Vivo Applications, *IEEE Sens. J. 14*, 2975-2980.

[124] Belle, A. M., Owesson-White, C., Herr, N. R., Carelli, R. M., and Wightman, R. M. (2013) Controlled Iontophoresis Coupled with Fast-Scan Cyclic Voltammetry/Electrophysiology in Awake, Freely Moving Animals, *ACS Chem. Neurosci. 4*, 761-771.

[125] Kita, J. M., Parker, L. E., Phillips, P. E., Garris, P. A., and Wightman, R. M. (2007) Paradoxical modulation of short-term facilitation of dopamine release by dopamine autoreceptors, *J. Neurochem. 102*, 1115-1124.

[126] Ciliax, B. J., Heilman, C., Demchyshyn, L. L., Pristupa, Z. B., Ince, E., Hersch, S. M., Niznik, H. B., and Levey, A. I. (1995) The dopamine transporter: immunochemical characterization and localization in brain, *J. Neurosci. 15*, 1714-1723.

[127] Freed, C., Revay, R., Vaughan, R. A., Kriek, E., Grant, S., Uhl, G. R., and Kuhar, M. J. (1995) Dopamine transporter immunoreactivity in rat brain, *J. Comp. Neurol. 359*, 340-349.

[128] Sesack, S. R., Hawrylak, V. A., Matus, C., Guido, M. A., and Levey, A. I. (1998) Dopamine axon varicosities in the prelimbic division of the rat prefrontal cortex exhibit sparse immunoreactivity for the dopamine transporter, *J. Neurosci. 18*, 2697-2708.

[129] Winslow, B. D., Christensen, M. B., Yang, W. K., Solzbacher, F., and Tresco, P. A. (2010) A comparison of the tissue response to chronically implanted Parylene-C-coated and uncoated planar silicon microelectrode arrays in rat cortex, *Biomaterials. 31*, 9163-9172.

[130] Bezard, E., Dovero, S., Imbert, C., Boraud, T., and Gross, C. E. (2000) Spontaneous long-term compensatory dopaminergic sprouting in MPTP-treated mice, *Synapse. 38*, 363-368.

[131] Finkelstein, D. I., Stanic, D., Parish, C. L., Tomas, D., Dickson, K., and Horne, M. K. (2000) Axonal sprouting following lesions of the rat substantia nigra, *Neuroscience. 97*, 99-112.

[132] Barlow, A. L., Macleod, A., Noppen, S., Sanderson, J., and Guerin, C. J. (2010) Colocalization analysis in fluorescence micrographs: verification of a more accurate calculation of pearson's correlation coefficient, *Microsc. Microanal. 16*, 710-724.

[133] Dunn, K. W., Kamocka, M. M., and McDonald, J. H. (2011) A practical guide to evaluating colocalization in biological microscopy, *Am. J. Physiol.: Cell Physiol. 300*, C723-742.

[134] Costes, S. V., Daelemans, D., Cho, E. H., Dobbin, Z., Pavlakis, G., and Lockett, S. (2004) Automatic and quantitative measurement of protein-protein colocalization in live cells, *Biophys. J. 86*, 3993-4003.

[135] Adler, J., and Parmryd, I. (2010) Quantifying colocalization by correlation: the Pearson correlation coefficient is superior to the Mander's overlap coefficient, *Cytometry A. 77*, 733-742.

[136] Manders, E. M., Stap, J., Brakenhoff, G. J., van Driel, R., and Aten, J. A. (1992) Dynamics of three-dimensional replication patterns during the S-phase, analysed by double labelling of DNA and confocal microscopy, *J. Cell Sci. 103 (Pt 3)*, 857-862.

[137] Manders, E. M. M., Verbeek, F. J., and Aten, J. A. (1993) Measurement of co-localization of objects in dual-colour confocal images, *J. Microsc. 169*, 375-382.

[138] Qian, J., Wu, Y., Yang, H., and Michael, A. C. (1999) An Integrated Decoupler for Capillary Electrophoresis with Electrochemical Detection: Application to Analysis of Brain Microdialysate, *Anal. Chem. 71*, 4486-4492.

[139] Walters, S. H., Robbins, E. M., and Michael, A. C. (2015) Modeling the Kinetic Diversity of Dopamine in the Dorsal Striatum, *ACS Chem. Neurosci. 6*, 1468-1475.

[140] Graeber, M. B., Streit, W. J., and Kreutzberg, G. W. (1989) Identity of ED2-positive perivascular cells in rat brain, *J. Neurosci. Res. 22*, 103-106.

[141] Ferrari, C. C., Depino, A. M., Prada, F., Muraro, N., Campbell, S., Podhajcer, O., Perry, V. H., Anthony, D. C., and Pitossi, F. J. (2004) Reversible demyelination, blood-brain barrier breakdown, and pronounced neutrophil recruitment induced by chronic IL-1 expression in the brain, *Am. J. Phathol. 165*, 1827-1837.

[142] Lecca, D., Cacciapaglia, F., Valentini, V., Acquas, E., and Di Chiara, G. (2007) Differential neurochemical and behavioral adaptation to cocaine after response contingent and noncontingent exposure in the rat, *Psychopharm. 191*, 653-667.

[143] Lecca, D., Cacciapaglia, F., Valentini, V., Gronli, J., Spiga, S., and Di Chiara, G. (2006) Preferential increase of extracellular dopamine in the rat nucleus accumbens shell as compared to that in the core during acquisition and maintenance of intravenous nicotine self-administration, *Psychopharm. 184*, 435-446.

[144] Bassareo, V., Cucca, F., Frau, R., and Di Chiara, G. (2015) Monitoring dopamine transmission in the rat nucleus accumbens shell and core during acquisition of nose-poking for sucrose, *Behav. Brain Res. 287*, 200-206.

[145] Dietrich, J., Rao, K., Pastorino, S., and Kesari, S. (2011) Corticosteroids in brain cancer patients: benefits and pitfalls, *Expert Rev. Clin. Pharmacol. 4*, 233-242.

[146] Iasevoli, F., Aloj, L., Latte, G., Avvisati, L., Marmo, F., Tomasetti, C., Buonaguro, E., Simeoli, C., Pivonello, R., Colao, A., and Bartolomeis, A. (2014) The Glucocorticoid Analog Dexamethasone Alters the Expression and the Distribution of Dopamine Receptors and Enkephalin within Cortico- Subcortical Regions, *Curr. Mol. Pharmacol. 6*, 149-155.

[147] Lammers, C. H., D'Souza, U. M., Qin, Z. H., Lee, S. H., Yajima, S., and Mouradian, M. M. (1999) Regulation of striatal dopamine receptors by corticosterone: an in vivo and in vitro study, *Mol. Brain Res. 69*, 281-285.

[148] Gasser, P. J., Lowry, C. A., and Orchinik, M. (2006) Corticosterone-sensitive monoamine transport in the rat dorsomedial hypothalamus: potential role for organic cation transporter 3 in stress-induced modulation of monoaminergic neurotransmission, *J. Neurosci. 26*, 8758-8766.

[149] Lindley, S. E., Bengoechea, T. G., Schatzberg, A. F., and Wong, D. L. (1999) Glucocorticoid effects on mesotelencephalic dopamine neurotransmission, *Neuropsychopharmacology. 21*, 399-407.

[150] Lindley, S. E., Bengoechea, T. G., Wong, D. L., and Schatzberg, A. F. (2002) Mesotelencephalic dopamine neurochemical responses to glucocorticoid administration and adrenalectomy in Fischer 344 and Lewis rats, *Brain Res. 958*, 414-422.

[151] Paxinos, G., and Watson, C. (1998) *The Rat Brain in Stereotaxic Coordinates*, 4th Edn, Academic Press, San Diego, CA.

[152] Leao, A. A. P. (1944) SPREADING DEPRESSION OF ACTIVITY IN THE CEREBRAL CORTEX, *J. Neurophysiol. 7*, 359-390.

[153] Leao, A. A. P. (1947) FURTHER OBSERVATIONS ON THE SPREADING DEPRESSION OF ACTIVITY IN THE CEREBRAL CORTEX, *J. Neurophysiol. 10*, 409-414.

[154] Strong, A. J., Fabricius, M., Boutelle, M. G., Hibbins, S. J., Hopwood, S. E., Jones, R., Parkin, M. C., and Lauritzen, M. (2002) Spreading and synchronous depressions of cortical activity in acutely injured human brain, *Stroke. 33*, 2738-2743.

[155] Hinzman, J. M., Andaluz, N., Shutter, L. A., Okonkwo, D. O., Pahl, C., Strong, A. J., Dreier, J. P., and Hartings, J. A. (2014) Inverse neurovascular coupling to cortical spreading depolarizations in severe brain trauma, *Brain 137*, 2960.

[156] Vespa, P., Bergsneider, M., Hattori, N., Wu, H.-M., Huang, S.-C., Martin, N. A., Glenn, T. C., McArthur, D. L., and Hovda, D. A. (2005) Metabolic crisis without brain ischemia is common after traumatic brain injury: a combined microdialysis and positron emission tomography study, *J. Cereb. Blood Flow Metab. 25*, 763-774.

[157] Vespa, P. M., McArthur, D., O'Phelan, K., Glenn, T., Etchepare, M., Kelly, D., Bergsneider, M., Martin, N. A., and Hovda, D. A. (2003) Persistently low extracellular glucose correlates with poor outcome 6 months after human traumatic brain injury despite a lack of increased lactate: a microdialysis study, *J. Cereb. Blood Flow Metab. 23*, 865-877.

[158] Hartings, J. A., Shuttleworth, C. W., Kirov, S. A., Ayata, C., Hinzman, J. M., Foreman, B., Andrew, R. D., Boutelle, M. G., Brennan, K. C., Carlson, A. P., Dahlem, M. A., Drenckhahn, C., Dohmen, C., Fabricius, M., Farkas, E., Feuerstein, D., Graf, R., Helbok, R., Lauritzen, M., Major, S., Oliveira-Ferreira, A. I., Richter, F., Rosenthal, E. S., Sakowitz, O. W., Sanchez-Porras, R., Santos, E., Scholl, M., Strong, A. J., Urbach, A., Westover, M. B., Winkler, M. K., Witte, O. W., Woitzik, J., and Dreier, J. P. (2017) The continuum of spreading depolarizations in acute cortical lesion development: Examining Leao's legacy, *J. Cereb. Blood Flow Metab. 37*, 1571-1594.

[159] Feuerstein, D., Parker, K. H., and Boutelle, M. G. (2009) Practical Methods for Noise Removal: Applications to Spikes, Nonstationary Quasi-Periodic Noise, and Baseline Drift, *Anal. Chem. 81*, 4987-4994.